

# **RELIABILITY ASSESSMENT OF THE LANSCE ACCELERATOR SYSTEM**

**BY  
MARCUS ERIKSSON**

**STOCKHOLM 1998**



# **RELIABILITY ASSESSMENT OF THE LANSCE ACCELERATOR SYSTEM**

**BY**

**MARCUS ERIKSSON**



**M.Sc. THESIS AT THE  
ROYAL INSTITUTE OF TECHNOLOGY**

**Examiner: Waclaw Gudowski  
Supervisor: Christopher Piaszczyk, Northrop Grumman Corp.**

**The thesis is available at the Dep. of Nuclear & Reactor Physics and the University  
Library of the Royal Institute of Technology**

**DEP. NUCLEAR & REACTOR PHYSICS  
ROYAL INSTITUTE OF TECHNOLOGY  
S-100 44 Stockholm, Sweden**

## **Preface**

This report is a M.Sc Thesis prepared at the Department of Nuclear and Reactor Physics at the Royal Institute of Technology, Stockholm. For the most time the analyses were conducted at Los Alamos National Laboratory, USA.

The objective is to present the reliability and availability of the high current linear proton accelerator at LANSCE (Los Alamos Neutron Science Center). The reliability and the underlying cause of failure in major accelerator systems and components are investigated. The distribution of beam failures and down time for 6 consecutive run cycles (1996-97 accelerator operation) are analyzed. The investigation offers the opportunity to evaluate power fluctuations and long-term reliability and availability of high power linear accelerators.

The analysis was initiated with the intention to examine the reliability and availability of an accelerator for the purpose of transmutation of nuclear waste. It may as well be valuable in availability assessment of similar accelerators for use in other applications. Results may also be helpful in development of a reliability and availability model of high power accelerator systems.

## Abstract

High availability is of vital importance for future high power proton accelerator applications such as the Accelerator driven Transmutation of Waste (ATW). The ATW accelerator demand excellent year round availability in order to match the desired transmutation performance. In order to estimate the availability and reliability of accelerator designs, data from existing accelerators are analyzed. The Los Alamos Neutron Science Center (LANSCE) is an accelerator facility with enough operating history to supply meaningful reliability data. The report describes the data collection and analysis effort of the LANSCE accelerator operational data which was initiated to supply the accelerator reliability models with credible input data. A preliminary database of beam trips was assembled using operational data records, Central Control Room Logbook, and Operations Shift Supervisors' Summary Reports covering 1996-97. The events were classified according to the underlying cause into categories corresponding to typical accelerator subsystems. The ambition has been to identify the root cause of the down times. Mean Time Between Failures (MTBF) and Mean Down Time (MDT) estimates were obtained for magnets, RF stations, power supplies, etc. The results are useful for identifying development issues in high power accelerators.

Persistent power fluctuations in the accelerator may effect beam window characteristics and have a negative influence on a hybrid system. At LANSCE, beam delivery is frequently measured by current monitors near the target. The thesis investigates the beam current history and a better insight into power fluctuations of the LANSCE accelerator is achieved.

# Table of Contents

<b>PREFACE</b>	<b>3</b>
<b>ABSTRACT</b>	<b>4</b>
<b>TABLE OF CONTENTS</b>	<b>5</b>
<b>1 INTRODUCTION</b>	<b>7</b>
<b>2 NUCLEAR WASTE</b>	<b>8</b>
2.1 TRANSMUTATION OF WASTE	8
2.2 SPALLATION	8
2.3 ACCELERATOR DRIVEN TRANSMUTATION OF WASTE	9
<b>3 INTRODUCTION TO ACCELERATORS</b>	<b>10</b>
3.1 ACCELERATOR TECHNOLOGY	11
3.2 LINEAR ACCELERATORS	13
3.3 CIRCULAR ACCELERATORS	15
<b>4 THE ATW ACCELERATOR</b>	<b>19</b>
4.1 THE ATW LINAC	20
4.2 THE ATW CYCLOTRON	22
4.2.1 <i>The Injector Cyclotron</i>	23
4.2.2 <i>Intermediate cyclotron</i>	23
4.2.3 <i>Booster cyclotron</i>	23
4.3 LINACS VS CYCLOTRONS	24
<b>5 THE LANSCE ACCELERATOR</b>	<b>25</b>
5.1 SHORT HISTORY	25
5.2 GENERAL	26
5.3 INJECTOR BUILDING	27
5.4 LOW ENERGY BEAM TRANSPORT SYSTEM	28
5.5 DRIFT TUBE LINAC	29
5.6 TRANSITION REGION	31
5.7 SIDE COUPLED LINAC	32
5.8 SWITCHYARD	33
5.9 PROTON STORAGE RING	33
5.10 MANUEL JR. NEUTRON SCATTERING CENTER	34
5.11 WEAPONS NEUTRON RESEARCH CENTER	34
<b>6 LANSCE ACCELERATOR OPERATIONS</b>	<b>35</b>
6.1 INTRODUCTION	35
6.2 DOWN TIME ASSIGNMENT	35
6.3 DATABASES	36
6.4 BEAM SCHEDULE	37
<b>7 OVERALL LANSCE RELIABILITY</b>	<b>39</b>
7.1 INTRODUCTION	39
7.2 DEFINITIONS	39
7.3 OPERATIONAL STATISTICS	39
7.3.1 <i>H+ Beam line (Area A)</i>	39
7.3.2 <i>H- Beam line (Lujan)</i>	44
7.3.3 <i>Conclusions</i>	49

<b>8</b>	<b>SUBSYSTEM AND COMPONENT RELIABILITY</b>	<b>52</b>
8.1	INTRODUCTION	52
8.2	METHOD	52
8.2.1	<i>Input data</i>	52
8.2.2	<i>Subsystems</i>	53
8.2.3	<i>Database</i>	54
8.3	SCHEDULED BEAM TIME	55
8.4	LANSCE SUBSYSTEMS	56
8.4.1	<i>805 RF System</i>	56
8.4.2	<i>RF Reference System</i>	57
8.4.3	<i>The Klystron System</i>	58
8.4.4	<i>High Voltage System</i>	61
8.4.5	<i>DC Magnets</i>	61
8.4.6	<i>Magnet Power Supplies</i>	62
8.4.7	<i>Pulsed Power System</i>	62
8.4.8	<i>Summary of Subsystems</i>	64
8.5	OPERATIONAL STATISTICS	65
8.5.1	<i>Reliability Calculations</i>	66
8.5.2	<i>Results</i>	70
8.6	CONCLUSIONS	71
<b>9</b>	<b>BEAM CURRENT ANALYSIS</b>	<b>72</b>
9.1	INTRODUCTION	72
9.2	INPUT DATA	72
9.3	METHOD	72
9.3.1	<i>Beam Schedule</i>	73
9.4	RESULTS OF BEAM CURRENT ANALYSIS	74
9.4.1	<i>Threshold Factor 0.5</i>	75
9.4.2	<i>Threshold Factor 0.8</i>	77
9.5	RELIABILITY ESTIMATES	80
9.6	CONCLUSIONS	81
<b>10</b>	<b>ACKNOWLEDGEMENT</b>	<b>82</b>
<b>11</b>	<b>REFERENCES</b>	<b>83</b>
<b>APPENDIX 1</b>		<b>84</b>
A1	BEAM SCHEDULES	84
<b>APPENDIX 2</b>		<b>86</b>
A2	DC MAGNETS AND POWER SUPPLIES AT LANSCE	86
<b>APPENDIX 3</b>		<b>87</b>
A3	SUMMARY OF COMPONENTS IN THE PULSED POWER SYSTEM	87
<b>APPENDIX 4</b>		<b>90</b>
A4	STATISTICS OF FAILURE CAUSES IN INDIVIDUAL SYSTEMS	90
<b>APPENDIX 5</b>		<b>97</b>
A5	INSTANTANEOUS BEAM CURRENT	97

# 1 Introduction

One of the most important specifications on an ion accelerator for transmutation of waste is the overall beam availability and reliability. Such large accelerators are major capital investments and the availability determines the return of investment. A year round availability of 90% is necessary to match the desired transmutation performance. High component reliability is also essential to minimize power fluctuations, radiation hazards, and activation of structure material. Power fluctuations are particularly important in applications for transmutation since the accelerator is coupled with a subcritical reactor. In a hybrid system, short beam trips creates a loss of heat generation and causes thermal shock to the structure material and fuel rods.

The LANSCE accelerator is the world's most powerful linear proton accelerator. It delivers 800 MeV protons at 1 mA of beam current. It has been in operation for many years and offers considerable quantities of operational data.

In chapter 2, the option for transmutation of nuclear waste will be briefly reviewed.

For the general reader, an introduction to particle accelerators will be made in chapter 3, "Introduction to Accelerators". The principle of particle acceleration, accelerator development, different types of accelerators and some basic definitions are discussed. In this chapter, formulas will not be described but rather focus on different technical realizations of particle acceleration.

Chapter 4 presents the current Los Alamos National Lab concept for linear accelerator design for transmutation of waste. Also, the circular accelerator design proposed by the CERN group is presented. At the end of this chapter advantages and disadvantages of both accelerators are discussed.

In chapter 5, the LANSCE accelerator complex is outlined. A general description of different beam lines and important areas is made. Major parts of the accelerator are explained.

Information on LANSCE accelerator operations are discussed in Chapter 6. The method for classification, organization, and recording of beam interruptions are shown. Run cycles and beam schedules are explained.

Chapter 7 investigates the overall reliability of the LANSCE accelerator. Statistics of beam interruptions and down time for the H<sup>+</sup> and H<sup>-</sup> beams are analyzed. For the most part operational statistics for 1996-97 is presented but some previous historical reliability data is also shown. Mean Time Between Failure and Mean Down Time for the entire accelerator are calculated. Conclusions and proposals for reliability improvements are summarized.

In Chapter 8, a more detailed reliability assessment of major systems and subsystems is carried out. Particular emphasis is made for systems which are used in modern rf accelerator systems such as rf stations, rf drives, rf transport, magnets, magnet power supplies, cooling and vacuum.

In Chapter 9, statistics of beam monitor data during 1997 for the H<sup>+</sup> beam is shown. Analysis of 163,000 beam current recordings is performed. The analysis verifies the true beam performance. It does not investigate the cause of the beam failure. These results are compared with results from Chapter 7 "Overall LANSCE Reliability". Important conclusions with respect to both analyses are summarized.

## 2 Nuclear Waste

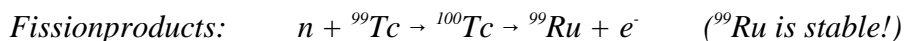
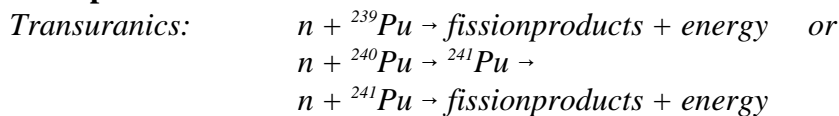
If one assumes the same level of global nuclear power generation for the future as it exists today there will be more than 250.000 tons of spent reactor fuel in the world by the year 2015. The spent fuel contains large quantities of long lived transuranics and fission products. This amount of long lived radiotoxic waste presents a major threat to all living organisms if released to the environment.

Due to different geological conditions, national views on nuclear energy, reprocessing, and proliferation concerns various programs have evolved for dealing with nuclear waste. One option is storing unprocessed spent fuel in geological repositories. Other options involves utilization of the fissile material contained in the spent fuel before storage in waste repositories. Long term uncertainties, the possibility for dilution of radiotoxic elements and extraction of weapon grade plutonium are the main concerns for the geological repository.

### 2.1 Transmutation of Waste

Nuclear waste may be eliminated in a nuclear way. One option for dealing with nuclear waste and weapon plutonium is transmutation. Transmutation is the conversion of one element into another. A nuclear transmutation entails a change in the structure of atomic nuclei. The transmutation reaction (see examples below) may be induced by a nuclear reaction such as neutron capture, or occur spontaneously by radioactive decay, such as alpha decay and beta decay. Chemical reactions are not capable of effecting the nuclear changes required for transmutation.

#### Examples of transmutation reactions in nuclear waste:



Transmutation of waste aims to enhance the viability of the geological repository. By transmuting the long lived transuranics by fission and the long lived fission products by neutron absorption the waste repository would have substantially reduced inventories of the long term radioactivity and heat sources. This will transform the time scale of repository performance requirements from a geological scale (tens of thousands years) to an engineering scale (hundreds of years). Transmutation of waste has the potential to provide added flexibility to the design of the waste repository and reduce the uncertainties about its performance.

### 2.2 Spallation

Large neutron availability is essential for transmutation of waste. Lack of neutrons make transmutation of waste in normal reactors less effective. A high intensity neutron source may be achieved in a process called spallation. Spallation occurs when high energy particles strike a target of heavy elements. The target material is usually tungsten, lead or an lead-bismuth alloy. In the collision, the incoming particle may tear



out protons, neutrons and nuclear fragments. Protons knocked out in the initial collision may strike a second tungsten nucleus, causing a "cascade" of nuclear fragments. The remaining nucleus is left in an excited state. In the deexcitation process the nucleus emits additional nuclei. Most of these nuclei are neutrons which are emitted isotropically.

### 2.3 Accelerator driven Transmutation of Waste

Several options of transmutation methods have been proposed. Up today the most reasonable suggestions utilize high power proton accelerators. In Accelerator driven Transmutation of Waste (ATW) protons are accelerated to high energy ( $\approx 1$  GeV) and then hit a heavy metal target. The result is an intense spallation neutron source.

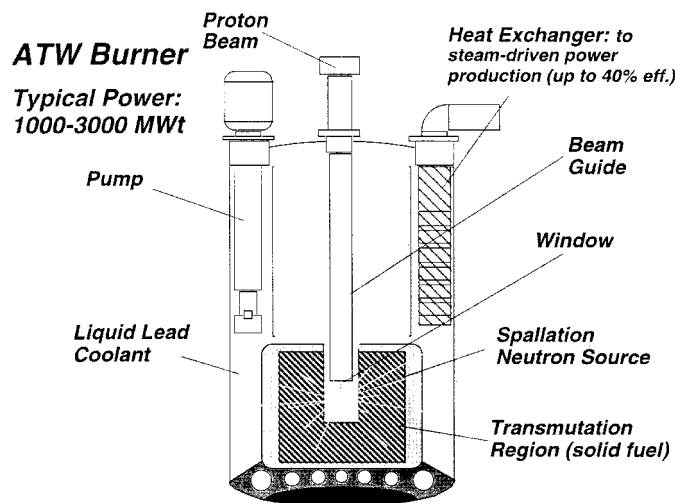


Figure 2.1 Illustration of the ATW burner, the Los Alamos National Lab concept [1]

In the ATW burner (see Figure 2.1), the target is surrounded by a subcritical transmutation region containing the fuel, "transmutation assemblies". The fuel consists of spent fuel and recycled ATW fuel. Since considerable neutron multiplication and heat production arises from fissioning of waste actinides, adequate heat removal must be present. The ATW burner may use an alloy of liquid lead-bismuth both as coolant and spallation target material. Because of its subcritical mode of operation the ATW system do not rely on delayed neutrons for control and power change, it is only driven by the externally generated neutron source. Control rods and reactivity changes have very low importance. Subcriticality allows the ATW burner to work with any composition of fuel. The neutron poor thorium-uranium fuel cycle may for example be used rather straightforwardly in the ATW burner. Extended burnup is achieved with appropriate accelerator operation. If desirable, significant electric power may be generated in a steam-cycle connected to the ATW burner.

### 3 Introduction to Accelerators

A particle accelerator is a device that produces a beam of fast-moving, electrically charged atomic or subatomic particles [2]. Physicists use accelerators in fundamental research on the structure of nuclei, the nature of nuclear forces, and the properties of nuclei not found in nature, such as the transuranic elements and other unstable elements. Their application as research tools in nuclear and high energy particle physics require the biggest and most energetic facilities. One of the ironies of modern physics is that the study of tiny nuclear particles and interactions often requires an extremely large apparatus, such as an accelerator. The world's longest electron linac is the 3.2-kilometre (2-mile) machine at the Stanford (University) Linear Accelerator Center, California (see Figure 3.1). SLC can accelerate electrons to 50 billion electron volts (50 GeV).

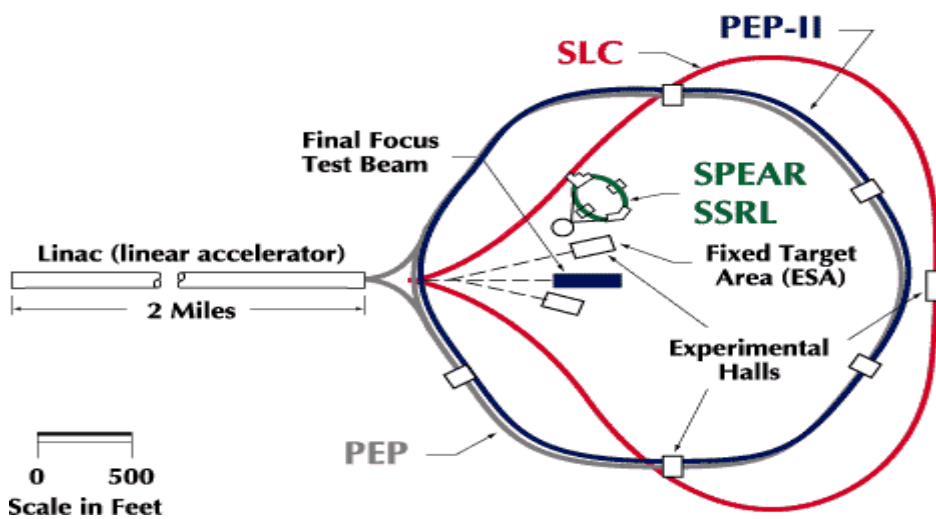


Figure 3.1 The Stanford Linear Accelerator

The Stanford Linear Accelerator Center has a 3.2-kilometre linear accelerator that produces one of the highest-energy electron beams in the world. At the far end of the accelerator, the electrons and positrons can be directed into the Stanford Linear Collider (SLC), which consists of two separate arcs of magnets forming a loop to bring the two beams into head-on collision at a total energy of about 100 GeV.

Much smaller accelerators, however, have found broad applications in a wide variety of basic research and technology, as well as medicine. Examples of such applications are radioisotope production, industrial radiography, cancer therapy, sterilization of biological materials and polymerization of plastics. Today, large particle accelerators are proposed for new applications, such as transmutation of waste, energy production, and production of tritium for use in nuclear weapons.

The particles that are accelerated most often are electrons or protons, and their antiparticles, or heavier ionized atoms. All electric charged particles may be accelerated, but for neutron production in a spallation target high energy protons are generally used.

Sometimes the primary beam is used, in other cases, the primary beam is directed onto a fixed target to produce a beam of secondary particles, such as X rays, neutrons, mesons, hyperons, or neutrinos. Such fixed target experimentation dominated nuclear and high energy particle experimentation from the first applications of artificially accelerated

particle beams far into the seventies and is still a valuable means of basic research. Obviously, it is also this method in conjunction with a heavy metal target which is used to produce secondary particles like neutrons for use in a ATW burner.

To increase the energy available for interaction the particles are sometimes aimed not at fixed targets but to collide head on with other particles. By this, almost all kinetic energy come to use in the collision. This is the main goal for the construction of colliding beam facilities (see figure 3.1).

A few circular accelerators are operated as sources of the intense radiation, called synchrotron radiation, emitted by electrons moving at almost the speed of light along curved paths. This radiation is highly collimated in the forward direction, of high brightness and therefore of great interest for basic research, technology, and medicine.

### **3.1 Accelerator technology**

Particle accelerators come in many forms applying a variety of technical principles. All are based on the interaction of the electric charge with static and dynamic electromagnetic fields and it is the technical realization of this interaction that leads to different types of particle accelerators.

The development of charged-particle accelerators has progressed along double paths which by the appearance of particle trajectories are distinguished as linear accelerators and circular accelerators. Particles travel in linear accelerators only once through the accelerator structure while in a circular accelerator they follow a closed orbit periodically for many revolutions accumulating energy at every traversal of the accelerating gaps. No fundamental advantage or disadvantage can be claimed for one or the other class of accelerators. It is mostly the particular application and sometimes the available technology that determines the choice between both classes. Both types have been invented and developed early in this century, and continue to be improved and optimized as associated technologies advance.

Since the late 1920's, when the first accelerators were built, the highest energies accessible have risen from around 1 MeV to 1 TeV. Several specific developments have allowed this progress to successively higher energies, but the basic principles of particle acceleration have remained essentially the same. For example, superconductivity has been employed to extend the reach of the highest-energy machines, but the machines themselves are still direct descendants of the first accelerators.

The effectiveness of an accelerator is usually characterized by the kinetic energy, rather than the speed, of the particles. The unit of energy commonly used is the electron volt (eV), which is the energy acquired by a particle that has a charge of the same magnitude as that of the electron when it passes between electrodes that differ in potential by one volt; it is equivalent to  $1.602 \cdot 10^{-19}$  J. The protons in the proposed ATW accelerator reaches an energy of 1 GeV and travel about 87 percent of the speed of light.

The particle beam current is measured generally in Amperes, no matter what general system of units is used but occasionally in terms of the total charge or number of particles. In a simple case, if the particles come by in a continuous stream the beam current is proportional to the particle flux. This case, however, occurs very rarely since particle beams are generally accelerated by rf fields. As a consequence there is no continuous flux of particles. The particle flux is better described as series of bunches separated by a number of wavelengths of the accelerating rf field. In these cases the

current is distinguished between different definitions. The peak current is the peak instantaneous beam current for a single bunch, while the average current is defined as the particle flux averaged over the duration of the beam pulse.

Particle accelerators consist of two basic units, the particle source or injector and the main accelerator structure. The region in which the particles are accelerated must be highly evacuated to keep the particles from being scattered out of the beam, or even stopped, by collisions with molecules of air.

The most successful acceleration of particles is based on the use of radio frequency alternating electromagnetic waves (rf fields). Acceleration occurs in resonant cavities (see figure 3.2) which are fed by rf power. Very high accelerating voltages can be achieved in resonant rf cavities, far exceeding those obtainable in electrostatic accelerators of similar dimensions. Particle acceleration in linear accelerators as well as in circular accelerators are based on the use of rf fields.

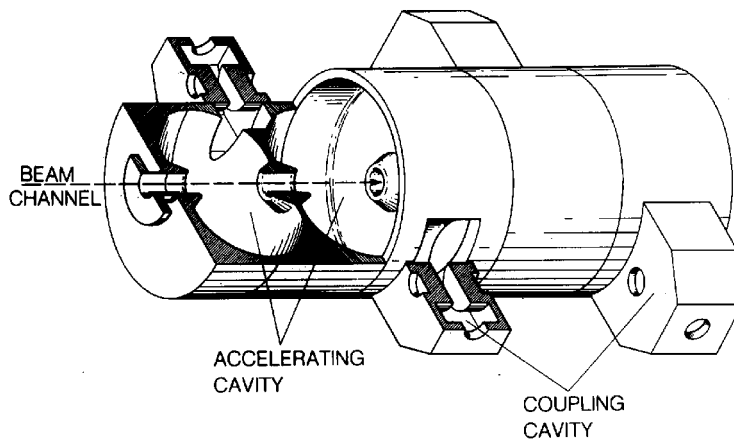


Figure 3.2 Illustration of the Side Coupled Cavity at LANSCE

RF accelerators require very powerful sources of electromagnetic fields. RF fields are produced by large klystrons (high-frequency vacuum-tube amplifiers) with power outputs of 20-30 megawatts.

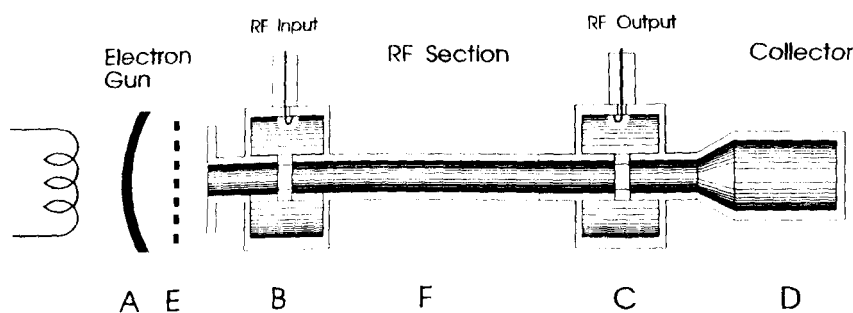


Figure 3.3 Picture of the 2-cavity Klystron Amplifier [3]

The principle of the two-cavity klystron amplifier can be understood from figure 3.3. A is an electron emitter and D is a collector for the beam. E is a modulating element, often used when pulses of power are required. Power is coupled into cavity B (input

cavity) and the rf voltage developed across the gap of the cavity modulates electrons in the beam. The tunnel between cavities B and C is called the drift tube (F) and its length is designed to provide optimum bunching of the beam at the gap of cavity C (output cavity). The electron bunches induce an rf current in the output cavity which can be coupled out as rf power. Depending on the resonant frequency of the second cavity (C) compared with the frequency of the input signal, an rf voltage will be excited in the second cavity which will be larger than that in the first cavity. Thus an amplified signal can be coupled out from the second cavity. In a multi-stage klystron (for example the LANSCE klystron) several cavities are connected in series and the rf energy grows in successive cavities as the beam flows from cathode to collector.

### 3.2 Linear Accelerators

In linear accelerators the particles are accelerated by definition along a straight path by either electrostatic fields or oscillating rf fields. When rf fields are used the linear accelerator is commonly called a linac [2].

The final energy of the particles is proportional to the sum of the voltages produced by the accelerating devices along that line. The linac consists of a linear sequence of many units where accelerating rf fields are generated and timed such that particles absorb and accumulate energy from each acceleration unit.

The principle of the linear accelerator based on alternating fields and drift tubes was proposed by Ising in 1925 and demonstrated by Widerö in 1928. In this method particles are accelerated by repeated application of rf fields (see figure 3.4).

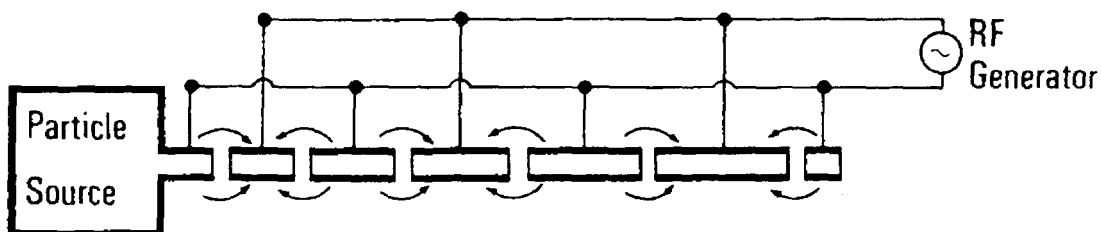
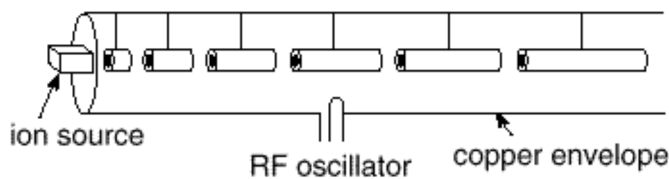


Figure 3.4 Principle of the Widerö accelerator [4]

While the principle of the linear accelerator is simple, the realization requires specific conditions to ensure that the particles are exposed to only accelerating rf fields. For efficient acceleration the motion of the particles must be synchronized with the rf fields in the accelerating sections. During the half period when the fields reverse sign the particles must be shielded from the fields in order not to be decelerated again. Technically this requirement is realized by surrounding the beam path with metallic drift tubes as shown in figure 3.5. The electric field is zero inside the drift tubes, and the length of the tube segments are chosen such that the particles reach the gap between two successive tubes at the moment the rf field is accelerating. The length of the tubes are therefore almost as long as it takes the particles to travel for half an rf period.

In the twenties when this principle was developed it was difficult to build high frequency generators at significant power. In 1928 rf generators were available only up to about 7 MHz and this principle was useful only for rather slow particles like low energy protons and ions. The drift tubes can become very long for low rf frequencies. At higher

frequencies, however, the capacitive nature of the Widerö structure becomes very lossy due to electromagnetic radiation. To overcome this difficulty, Alvarez proposed to enclose the drift tubes in a long cylindrical metal tank, or cavity. The Alvarez linac is based on the formation of standing electromagnetic waves inside the tank. The electric field is parallel to the axis of the tank. Most of these accelerators operate at frequencies of about 200 MHz. Focusing is usually provided by magnetic quadrupoles placed inside the drift tubes. The Alvarez linac is suitable for acceleration of protons and ions from a few hundred keV to a few hundred MeV. That energy range makes the Alvarez structure useful in the first accelerating stage in a linear accelerator or as a preaccelerator into a synchrotron.



*Figure 3.5 The Alvarez linac*

*The acceleration chamber is an evacuated cylindrical pipe that serves as a waveguide for the accelerating field.*

Linear accelerators fall into two distinct types: standing-wave linear accelerators (used for heavy particles) and traveling-wave linear accelerators (used to accelerate electrons). The reason for the difference is that after electrons have been accelerated to a few MeV in the first few metres of a typical accelerator, they have speeds very close to that of light. Therefore, if the accelerating wave also moves at the speed of light, the particles do not get out of phase, their speeds do not change. Protons, on the other hand, must reach much higher energies before their speeds can be taken as constant, so that the accelerator design must allow for the prolonged increase in speed.

In most new linac designs RFQs (radio frequency quadrupole accelerators) are included. The RFQ is a low velocity, high current linear accelerator. Many laboratories have adopted the RFQ as a "front end" accelerator. The Alvarez linac is most efficient in a higher energy range (0.5-100 MeV). Below that range, RFQs are more appropriate. Separate bunching devices are not necessary in the RFQ. The RFQ receives a continuous stream of ions from the injector, forms it into bunches, and accelerates nearly 100 % of the beam. In other linacs the bunching process usually discards 30 to 50 % of the beam. The RFQ has eliminated the historic requirement of operating the ion source at several hundred kilovolts above ground before injection into a drift tube linac. Increased accelerator reliability is gained due to a lower probability of high voltage sparking in the injector column.

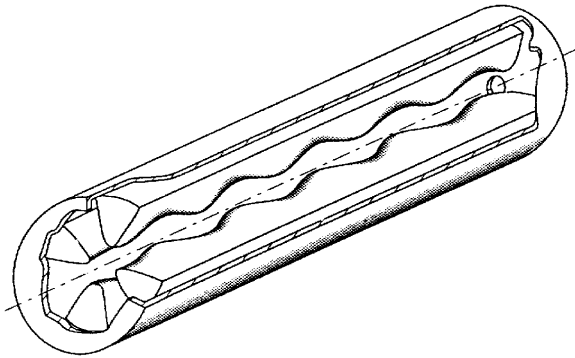


Figure 3.6 Illustration of a Radio Frequency Quadrupole [5]

The RFQ, as shown in figure 3.6, is a focusing structure to which acceleration is added as a perturbation. Other linac designs impose focusing onto an accelerating structure. This fundamental focusing attribute of the RFQ gives rise to very good beam stability in all three dimensions.

### 3.3 Circular Accelerators

In a circular accelerator, the path of the particles is bent by the action of a magnetic field into a spiral or a closed curve that is approximately circular. In this case, the particles pass many times through the same accelerating devices. This simplifies the rf system compared to the large number of energy sources and accelerating sections required in a linear accelerator. While this approach seemed at first like the perfect solution to produce high energy particle beams, its progress soon became limited for the acceleration of electrons by the generation of synchrotron radiation.

The simplicity of circular accelerators and the absence of significant synchrotron radiation for protons and heavier particles like ions has made circular accelerators the most successful and affordable principle to reach the highest possible proton energies for fundamental research in high energy physics.

In circular accelerators, the final energy depends on the magnitude of the voltages multiplied by the number of times the particles pass through the accelerating gaps. Because the total distance traveled by the particles in a cyclic accelerator may be more than a million kilometres, cumulative effect of small deviations from the desired trajectory would be dissipation of the beam. Therefore, the beam must be continually focused by the magnetic fields, which are precisely shaped by powerful magnets.

The magnetic resonance accelerator, or cyclotron, was the first cyclic accelerator and the first resonance accelerator that produced particles energetic enough to be useful for nuclear research. For many years the highest particle energies were those imparted by cyclotrons modeled upon Lawrence's archetype. In these devices, commonly called classical cyclotrons, the accelerating electric field oscillates at a fixed frequency and the bending magnetic field has a fixed intensity (see figure 3.7). The principle of the cyclotron is basically the application of the Widerö linac in a coiled up version to save space and rf equipment.

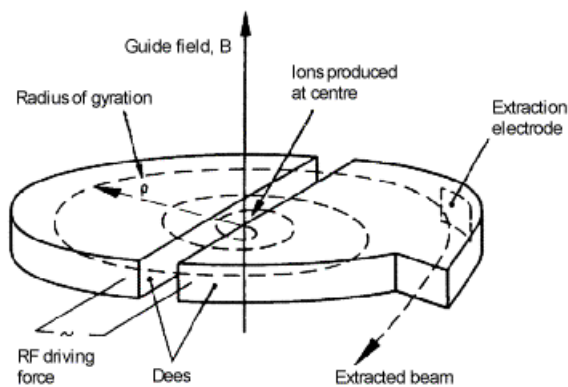


Figure 3.7 Classical cyclotron

*The magnetic resonance accelerator, or cyclotron, conceived by Lawrence as a modification of Widerö's linear resonance accelerator.*

The accelerating cavity has basically the form of a circular pillbox cut in two halves, where the accelerating fields are generated between those halves and are placed between the poles of the magnet. Because of the form of the half pillbox, these cavities are often called the Dees of a cyclotron. The particle orbits occur mostly in the field free interior of the Dees and traverse the accelerating gaps between the two Dees twice per revolution. Due to the increasing energy, the particle trajectories spiral to larger and larger radii.

The bending magnet field serves only as a beam guidance system to allow the repeated passage of the particle beam through the cavity. Since the cavity fields are oscillating, acceleration is not possible at all times and for multiple accelerations we must meet specific conditions of synchronization between the motion of particles and the field oscillation. The time it takes the particles to travel along the orbital path must be an integer multiple of the oscillation period for the rf field.

The energy gained by a particle in a classical cyclotron is limited by the relativistic increase in the mass of particle, a phenomenon that causes the orbital frequency to decrease and the particles to get out of phase with the alternating voltage. This effect can be reduced by applying higher accelerating voltages and shorten the overall acceleration time. The highest energy imparted to protons in a classical cyclotron is less than 25 MeV, and this achievement requires the imposition of hundreds of kilovolts to the Dees.

Cyclotrons in which the frequency of the accelerating voltage is changed as the particles are accelerated are called synchro cyclotrons, frequency-modulated (FM) cyclotrons. Because of the frequency modulation, the particles do not get out of phase with the accelerating voltage, so that the relativistic mass increase does not impose a limit on the energy. The particles reach the maximum energy in bunches, one for each time the accelerating frequency goes through its program. In other words, the particle flux has a pulsed macro structure equal to the cycling time of the rf modulation. The average intensity of the beam is much lower than that of a classical cyclotron.

The isochronous cyclotron is another modification of the classical cyclotron that also evades relativistic constraint on its maximum energy. The isochron cyclotron is the solution to obtain high intensity (classical cyclotron) at high energy (synchrocyclotron). Its advantage over the synchrocyclotron is that the beam is not pulsed and therefore more



intense. The frequency of the accelerating voltage is constant, and the orbital frequency of the particles is kept constant as they are accelerated by causing the average magnetic field on the orbit to increase with orbit radius. This ordinarily would cause the beam to defocus axially. Hence, the magnetic field in an isochronous cyclotron would not be axially symmetric. But, if the magnetic poles are constructed from sectors, the particles in the cyclotron would experience azimuthal variation of the magnetic field. This in turn introduces an axially restoring force on the particles at the edges of the sectors.

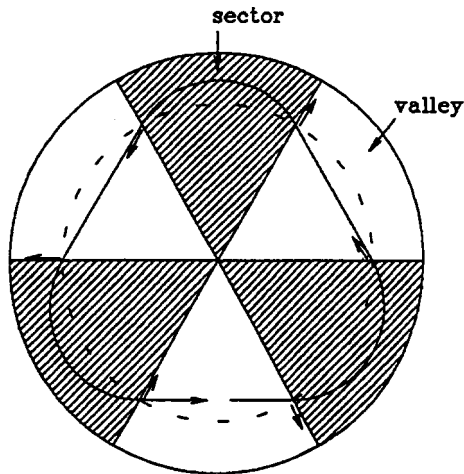
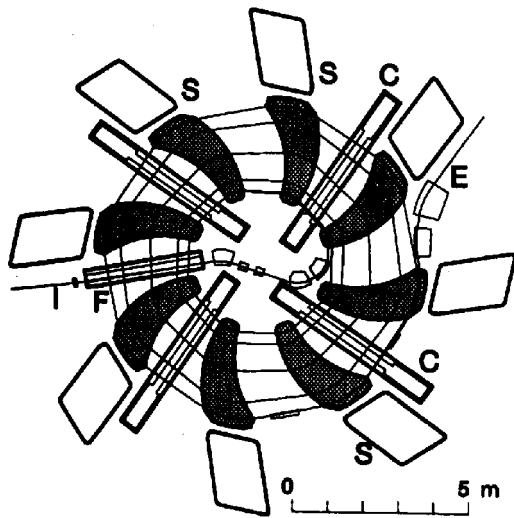


Figure 3.8 Isochronous cyclotron

If the sectors are twisted to a spiral form we get some additional axial focusing since the particles enter and leave the magnet edges with a larger spiral angle.

The development of circular accelerators has finally made a full circle. Starting from the use of a constant rf field, in classical cyclotrons, the need for frequency modulation was obvious to meet the synchronicity condition for particles through the relativistic transition region. Application of technically complicated focusing schemes allowed to revert back to the most efficient way of particle acceleration with constant fixed frequency fields.

Accelerating protons with isochronous cyclotrons is usually limited by the focusing limit of the magnet. The ultimate focusing limit for this is a separated sector cyclotron. In the separated sector cyclotron (or ring cyclotron) the magnets consist of sectors only (see figure 3.9). In the valley between the sectors there is no iron and practically no magnetic field. RF cavities, extraction and other beam diagnostic equipment may be installed in the space between the sectors. This type of cyclotron is a possible candidate for transmutation of waste purposes (see section 4.2).



*Figure 3.9 Sector Separated Cyclotron at PSI*  
*The Ring Cyclotron at Paul Scherrer Institute (PSI). The cyclotron accelerates protons to 590 MeV at 1.5 mA.*

## 4 The ATW Accelerator

To produce enough neutrons in a spallation target the accelerator must deliver energetic protons at high current (see figure 4.1). Since the neutron yield increases almost linearly (in the range 0.8-4 GeV) with proton energy the energy and current may be exchanged. For example, if the proton energy is doubled and the beam current is divided by two the neutron yield stays approximately the same. Typical specifications of an ATW linac are 30-40 mA at 1 GeV. Such high power accelerators do not exist today, but considering recent progress in accelerator technology there is a good confidence in realization of these accelerators.

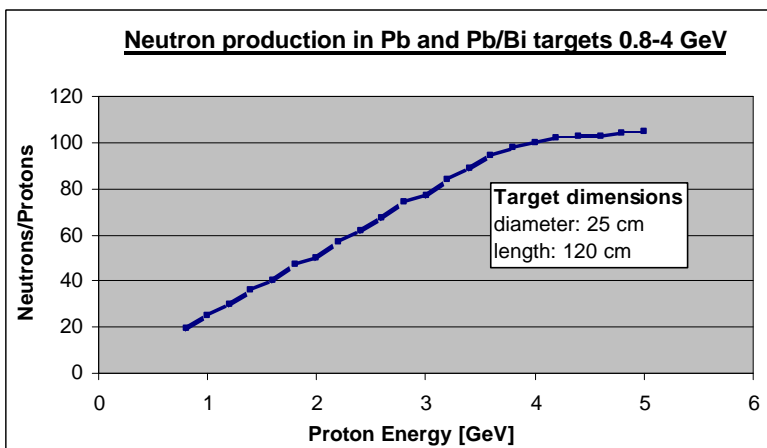


Figure 4.1 Illustration of neutron yield in a spallation target [6]

The ATW accelerator must be designed to deliver large beam currents to a target facility with very little beam losses along the accelerator. Several types of difficulties arise when one tries to increase the beam intensity. One effect is the mutual repulsion of particles due to their electric charge. This repulsion affects phase stability as well as focusing. In the case of beam loss, relative losses increase with intensity and there is a risk for contamination, local heating and damage of the accelerator structure. Light ions, such as protons, have long stopping ranges, penetrate deeply, and have nuclear reactions that cause radioactivity buildup in the structure [7]. This activation is the main problem with beam losses in light ion accelerators. It is desirable to be able to perform maintenance activities without using remote manipulators (hands-on maintenance) over the lifetime of the facility.

## 4.1 The ATW Linac

In this section the linear accelerator design for transmutation of waste purpose is outlined. The proposed accelerator is the Los Alamos National Lab concept for accelerator design. Most of the text is based on the ATW accelerator design by George Lawrence of Los Alamos National Lab [8].

### A linac for an ATW facility should be designed:

- To have high availability and operational flexibility
- To have high reliability and minimal power fluctuations
- To have very high electrical efficiency (ac to beam power)
- For minimum capital and operating costs
- To have short length
- To vary the power on target over a wide range

The ATW linac design is based on the APT (Accelerator Production of Tritium) linac design and technology. Extensive Research and Development on the APT linac has been in progress for several years. The baseline accelerator design for the ATW linac is a normalconducting-superconducting proton linac that produces a continuous wave beam power of 40 MW at 1 GeV. The ATW linac is illustrated in figure 4.2.

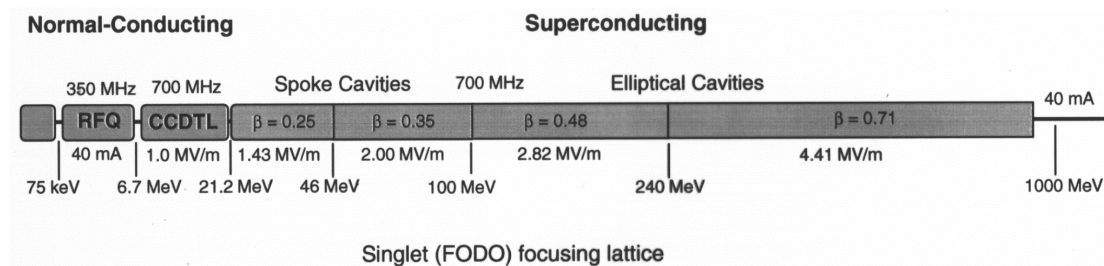


Figure 4.2 The ATW linac proposal [8]

Normalconducting (nc) linac is used for low energies. This facilitates a high-density magnetic focusing lattice and smoothly varying accelerating and focusing parameters. It also allows for excellent emittance control of the high-current beam and minimal generation of halo. Halo is the formation of an outer ring of particles surrounding the inner core of the beam. The beam halo affects particle losses in an accelerator. This of great concern for the next generation of high power proton linacs.

At high energies superconducting cavities and quadrupoles are used. This eliminates RF cavity losses and provides very high power efficiency. Large aperture dramatically reduces beam loss threat. Short cavities provide wide velocity acceptance bandwidth.

The ATW linac design is more advanced than APT. Some of the most important aspects an the linac proposal for ATW are:

- **High accelerating gradients in the superconducting section**
  - gradients of 15MV/m in superconducting section. These gradients have been achieved in cavity tests (TESLA).
  - short linac (only 345 m) ⇒ reduces size as well as costs
- **Cryomodules contain superconducting quadrupoles**
  - stronger focusing ⇒ larger aperture/beam-size ratio ⇒ less contamination
  - higher electrical efficiency ⇒ minimizes quadrupole power
- **Superconduction starts at lower energy (20 MeV)**
  - reduces RF losses in low energy linac ⇒ increases efficiency
  - increases aperture size at low energies
  - makes use of 1/2-wave (spoke-type) superconducting resonators

Table 4.1 Global ATW accelerator parameters

Parameter	Value
Output proton current	40 mA
Duty factor	100%
Final energy of nc linac	21.2 MeV
Final energy of sc linac	1000 MeV
Length	345 m
RF power	44.6 mA
Number of klystrons	3 at 350 MHz; 53 at 700 MHz
Number of cryomodules	31
Number of nc accelerating cavities	106*2
Number of sc accelerating cavities	134
Number of nc quadrupoles	105*2
Number of sc quadrupoles	165

At Los Alamos a 110 mA, 75 keV proton injector is being developed for the APT project. The new injector is based on a microwave proton source which operates at 2.45 GHz. The ion source is coupled with a two-solenoid, LEBT system for matching into a RFQ [9].

A low-energy demonstration accelerator (LEDA) has been developed. LEDA is virtually identical to the first 20 MeV of the APT accelerator. It is used to confirm beam parameters, system availability, component reliability, provide experimental determination of the beam halo distribution, develop a commissioning plan for a continuous wave system, and prototype the low-energy portion of the APT plant accelerator. As far as now the LEDA injector has demonstrated APT beam performance requirements and reliability. In 1997, the injector was operated for 168 hours. In this time, the injector operated at 75 keV, > 120 mA with an availability of 96-98 % [9]. The ion source accounted for 3.4 hours of down time (see definition in section 8.5.1) because of recovery from high voltage sparks.

## 4.2 The ATW Cyclotron

In the section the solution based on circular machines for accelerator driven transmutation projects is presented. The proposal is made by the transmutation group at CERN (European Organization for Nuclear Research). The text is a summary of the proposition in the IAEA Status report on Accelerator driven systems [10]. The accelerator complex is based on a three-stage cyclotron accelerator (figure 4.1)

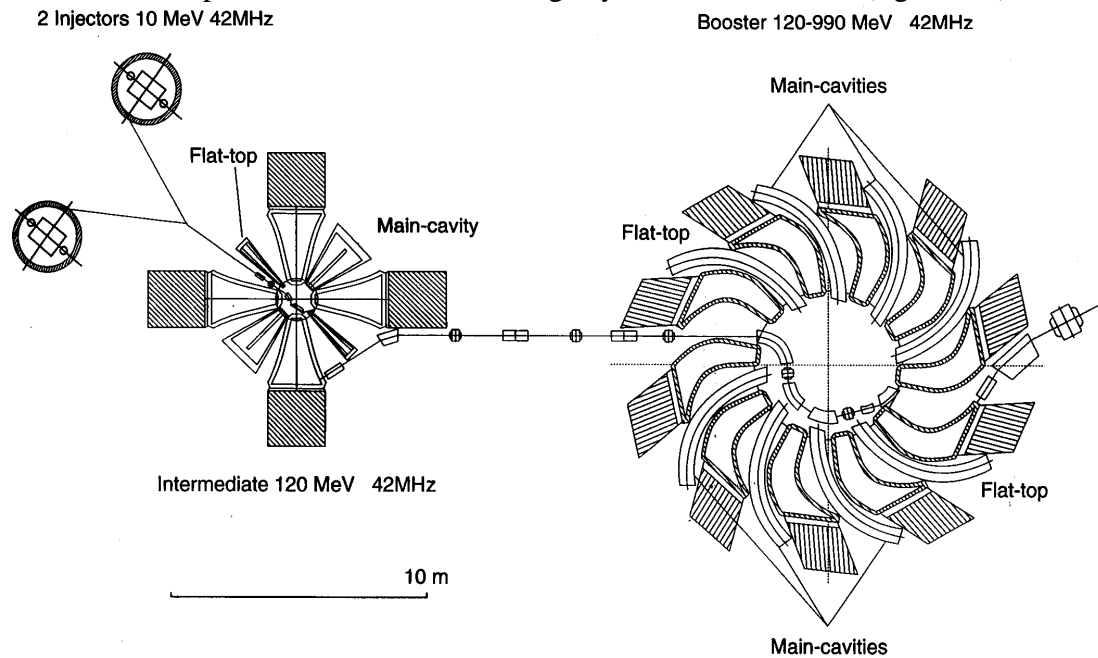


Figure 4.1 General layout of the CERN group accelerator complex [10]

The injector is made of two 10 MeV, Compact Isochronous Cyclotrons (CIC). Beams are merged with the help of negative ion stripping to the intermediate stage, a cyclotron with four separated sectors (ISSC) bringing the beam up to 120 MeV. In the final booster, a ten separated and six cavities cyclotron (BSSC), the kinetic energy is raised up to 1 GeV. The main parameters of the cyclotrons are presented in table 4.2.

Table 4.2 Main parameters of the cyclotrons

Parameter	Injector	Intermediate	Booster
Injection energy	100 keV	10 MeV	120 MeV
Extraction energy	10 MeV	120 MeV	990 MeV
Frequency	42 MHz	42 MHz	42 MHz
Harmonic	4	6	6
Magnet gap	6 cm	5 cm	5 cm
Niobium sectors	4	4	10
Sector angle (injection/extraction)	15°/34°	26°/31°	10°/20°
Sector spiral extraction	0°	0°	12°
Niobium cavities	2	2	6
Type of cavity	delta	delta	single gap
Gap peak voltage	110 kV	170 kV	550 kV
Gap peak voltage extraction	110 kV	340 kV	1100 kV
Radial gain per turn extraction	16 mm	12 mm	10 mm

### 4.2.1 The Injector Cyclotron

The injector cyclotron consists of a four sector isochronous cyclotron capable of delivering 5 mA. The beams of two such injectors working at the same frequency are then merged before injecting them into the intermediate stage (ISSC) and the final booster. Since high current is required the injection energy must be about 100 keV in order to avoid space charge effects. A stripper is installed at the end of the injection line, before beams enters the ISSC to convert the H<sup>-</sup> beam into a H<sup>+</sup> beam. As a result the particle density in the phase space is doubled at no increase of the single beam emittance.

### 4.2.2 Intermediate cyclotron

A four-separated-sector cyclotron has been chosen as the intermediate stage. Acceleration of the beam is provided by two main resonators located in opposite valleys giving an energy gain per turn of 0.6 MeV at injection and 1.2 MeV at extraction, increasing the beam energy from 10 MeV to 120 MeV. The RF frequency of the accelerating cavities has been chosen equal to 42 MHz. The choice of the injection energy into the ISSC is certainly one of the most important parameters which influences the overall performances of the cyclotron complex. The space charge effects are strong at low energy. They are present in both transversal and longitudinal directions of the beam. Results of simulations show that a nominal 10 mA beam can be handled at an injection energy of the order of 10 MeV.

Double gap cavities have been selected because their radial extension is much smaller leaving more space in the centre of the machine for the bending and injection magnets and the beam diagnostics.

### 4.2.3 Booster cyclotron

The magnet of the final booster consists of 10 identical C-shaped sector magnets with a strong spiral in order to obtain sufficient vertical focusing at high energies. Acceleration of the beam is provided by 6 main resonators located in the valleys. They should provide an energy gain per turn of 3 MeV at injection and 6 MeV at extraction, increasing the beam energy from 120 MeV to 990 MeV. In order to compensate the effects of the space charge forces, two flat-topping cavities are needed (flat-topping is a technique to achieve a constant accelerating voltage at a phase width of 30°). The RF frequency is equal to 42 MHz. A voltage ratio of 2.0 is used between injection and extraction in order to reduce the number of turns in the cyclotron and to have sufficient turn separation at extraction.

### 4.3 *Linacs Vs Cyclotrons*

As mentioned before, both linear and circular accelerator designs are proposed for transmutation of waste and energy production. Both accelerators use radio frequency (rf) electromagnetic waves for acceleration. The main advantage for the linac is the possibility to produce high currents. For the cyclotron, the main advantages are low cost and compact size.

Due to longitudinal space charge effects and extraction losses the maximum beam current is limited for the cyclotron. For the current state of the art at about 10-20 mA. Since the space charge influence is strong at high current and low energy it is suitable to inject protons at high energy. To achieve high intensities in a circular accelerator one may utilize a multistage sector separated cyclotron, consisting of several low energy, low current cyclotrons feeding into one high energy, high current cyclotron.

The cyclotron can be made very compact in size due to repeated use of the same accelerating cavities and not requiring a long beam transport system. The beam is held on a circular path by magnetic fields in bending magnets. The cyclotron is cheaper, but to deliver a beam current comparable to a linac one must use two or three cyclotron facilities. To increase particle energy is less costly. Since the neutron yield per incident proton is proportional to beam power in the region 1-4 GeV, beam current and beam energy may be exchanged.

One problem in cyclotrons is beam extraction. In order to get a high extraction efficiency, it is necessary to achieve a large radial separation of the last turns. This may be accomplished by a low average magnetic field and a high energy gain per turn.

For very high beam energies linear accelerators become very long, often several hundred meters long, and more expensive than cyclotrons. The linac length determines the total cost and the maximum energy hence the cost is proportional to the particle energy. Increase of particle energy in a linac is much more costly than for the cyclotron. New superconducting linac structures offers high accelerating gradients this reduces the size of the linac. Superconduction also reduces operational costs as rf losses in cavities are negligible. Most of the existing cyclotrons utilize room temperature magnets (conventional magnets) where the maximum magnetic field is limited to 2 T due to iron saturation. Superconducting cyclotrons offer higher energies as compared with conventional cyclotrons. Also, superconductivity offers a way to build small magnets to give relatively high energies. However, superconduction in cyclotrons is complicated since presence of a strong magnetic field destroys the superconducting state.

Linear electron accelerators constructed of superconducting materials have been developed. Such structures dissipate far less energy than conventional metal structures, allowing a continuous electron beam, rather than a pulsed beam, to be accelerated.



## 5 The LANSCE Accelerator

### 5.1 Short History

Operated by the Los Alamos National Laboratory of the University of California for the United States Department of Energy, Los Alamos Neutron Science Center (LANSCE) is a national research facility for nuclear physics.

The initial name of the facility was LAMPF, Los Alamos Meson Physics Facility. Later, the complex was renamed as the Clinton P. Anderson Meson Physics Facility because of the late senator's long-time interest in and support of Los Alamos National Laboratory. In the 1990's, Los Alamos National Laboratory decided to focus on neutron research and applications. In October 1995, the accelerator complex was renamed to the present Los Alamos Neutron Science Center (LANSCE).

LANSCE is a pulsed spallation neutron source facility that includes the world's most powerful proton linear accelerator. LANSCE is ideal for research in neutron scattering, neutron physics, and transmutation technologies. The linac was brought into initial operation at 800 MeV with a low intensity beam on June 9, 1972, within the time schedule and the revised cost estimate of \$57 000 000. By January 1983 the accelerator produced a beam current of 1.2 mA. Routine operation now is at 1 mA and 800 MeV.

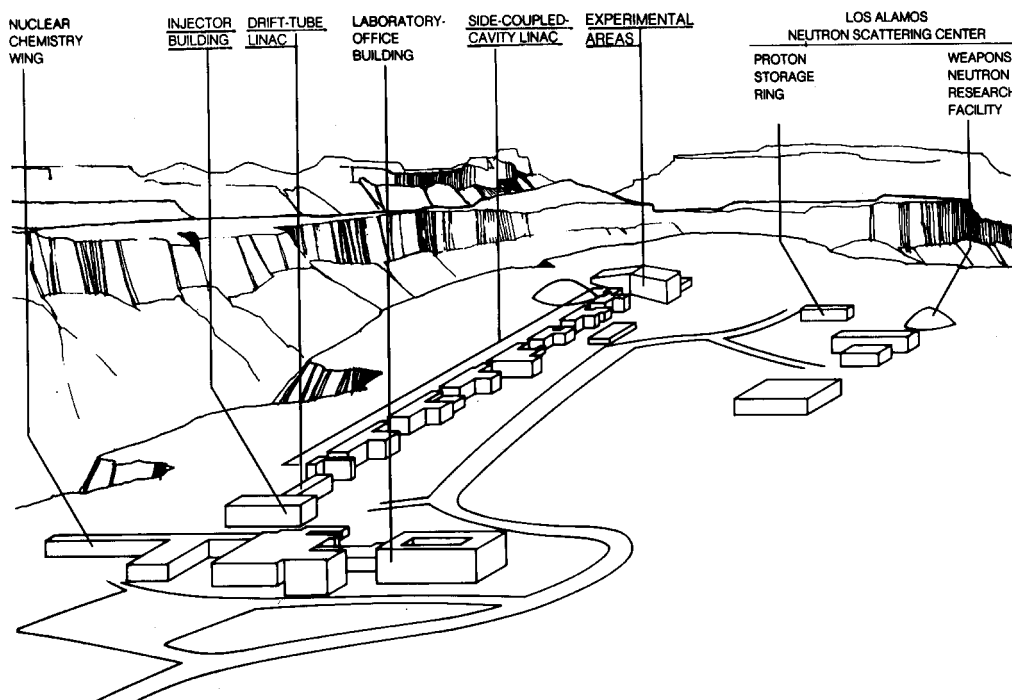


Figure 5.1 Overview of LANSCE

## 5.2 General

Two particle beams are available at LANSCE: H<sup>+</sup> and H<sup>-</sup> (the third polarized H-beam is not in use). Both ions are accelerated simultaneously by alternating electric fields in the accelerator cavities. The first stage of the accelerator contains the injector systems, one for each kind of particle (see figure 5.2). The beams are passed through Low Energy Beam Transport (LEBT) systems before injection into the second stage of the accelerator which is an Alvarez Drift Tube Linac (DTL). The DTL accelerate protons from an energy of 750 keV to 100 MeV. The beams are then transported through a transition region for matched injection into the third section, the Side Coupled Linac (SCL). The SCL is the main section of the linac, it can accelerate protons to energies varying from 113 MeV to 800 MeV.

At the end of the linac the beams enter a switchyard in which the beams are separated, focused and diverted into their final beam lines.

The high intensity proton beam (H<sup>+</sup>) is directed through Line A (LA) to experimental area A, passing through secondary beam production targets as desired, and culminating at the isotope production, radiation effects, and beam stop area.

The negative hydrogen ion beam (H<sup>-</sup>) may be directed to Line D. Selected pulses are then delivered to the Proton Storage Ring (PSR) for accumulation and delivery to the Manuel Lujan Jr. Neutron Scattering Center (Lujan or LANSCE) target or to the Weapons Neutron Research area (WNR, Target 2 and 4).

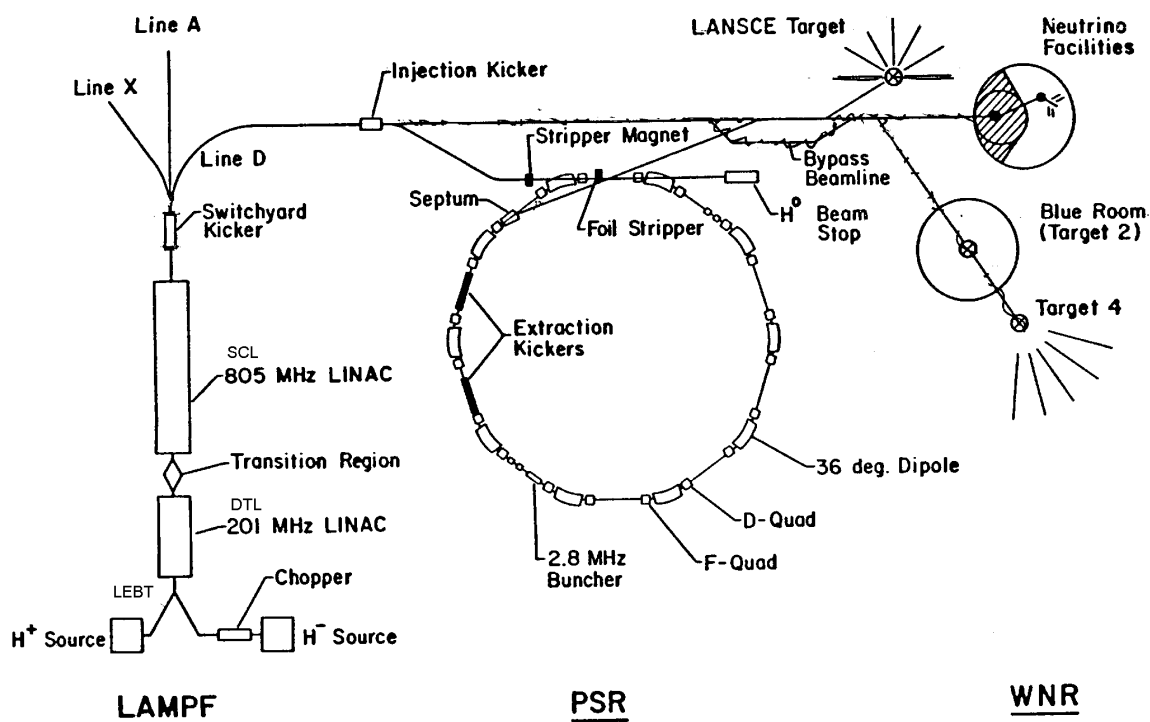


Figure 5.1 Major Accelerator Sections and beam lines at LANSCE

The accelerator is divided into different sectors. Beam transport systems and experimental facilities are designated as beam lines and target areas.

*Table 5.1 Description of sectors of the accelerator*

Sector	Sector Description	Detailed Sector Description
Sector J	Injector Building	The injector building houses the injectors and Low Energy Beam Transport (LEBT) Systems.
Sector A	Drift Tube Linac (DTL)	Sector A houses the DTL and the Transition Region (TR) which permits matching of the different beams from the DTL to the SCL.
Sectors B-H	Side Coupled Linac (SCL)	These sectors includes the SCL structure. Six or seven klystrons and a high voltage capacitor room are associated to each sector.
Sector S	Switchyard (SY)	The Switchyard (SY) provides magnetic separation of the beams at the end of the SCL.

*Table 5.2 Description of beam lines and target areas*

Beam line	Target Area Description	Detailed Line and Area Description
Line A	Area A	Line A delivers the H+ beam to a number of targets in Area A.
Line D	Lujan and Weapons Neutron Research	Line D provides H- beam to the Proton Storage Ring (PSR), Lujan Neutron Scattering Center, and the Weapons Neutron Research (WNR) area.
Line X	Area B and C	Line X provides H- beam to experiments in Area B or C.

### **5.3 Injector Building**

Each injector system has a 750 keV Cockcroft-Walton type generator and an duoplasmatron type ion source (see figure 5.4) to produce positive and negative charged protons. The ion source is positioned within the high voltage terminal of the Cockcroft-Walton generator. These units are located within large electrically shielded bays in the injector building. Created inside the high voltage dome, the ions are accelerated by the electrostatic field as they travel in the injector column connecting the dome to a grounded plane. Beams from the two ion sources enter a beam transport (LEBT) area which directs each one into the entry of the DTL without interference with the other.

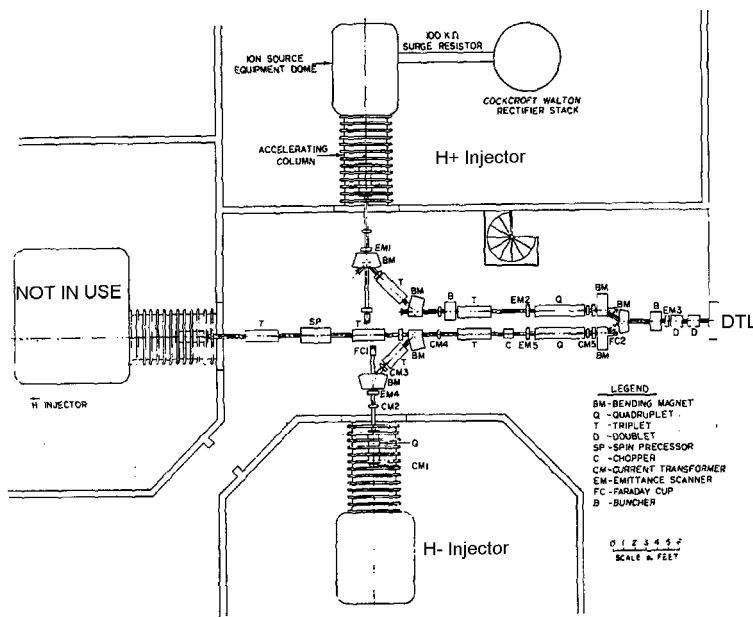


Figure 5.3 The Injector Building and LEBT system at LANSCE [11]

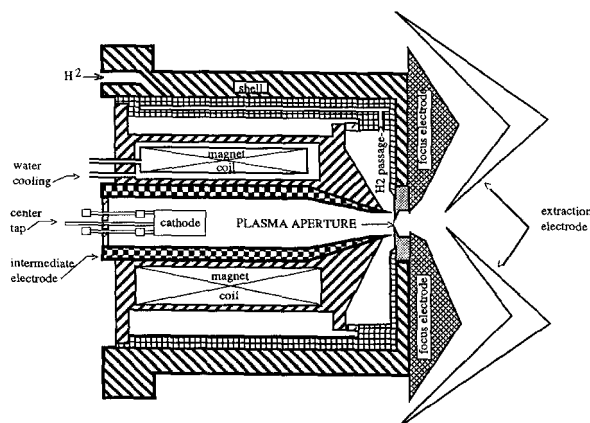


Figure 5.4 The H<sup>+</sup> ion source at LANSCE (Duoplasmatron)

## 5.4 Low Energy Beam Transport System

Before the protons enter the DTL the beams must pass through a Low Energy Beam Transport system (LEBT) where the protons are steered, focused and bunched (see figure 5.3). Timing when these bunches are injected into the drift tube linac is crucial to ensure their acceleration by the rf field.

Particles from the ion source enter the beam line in what appears to be a constant stream. This stream could be injected into the accelerator structure and a small percentage of the particles which entered the accelerator at the correct phase angle would be accelerated, the rest would be lost. For high beam densities it is desirable to compress the continuous stream of particles from the source into short pulses with the help of a prebuncher, figure 5.5.

Efficient acceleration by rf fields occurs only during a very short period per oscillation cycle and most particles would be lost without proper preparation. It is the purpose of the buncher to collect the particles into bunches and to time the progress of

these bunches so that they enter the accelerator at the most favorable phase angle. Early particles within a bunch are decelerated and late particles are accelerated. This process may be imitated to the bunching of vehicles that occurs as they go through a traffic light: protons are accelerated or slowed, as required, to group them into bunches. By this technique the percentage of the particles in the initial ion stream that are successfully accelerated is substantially increased.

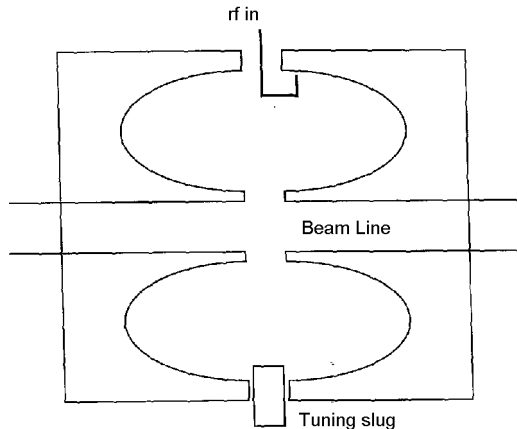


Figure 5.5 The prebuncher at LANSCE

The buncher itself is simply a resonant cavity that establishes an alternating potential across a gap in the beam line. In the LANSCE accelerator there are two bunchers between the ion generator and the drift tube linac. Both are driven at 201 MHz. The rf power for the two bunchers are in phase coherence with the rest of the 201 MHz rf system (DTL rf system). The first buncher is excited with relatively low power of 10-20 Watts, the second is excited with several hundred Watts.

### 5.5 Drift Tube Linac

The first section of the linac is of drift tube type developed from the original Alvarez design (figure 3.5). It uses four successive copper-lined tanks with drift tubes mounted along their axes to accelerate the beams from 750 keV to 100 MeV. An alternating electric field is set up in the tanks at a frequency of 201.25 MHz. The basic problem is to arrange for the particle bunches to reach each cavity at the exact time at which the rf fields is of the right sign and proper amplitude. This is done in the Alvarez linac by letting the particle bunches "drift" inside the tubes while the rf field goes through the decelerating part of its cycle (figure 5.6).

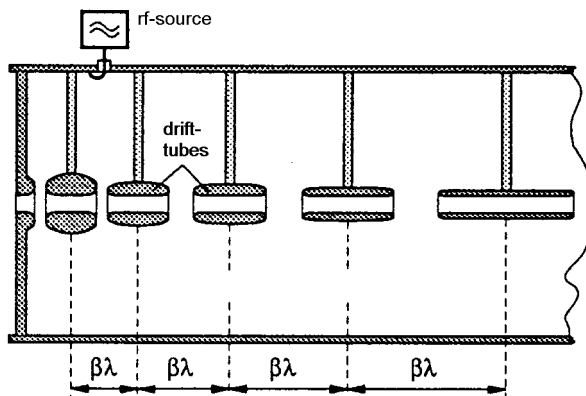


Figure 5.6 Illustration of drift tubes [12]

Electric field accelerates particles while they are in gap between drift tubes. Drift tubes shield particles while the field reverses direction.

In practice the cavities or cells at LANSCE are grouped together into four separate series known as a tank. There are a number of modes in which the particles can be accelerated in these tanks. In the  $2\pi$  mode (figure 5.7a), which is normally employed in Alvarez accelerators, the field is in the same direction in each cell at any given moment (standing wave). In the  $\pi$  mode, the fields are oppositely directed in adjacent cells (figure 5.7b). In the  $\pi/2$  mode the field also alternates in direction but in addition every other cell contains no field.

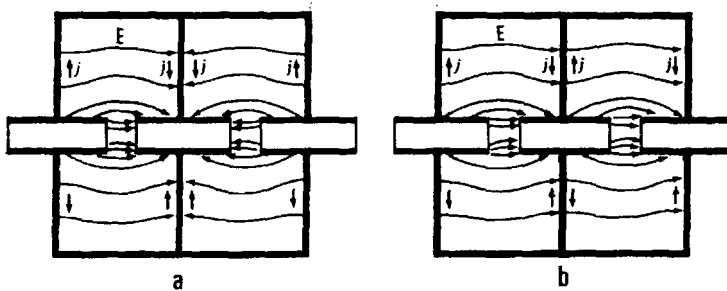


Figure 5.7 a)  $\pi$  mode and b)  $2\pi$  mode

At LANSCE resonant posts are placed facing the drift tubes, they will transform the mode of operation of the drift tube linac from the conventional  $2\pi$  mode to something which approximates a  $\pi/2$  mode. By this, a way has been found to stabilize the beam, by a factor of 100. However, although it works very well for low energy protons, the drift tubes must become ever longer as the particle velocity increases, and correspondingly more of the rf power is then dissipated in the copper walls of the tanks and drift tubes. Another accelerating structure is necessary if one is to go much beyond 100 MeV at high duty factor.

## 5.6 Transition Region

The beam transport section between the Drift Tube Linac and the Side Coupled Linac is called the Transition Region (TR). The main functions of the Transition Region is to:

- 1) Transversely match the output H+ and H- beams from the DTL to the acceptance of the SCL.
- 2) To increase the flight path of the H- beam by 8 cm compared with the H+ beam so that the H- particles enter the SCL at an instant one-half 805 MHz rf cycle later than the H+ particles [13].

The TR have three beam lines. These lines are called (from top to bottom in Figure 5.8) the short track (H+), the straight through section, and the long track (H-). Each line includes four quadrupole magnets. During normal operation, one 20° bending magnet in the beginning of the TR separates the H+ and H- beam, another 20° bending magnet at the end recombine the beams. The short track includes two bending magnets and the long track includes four bending magnets. All the bending magnets are of the same design.

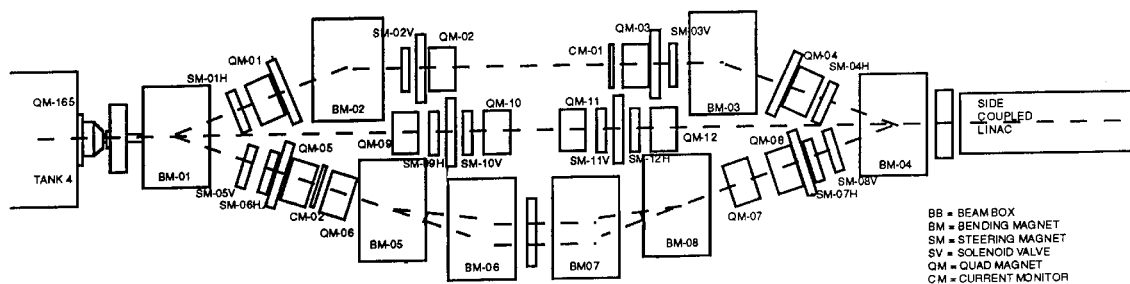


Figure 5.8 Transition Region at LANSCE [13]

## 5.7 Side Coupled Linac

The main section of the linac is a side coupled cavity system operated in the  $\pi/2$  mode at a rf frequency of 800 MHz. The side coupled linac (SCL) was developed at LANSCE over the years 1963 to 1970. The SCL allows the particles to be accelerated to high energy in much shorter distances than in the drift tube linac. With cells that are nearly enclosed instead of suspended drift tubes, the SCL is designed for maximum efficiency in space and power. Conversion of rf power to beam power is about four times more efficient in this section than in the DTL.

The unique field distribution in the  $\pi/2$  mode of operation provides a high degree of stability of the electromagnetic wave against effects due to heavy beam loading and manufacturing imperfections. The combination of efficiency and field stability allow high duty factor. The problem with the  $\pi/2$  mode, is that every other cavity carries no field and the accelerator is likely to be twice as long as a conventional one reaching the same energy.

From the mathematical model [14], it is realized that the  $\pi/2$  mode of operation allows a multitude of possible cavity configurations to be considered, all with the same excellent "mode" characteristics (see figure 5.9).

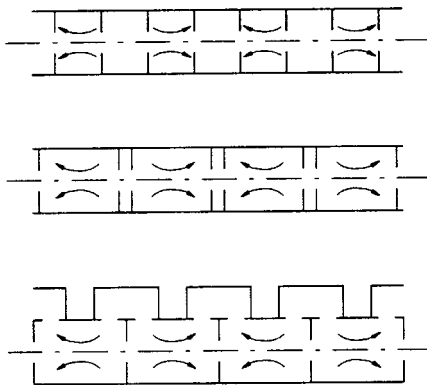


Figure 5.9 Illustration of different  $\pi/2$  mode structures [12]

All structures are excited in the  $\pi/2$  mode. Obviously the field free cavity may be completely moved off beam line.

In fact, the odd (empty) cavity may be completely moved off beam line. Of course, they still remain coupled via slots to the field carrying cavities.

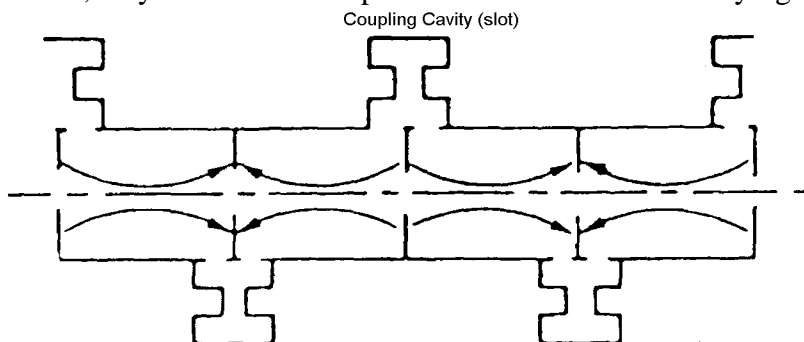


Figure 5.10 Side Coupled structure in  $\pi/2$  mode



This scheme has substantial advantages, namely (a) the a maximum length along the beam line is available for accelerating fields, (b) only small slots at the outer wall are required for coupling, allowing large amounts of freedom to design the online cavity for maximum efficiency, (c) the coupled cavity stores very little energy and thus little attention need to be paid to its geometry.

At LANSCE, the beam is accelerated in a series of 4962 resonant cavities, powered through coupling cavities on the side of the structure. The physical spacing between centers of resonant cavities increases steadily with increasing velocity of the particles, so each of the cavities has a different length. From a cell length of about 10 cm at 100 MeV to 20 cm at 800 MeV. A group of individual cells (12-18) are brazed into a section ranging from 1.5-2.5 m, including the side cavities, which forms a single vacuum-tight unit. A total of 352 such multi cell sections are spaced along the main linac. Various beam handling devices are mounted in the space between sections, such as quadrupole focusing magnets, beam monitors, and other control systems.

## 5.8 Switchyard

At the end of the linac the beams enter a beam switchyard in which a variety of focusing and deflecting magnets and other beam handling equipments are located. The beams are separated, focused, and diverted into the final beam lines and experimental areas. Deflection magnets provide simultaneous but separated H<sup>+</sup> and H<sup>-</sup> beams. A large switchyard kicker magnet deflects the H<sup>-</sup> beam by 1.2° to the Proton Storage Ring or Line X. The H<sup>+</sup> beam is deflected upwards and then into Line A.

## 5.9 Proton Storage Ring

The 30 m in diameter storage ring is located under ground and it became operable in April 1985. The Proton Storage Ring (PSR) acts as a bunch compressor, it converts the long beam pulses into short, intense proton pulses that provide the capability for precise neutron time-of-flight measurements. The Proton Storage Ring does not accelerate the particles. It compresses the 750 μs H<sup>-</sup> proton pulses from the accelerator into pulses about three thousand times shorter. These protons are used to produce neutrons in a target by spallation in either Manuel Jr. Lujan Neutron Scattering Center or the Weapons Neutron Research Center.

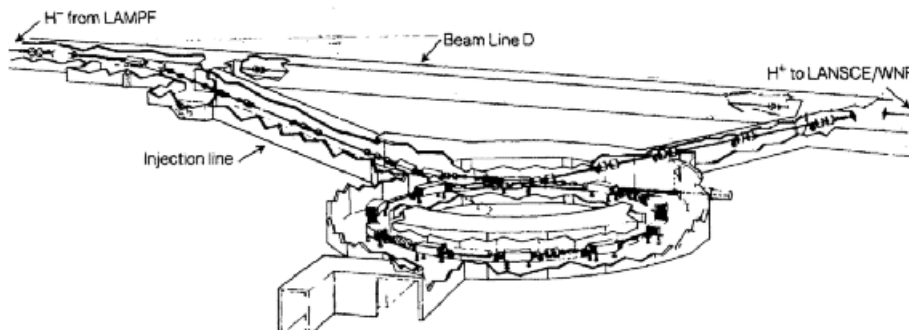


Figure 5.11 The Proton Storage Ring at LANSCE

### **5.10 Manuel Jr. Neutron Scattering Center**

The Manuel Jr. Neutron Scattering Center (Lujan) is a high power, pulsed source of spallation neutrons that is used in condensed matter science, nuclear physics, and nuclear applications. Neutrons are produced when the proton beam impinges on a tungsten target. Moderators adjacent to the target is used to slow down neutrons. Lujan includes 16 neutron flight paths [15].

### **5.11 Weapons Neutron Research Center**

In the Weapons Neutron Research Center (WNR) two target areas (target 2 and 4) are available, each with several flight paths aimed at bare target locations. Neutron beams with energies ranging from about 0.1 MeV to 600 MeV are produced in Target 4 (an unmoderated tungsten spallation source). In the Target-2 area (Blue Room) samples can be exposed to the direct 800 MeV proton beam. A H- chopper is installed to allow isolated micropulses of beam to be delivered to these targets. The WNR complex is used for national security research and basic nuclear physics research.

## 6 LANSCE Accelerator operations

### 6.1 Introduction

During operation beam delivery is measured by current monitors near the target. If the beam current for some reason is below a threshold current the beam is considered as interrupted. The event/trip generates a loss in scheduled beam time, commonly called down time. The underlying cause of the event is appointed a down time assignment, this is done by the operator (Beam Delivery Team) situated in the Central Control Room. The down time assignment is recorded in the logbook. An automated system extracts the down time assignments from the logbook and enter them along with current monitor data in a database (Excel spreadsheet). One database exists for each beam line or target area. From the database further down time statistics are obtained.

### 6.2 Down time assignment

The operator or the Beam Delivery Team is situated in Central Control Room (CCR). Whenever a beam loss occurs the operator appoints the trip a down time assignment. The computer presents a menu to the operator that requires entries of down time assignments. The computer also prompts the operator for comments on the cause of the beam trip.

Every down time assignment includes an Area assignment and a System assignment. A single set of Area and System categories are available to choose from. A list of System categories is presented in table 6.1.

The Area assignment indicates the geographical location in the accelerator complex where the failure occurred. The System assignment defines the kind of equipment responsible for the down time [16].

Table 6.1 System Definitions Used for Down Time Assignment [16]

SYSTEM	DEFINITION
201	201 MHz Radio Frequency System: pad power supplies, capacitor rooms, amplifier systems, interlocks (flow, temp, etc.), resonance controllers and valves.
805	805 MHz Radio Frequency System: pad power supplies, capacitor rooms, amplifier systems, klystron systems, interlocks (flow, temp, etc.), resonance controllers and valves. Includes prebunchers (but excludes Proton Storage Ring buncher.)
CTRL-HW	Control HardWare: Computer, control system and network hardware. Includes hardware on VAXes, Suns, remotes, CAMAC, VME, Remote Instrument and Control Electronic (RICE), Analog Digital System (ADS), networks, console equipment, printers, knobs, etc. Excludes Master Timer.
CTRL-SW	Control Software: Computer, control system and network software. Includes software on VAXes, Suns and remotes.
DIAG	Diagnostics: Problems with harps, wire scanners, current monitors, Delta T hardware, strippers, scrapers, emittance systems, and Beam Position Monitors.
DC-MAG	DC Magnets: Magnets, winding, DC cabling, flow and temperature switches, vacuum and water leaks, magnet water strainers. Does not include power supplies.
DC-MAG-PS	DC Magnet Power Supplies: electronics, trips, interlocks (flow, ripple, etc.), water leaks.
EXPT	Experimenter: Flight paths, shutters and secondary beam lines, experimenter requested beam-off. <i>Further clarification TBS by M. Zumbro.</i>
FACILITY	Facility problems not elsewhere on the list (water main leaks, compressed air, natural gas, etc.)

HVAC	Heating, Ventilation and Air Conditioning system problems.
INJECTOR	Ion sources, ion source support equipment, Cockcroft-Walton generator. Includes ion source power supplies, 80KV/670KV/750KV columns and power supplies.
INTLKS	Interlocks: Fast Protect, Run Permit, Hard Ware Transmission Monitor, Loss Monitors and Area Protect problems. Weekly Radiation Security System (RSS) checks. Interlock checks during scheduled production that are not required by an RSS trip. Failures of interlock hardware. If an RSS trip report is required, see RSS-TRIP.
OTHER	Cause is known but does not fit in above categories. Use comments to identify.
POWER	Site power, the AC electrical distribution system for 110V and above. Includes outlets, breaker failures, power line surges, etc.
PULS-PWR	Pulsed Power System: Kickers, Ring buncher, deflectors, inflector, choppers and their related power supplies, local controls and modulators.
RSS-TRIP	Radiation Security System (RSS) trips: RSS and Personal Security System (PSS) trips. E.g. SCRAM switch actuation, doors rattled, high spill on gamma detectors, current detector sees too high current, etc. Anything requiring an RSS trip report. RSS-TRIP is not part of INTLKS because an RSS trip is an important safety issue.
TARGETS	All production targets, target boxes, beam stops, proton inserts, degraders, isotope stringers and foils. Includes flow and temperature interlocks and water and vacuum leaks.
TIMING	Problems with Master Timer and timing signal distribution.
TUNE-RECOVERY	Tuning other than TUNE-UP. Spill. High losses. Off-energy beam, micropulse contamination, off-center beam at Lujan target, etc.
TUNING	Intentional tuning to bring beam to production status. Does not include tuning time require to recover from an equipment problem. Typically used for recovery from inter-cycle breaks and scheduled maintenance periods. ( <i>This system assignment was abandoned in 1996, hence only assignments made before 1997 may include "tuning".</i> )
TUNE-UP	Tuning to bring beam to production status after scheduled down-time periods such as inter-cycle breaks and maintenance days. Tuning to recover after down-time caused by equipment failure is attributed to the failed system.
UNKNOWN	Cause of down-time cannot be identified.
VACUUM	Vacuum system: Vacuum pumps, pump power supplies, roughing packages, valves, instrumentation, controls, pipes, flanges. Does not include leaks in individual components or loads such as magnets, targets, etc.
WATER	Cooling water systems: pumps, pump controls, makeup water, valves, pipes, heat exchanges. Does not include leaks and flow problems in individual cooled components such as magnets, amplifiers, cavities, etc. unless problem is caused by variations or limits in water system.

Usually the System assignment identifies the personnel responsible for attending the failure, although the same crew may be responsible for several Systems. In general, the assignment should point to the System to "cost effectively make the problem go away", not to the first-out system. This may in some cases result in misleading down time assignment. For example, if the prebuncher malfunctions the System assignment in the logbook is 805 since the 805 rf personnel is responsible for the prebuncher, but the prebuncher is actually driven by the 201 rf system and the correct assignment should be 201.

### 6.3 Databases

Beam trips that occur within the frame of scheduled production are recorded in the databases. Events affecting the beam that take place outside scheduled production may be available in the logbook but this information is not included in the databases.

Depending on which beam line or target the trip affects beam trips are sorted into different databases (Excel spreadsheets). Subsequently, beam trips are classified into five databases, namely:

*Table 6.2 Description of Databases*

Database	Description
<b>Area A</b>	Includes all beam trips affecting the H+ beam line from the H+ injector to target Area A.
<b>Lujan</b>	Includes beam trips affecting the H- beam when delivered to Manuel Jr. Neutron Scattering Center.
<b>WNR T2</b>	Includes beam trips affecting the H- beam when delivered to Weapons Neutron Research Center Target 2.
<b>WNR T4</b>	Includes beam trips affecting the H- beam when delivered to Weapons Neutron Research Center Target 4.
<b>Line X</b>	Includes beam trips affecting the H- beam when delivered to Line X.

A schematic overview in table 6.3 presents which accelerator section is an integral part of each database.

*Table 6.3 Schematic overview of equipment and beam lines corresponding to each database*

*LEBT - Low Energy Beam Transport located after the injector, before the Drift Tube Linac (DTL). In this table the Linac embraces all equipment associated with the Drift Tube Linac, Transition Region, and the Side Coupled Linac.*

Database	Accelerator Section								
	H+ Injector	H- Injector	H+ LEBT	H- LEBT	Linac	Line A	Line D	Line X	PSR
<b>Area A</b>	X		X		X	X			
<b>Lujan</b>		X		X	X		X		X
<b>WNR T2</b>		X		X	X		X		X
<b>WNR T4</b>		X		X	X		X		X
<b>Line X</b>		X		X	X			X	

Table 6.3 gives information in which database (or databases) a particular failure is recorded. For example, a failure in the H+ injector will only be recorded in the Area A database. Where a failure in the Linac will be recorded in all databases since all beam lines utilize the Linac section. **This allows for overlapping of beam trips in the databases.** Identical trips may be recorded in several databases. This must be taken in consideration when merging of databases is in question.

## 6.4 Beam Schedule

Ahead of time a beam schedule has been organized with respect to time-sharing between experiments, beam intensity, and beam energy. An overall schedule of commissioned beam time between different beam lines is set out.

Scheduled operation at LANSCE is divided into run cycles. During scheduled operation, the accelerator is operated almost 24 hours per day for an entire run cycle with only a few scheduled breaks. A run cycle is maintained for approximately 5-6 weeks

(800-1000 hours). In table 6.4 run cycles and beam schedules for the H- beam are presented.

Table 6.4 Run cycles and scheduled H- beam time

Year	Cycle	Scheduled Time [hours]
1993	63	648
	64	636
	65	549
1994	66	Not Scheduled
	67	Not Scheduled
	68	Not Scheduled
1995	69	1366
	70	998
1996	71	964
	72	1062
	73	654
1997	74	755
	75	956
	76	752

Between run cycles two or three maintenance days are scheduled. Usually there are three run cycles per year. An extended maintenance period is initiated at the end of the last run cycle each year. In figure 6.1 an illustration of the scheduled H- production for 1996 is displayed.

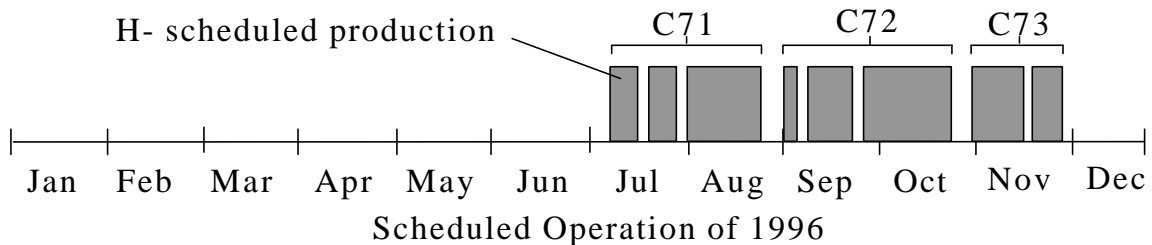


Figure 6.1 Illustration of Scheduled H- Production at LANSCE

Gray boxes are scheduled operation, white spaces in between represent maintenance period.

The LANSCE accelerator delivers two beams (H+ and H-) to different target areas and each target area has a separate schedule. In other words, Area A, which receives the intense H+ beam from Line A has a different schedule compared to the Lujan or WNR target facility which receives the H- beam via Line D.

## 7 Overall LANSCE Reliability

### 7.1 Introduction

In this chapter operational statistics of the entire LANSCE accelerator facility is presented. The overall reliability/availability of the accelerator is analyzed, all systems are included. For the most part, the reliability for cycles 71-76 is discussed, but some early reliability history will also be presented. A more penetrating reliability analysis for individual subsystems and components is performed in chapter 8.

The Area A and the Lujan databases for Cycles 71-76 (1996-97 operations) are used for all statistics.

#### Main reasons for utilization of Area A and Lujan databases are:

- At a rough estimate, Area A and Lujan covers >95% of all beam trips and scheduled beam time for 1996-97 operation.
- Area A includes all beam trips common to the powerful H<sup>+</sup> beam line.
- Lujan includes trips common to the H<sup>-</sup> beam line and the Proton Storage Ring.
- During 1996-97, commissioned beam time was longest for Area A and Lujan
- Most beam trips common to Lujan and WNR are overlapping. On comparison, only a small fraction of beam trips are unique for each beam line. Therefore it is little gain in processing the WNR database as well.
- Line X was hardly ever in operation during 1996-97.

Trips that arise in the Linac (DTL and SCL) structure will overlap in both databases. But, results are treated separately and comparison of beam trips is not necessary.

### 7.2 Definitions

down time - any unscheduled time recorded in the logbook when beam current is below a threshold current. For 1997 the threshold current was one-half the scheduled current.

availability - time beam was delivered at or above a threshold current divided by the scheduled time.

### 7.3 Operational statistics

#### 7.3.1 H<sup>+</sup> Beam line (Area A)

In this section, the distribution of beam trips and down time of the H<sup>+</sup> beam line are presented. The analysis considers accelerator operation during scheduled H<sup>+</sup> production for 1997 (Cycles 74-76).

##### 7.3.1.1 H<sup>+</sup> Beam schedule

The total scheduled beam time is an important factor **-beam trips are only recorded if they occur within scheduled production**. To obtain the total scheduled beam time it is necessary to investigate the beam schedule closely. In Appendix 1, a detailed beam schedule is available for the H<sup>+</sup> beam.

For 1997, the total scheduled beam time of the H+ beam was 2870 hours. The accelerator was operated in three run cycles (cycles 74-76), scheduled production started in 18<sup>th</sup> of March and ended the 27<sup>th</sup> of July. In general, one or two scheduled interruptions took place inside each run cycle. Each of these interruptions lasted for 1-2 days. At the end of each run cycle a two-day maintenance activity was performed. In figure 7.1, a perspective on the historical operation of the H+ beam is presented.

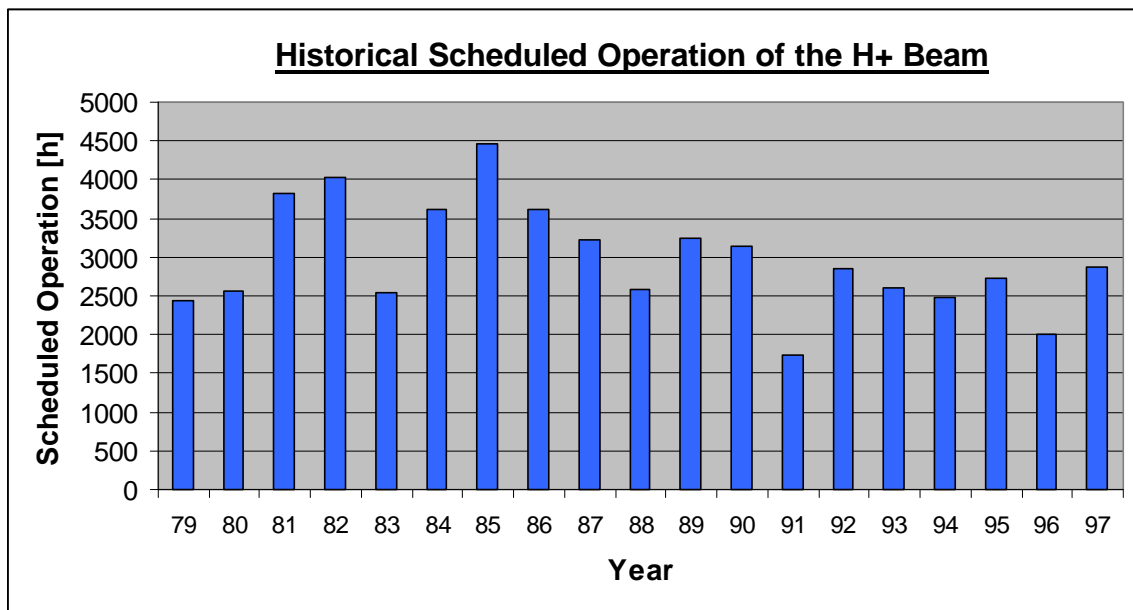


Figure 7.1 Scheduled Operation of the H+ Beam at LANSCE (1979-97) [17]

Scheduled operation is usually in the region of 2000-3000 hours per year, about 30 % of the year. In 1985, the longest schedule ever was practiced. The accelerator was commissioned for 4500 hours and it operated with normal availability (83 % in figure 7.5).

**7.3.1.2 H+ Beam statistics**

Beam trips and the distribution of down time of the H+ beam are shown and discussed.

From the Area A database, statistics of beam trips and the distribution of down time is obtained for the H+ beam. In figure 7.2 beam trips are sorted into down time intervals. In order to explicitly show the influence of the injector an extra column has been added which does not include any trips caused by the H+ injector.



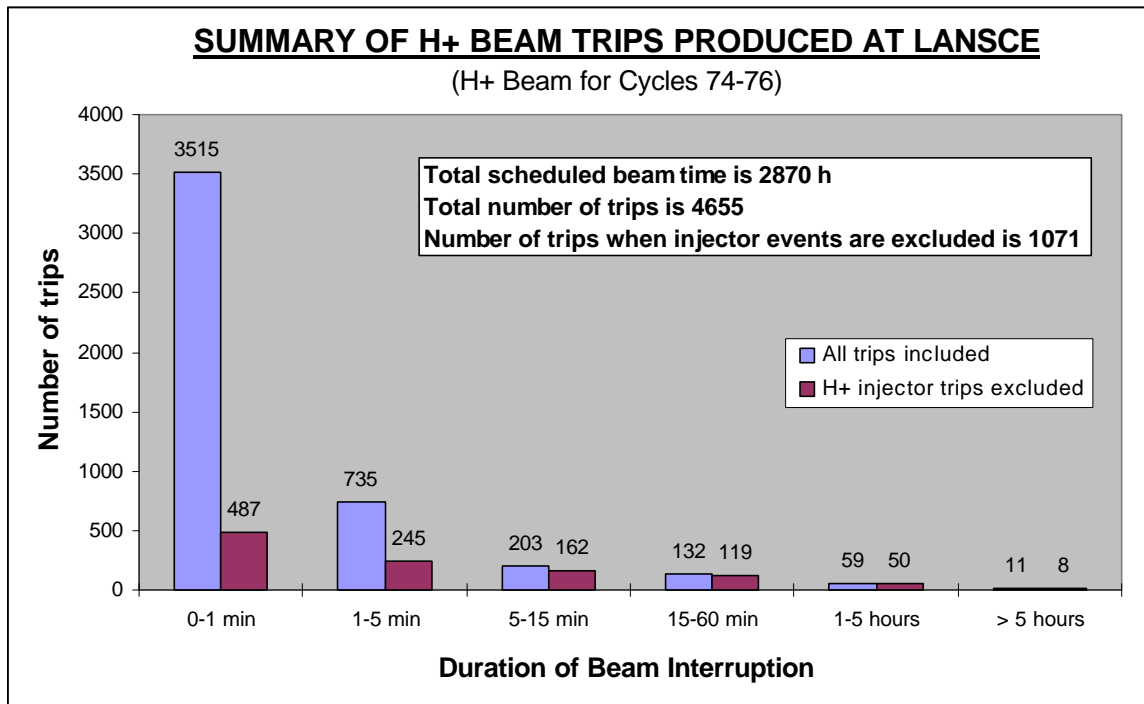


Figure 7.2 Summary of H+ Beam trips produced at LANSCE for Cycles 74-76

From figure 7.2 it is obvious that the H+ injector is causing many short beam interruptions. Using the numbers from figure 7.2 the average number of H+ trips per hour may be calculated:

**Average number of H+ trips per hour:**

$$4655/2870 = 1.62 \text{ trips/h}$$

The most common injector failure is arcing in the high voltage column. This may be due to a contaminated column, bad vacuum, dust on the column surface etc. The characteristic of the injector trip is the interruption length. It is shorter than 1 min, usually in the order of 10-20 seconds, the time it takes to reset the trip and re-energize the generator. In each downtime interval the three most dominating failures are presented in table 7.1. The Systems are ordered in the fraction of total number of trips the system is responsible for in each downtime interval (for System references see table 6.1).

H+ Beam Interruption length						
	Short		Medium		Long	
No	0-1 min	2-5 min	5-15 min	15-60 min	1-5 h	>5 h
1	Injector (86%)	Injector (67%)	Injector (20%)	805 RF (37%)	Injector (15%)	Targets (36%)
2	Unknown (3%)	201 RF (11%)	201 RF (18%)	201 RF (11%)	Targets (14%)	Injector (27%)
3	Tune-Recovery (3%)	Interlocks (4%)	805 RF (16%)	Injector (10%)	805 RF (12%)	805 RF (18%)

Table 7.1 Predominant H+ failures in each downtime interval

The Systems are ordered after the fraction of trips the system is responsible for. For example, in the downtime interval 15-60 min the 805 RF System is responsible for 37% of all trips.

In the interval of 0-1 min the injector is responsible for almost 90% of all H+ beam interruptions. For medium down times, the fraction of trips produced by the injector is much smaller. Some short trips were unknown, since they were short they were, at the time of occurrence, not investigated thoroughly. On the other hand, it was possible to assign a known system for all other trips with down time longer than 5 minutes. At medium down times (>5 min) the RF System contributes more to the total number of trips. In fact, the 805 RF System (includes the klystron system) dominates the failure cause in the interval of 15-60 minutes. For long down times the Targets and the Injector are responsible for a large portion of the trips. The injector was shutdown in order to investigate the reason for the short injector trips. Only a few trips with long down time occurs and a system causing only a small number of long trips is rather dominating.

In figure 7.3 all trips are classified into systems. The systems are presented in order of importance, starting at left-hand side with the System responsible for most of the trips.

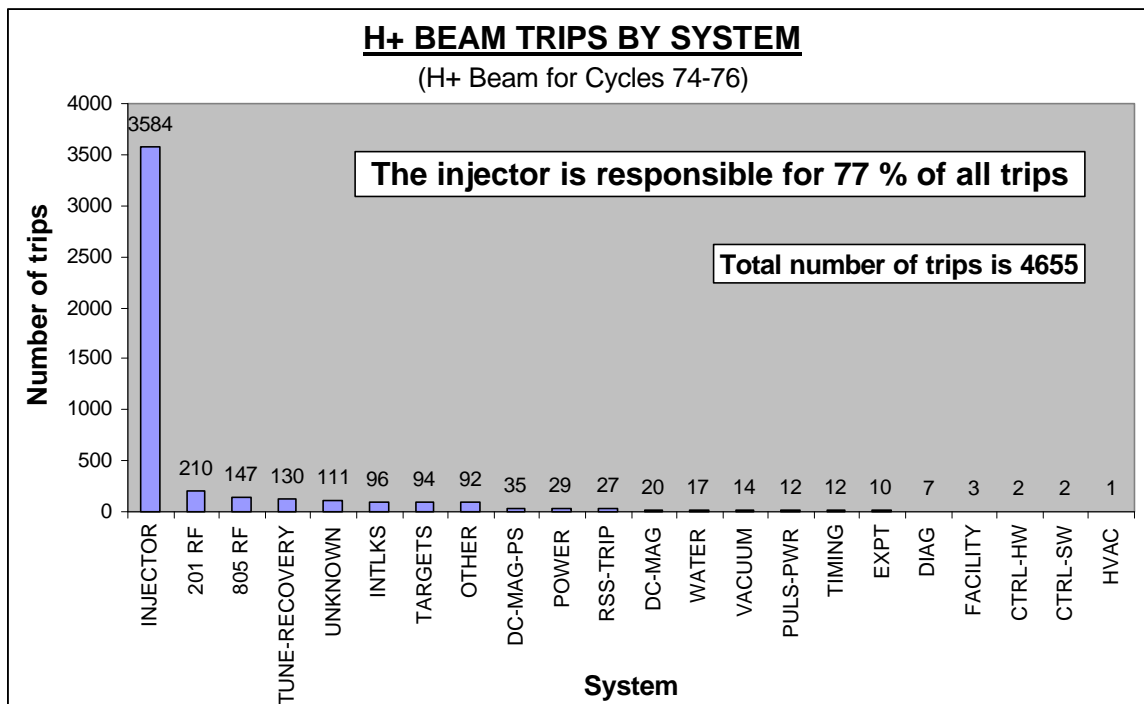


Figure 7.3 H+ Beam trips produced by each System

Again, it is obvious that the injector is the origin for most of the trips.

**Predominant failure causes of the H+ beam are:**

- 1) H+ Injector (77 % of all trips)
- 2) 201 RF System (5 % of all trips)
- 3) 805 RF System (3 % of all trips)

As far as now we have only looked at the number of **trips** (interruptions) each system is responsible for, another important point is the **down time**. In figure 7.4, the total down time produced by each system is presented.

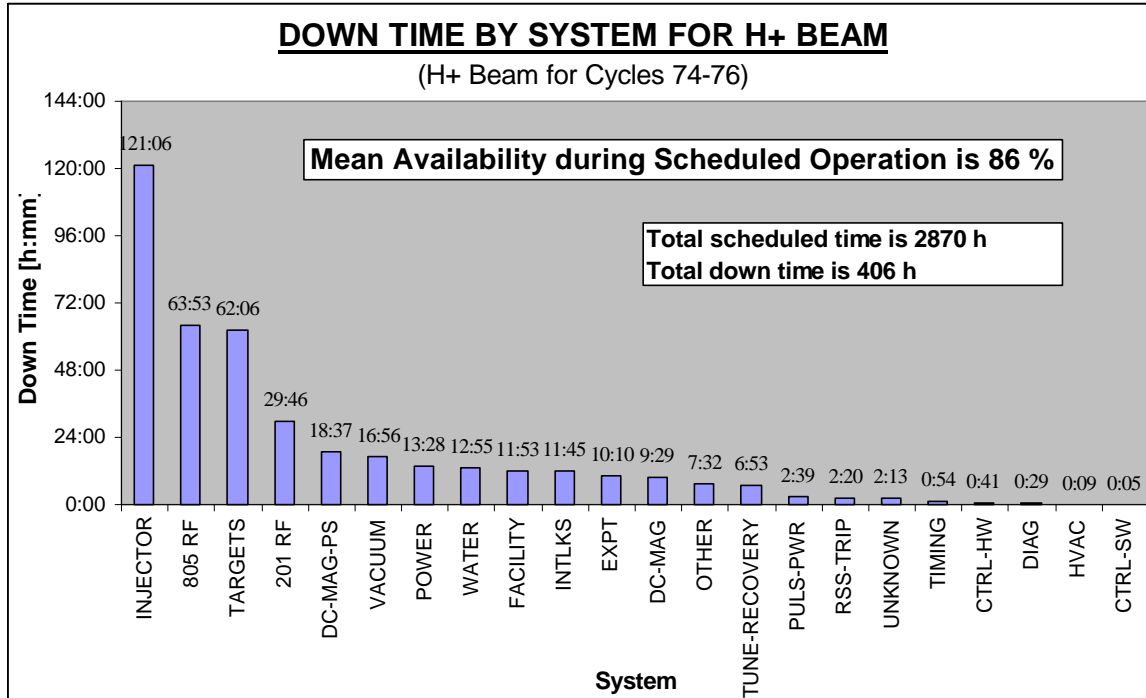


Figure 7.4 H+ down time produced by each System

Now the result looks a little bit different. While the injector is responsible for 77% of all trips it is "only" producing 30% of the down time. The 805 RF System is generating 3 % of the trips but is accountable for 16 % of the down time. This is a direct consequence of the fact that the injector is producing mainly short interruptions while the 805 RF System generates trips with long down time (15-60 min). Most of the H+ down time is concentrated to a few Systems, namely:

**The three largest contributors of H+ down time are:**

- 1) H+ Injector (30 % of all down time)
- 2) 805 RF System (16 %)
- 3) Targets (15 %)

**The availability of the accelerator is defined as:**

$$Availability = Total\ Up\ Time\ [h] / Scheduled\ Beam\ Time\ [h]$$

The availability is a measure of how large fraction of the scheduled beam time the accelerator is actually operating. Another interpretation would be what the probability is for a functioning accelerator at a given instant of time.

**For 1997, the availability of the H+ Beam at LANSCE was:**

$$H+ Availability = (2870-406)/2870 = 86 \%$$

It must be noted that the availability only measures the availability of the accelerator during **scheduled operation**. A common misunderstanding is that the availability of the machine is the availability over the whole year. If that was the case, the availability of LANSCE for 1997 would be  $(2870-406)/8760 = 28\%$ . A large fraction of the year the accelerator is not scheduled due to maintenance activities. In figure 7.5 historical H+ availability data for 1979-97 is presented [17].

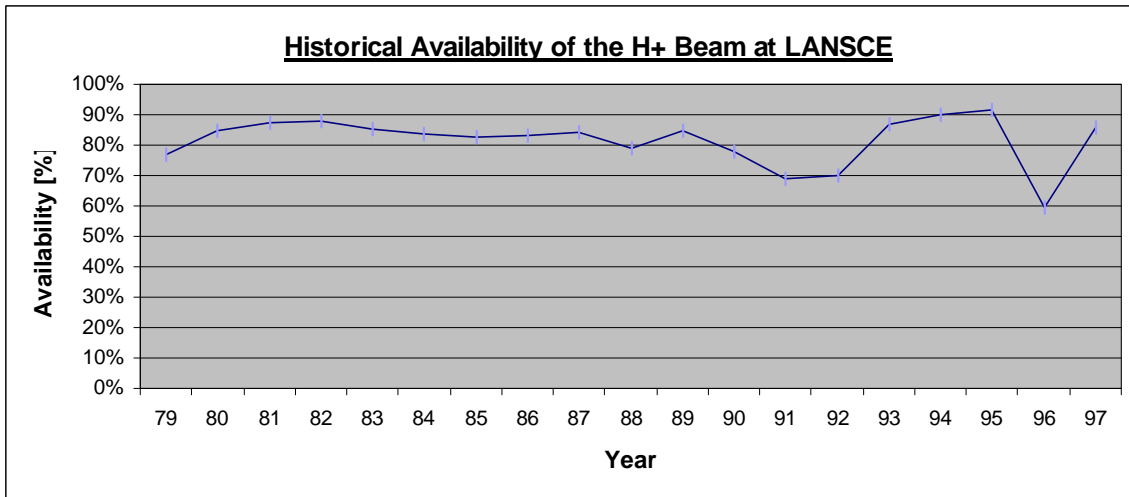


Figure 7.5 Perspective on the historical Availability of the H+ Beam at LANSCE (1979-97) [17]

In 1996, the availability experienced a decline due to a single water leak in one of the targets, otherwise the availability of LANSCE is usually in the region of 80-90 %. This level of availability is also in good agreement with other accelerators, for example at SLAC:

Accelerator	Year	Availability
SLC	1993	82.8 %
SLC	1994	80.7 %
SLC	1996	79.0 %

Table 7.2 Availability of the Stanford Linear Collider (SLC) ref SLAC Accelerator operations report.

### 7.3.2 H- Beam line (Lujan)

Similar analysis of beam trips and down time has been done for the H- beam. Operational statistics of the H- beam line to Lujan Neutron Scattering Center are investigated. The H- beam is analyzed during scheduled production for 1996-97 (Cycles 71-76).

#### 7.3.2.1 H- Beam schedule

During 1996 the H- beam was operated in three run cycles (Cycles 71-73). Cycle 71 started at the 10<sup>th</sup> of July and Cycle 73 ended at the 28<sup>th</sup> of November. Between each

run cycle the beam was off schedule for 4-8 days due to maintenance periods. Within each run cycle the beam was also off for shorter maintenance activities. The total scheduled H- beam time for 1996 was 2681 h.

In 1997 the H- beam was also operated in three run cycles (Cycles 74-76). Cycle 74 was initiated at the 7<sup>th</sup> of March and Cycle 76 ended at the 24<sup>th</sup> of July. During 1997 the H- beam was scheduled for 2463 h.

Since this section investigates the reliability for both 1996 and 1997 the important beam time is the total scheduled time. For 1996 and 1997 the total scheduled time was 5144 h. In Appendix 1 a detailed schedule of the H- beam during 1996-97 is available.

In figure 7.7 some historical scheduling information of the H- beam line at LANSCE is presented.

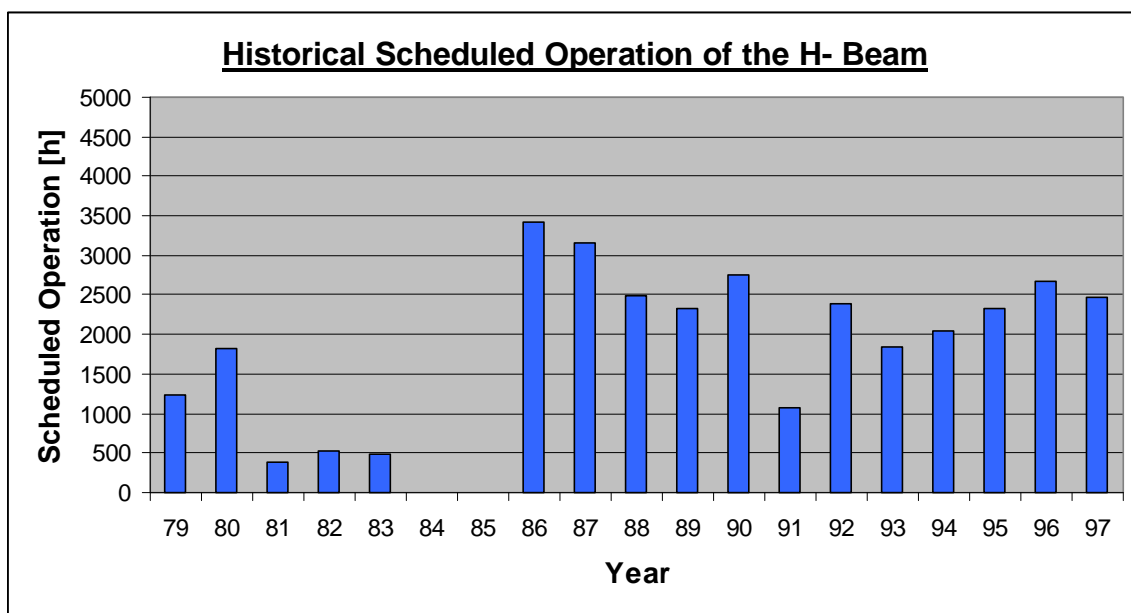


Figure 7.7 Scheduled Operation of the H- Beam at LANSCE (1979-97) [17]

Historically the H- beam has been scheduled less time than the H+ beam (compare with figure 7.1). During 1984-85 the Proton Storage Ring was under construction and hence the H- beam was not scheduled at all.

**7.3.2.2 H- Beam statistics**

The overall statistics of beam trips and down time produced by the H- beam are presented.

In fig 7.8 a summary of all beam trips is shown. An extra column has been added in order to point out the influence of the injector.

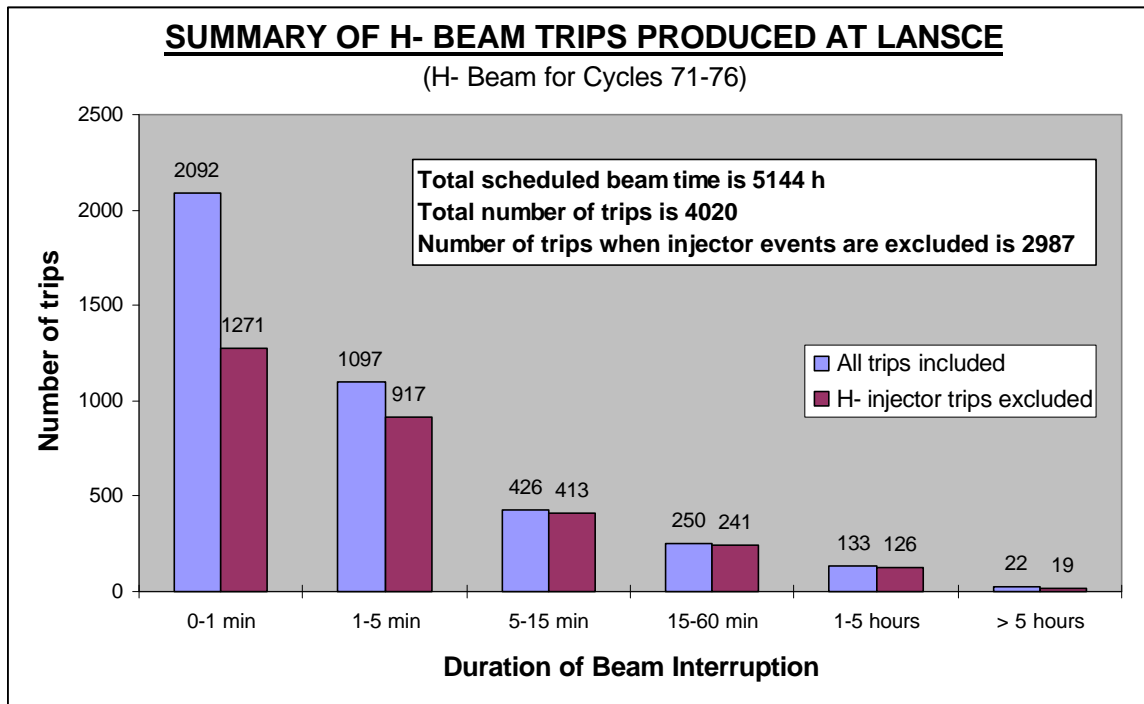


Figure 7.8 Summary of H- Beam Trips produced at LANSCE during 1996-97

The H- beam is more reliable than the H+ beam (compare with figure 7.2). This is mainly due to a more stable H- injector.

**Average number of H- trips per hour:**

$$4020/5144 = 0.78 \text{ trips/h}$$

In table 7.3 the predominant failures in each down time interval are presented.

H- Beam Interruption length						
	Short		Medium		Long	
No	0-1 min	2-5 min	5-15 min	15-60 min	1-5 h	>5 h
1	Injector (40%)	Other (21%)	805 RF (19%)	Targets (17%)	Targets (16%)	Mag PS(18%)
2	Interlocks (12%)	Injector (16%)	Other (13%)	805 RF (13%)	Water (11%)	Vacuum(18%)
3	Unknown (10%)	201 RF (11%)	Rss-trip(12%)	Rss-trip (9%)	Mag PS (9%)	Injector (14%)

Table 7.3 Predominant H- failures in each down time interval

The Systems are ordered after the fraction of trips the system is responsible for in each interval. For example, in the down time interval 5-15 min the 805 RF System is responsible for 19% of all interruptions.

In the interval 0-1 min the H- injector is "only" responsible for 40% of the trips. The H- injector produces only a few long down times. Again, as in the case with the H+ beam, the 805 RF System is responsible for many trips in the medium down time interval (5-60 min). It is natural these trips occur to both beams since both beam lines utilize the same RF System. In the medium and long down time interval the targets are troublesome. Many long H- trips occurred due to problems with the target moderator. A single Magnet

Power Supply in the Proton Storage Ring was causing very long interruptions during 1996.

In figure 7.9 all trips are classified into systems. The systems are presented in order of importance, starting at the leftmost with the system responsible for most of the trips. The diagram does not consider the duration of the interruption.

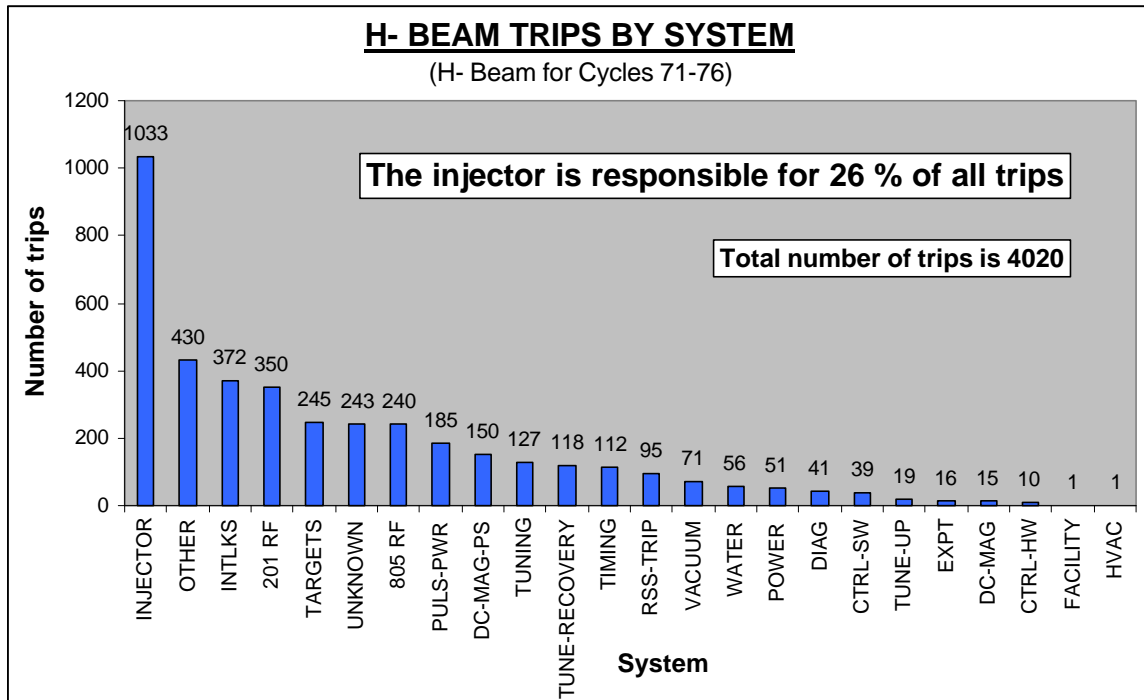


Figure 7.9 H- Beam trips produced by each System

**Predominant failure causes of the H- beam are:**

- 1) H- Injector (26% of all trips)
- 2) Other (11%)
- 3) Interlocks (9%)

Even though the H- injector is still the largest producer of trips (26% of all trips) it is obviously much more reliable than the H+ injector (77% of all trips). The assignment "Other" is responsible for 11 % of the trips. In most of these trips the accelerator is not subject to any actual component failure. Sometimes beam measurements are performed which prevents the beam from reaching the target. 9% of all H- beam trips are assigned "Interlocks". The underlying cause of these interruptions are sometimes unknown. For example, a loss monitor detects a high beam spill in the Proton Storage Ring and subsequently the Fast Protect System shuts the accelerator off, but the underlying cause of the beam spill is unknown.

In figure 7.10 the total down time produced by each system is displayed. The systems are presented in order of importance, starting with the largest contributor of down time on the left-hand side.

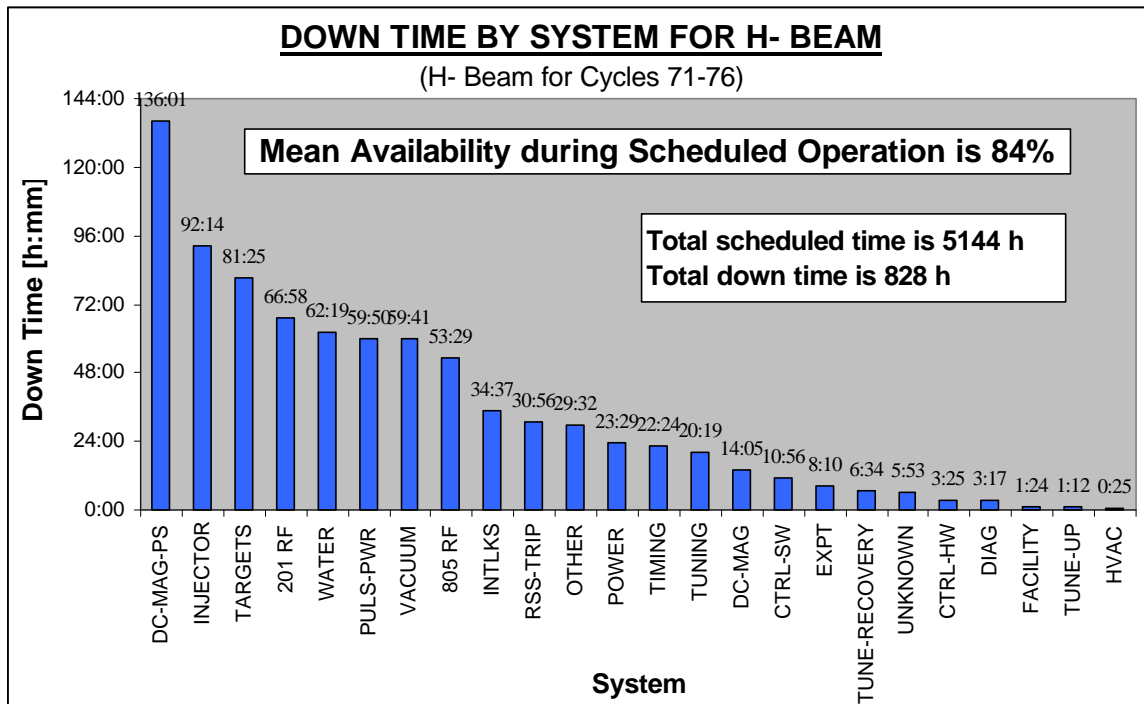


Figure 7.10 H- down time produced by each System

The H- down time is more evenly distributed among several systems in comparison with the H+ beam (see figure 7.4). It is interesting to note that the H- injector is not causing as much down time even though it is without doubt the largest producer of trips (see figure 7.9). Instead the Magnet Power Supply system is clearly the largest contributor of down time. During 1996 a single power supply in the Proton Storage Ring was causing very long interruptions (days). For that reason, the event may be regarded as extraordinary, it is not likely that the Magnet Power Supply System will cause a similar failure the following year. On the other hand, it is not unusual that one or a few extraordinary failures are responsible for a large portion of the total down time. For example, during 1996 the H+ beam was off for several days due to a single water leak in the target. Therefore, it is not justified to exclude the extraordinary down time, since they do occur, but the Magnet Power Supply System will not always be predominant. Almost any System may be responsible for a failure which causes long down time.

**For 1996 and 1997, the largest contributors of H- down time were:**

- 1) Magnet Power Supplies (16 % of all down time)
- 2) H- Injector (11%)
- 3) Targets (10%)

**The Availability of the H- Beam was:**

Availability 1996 =  $(2680-449)/2680 = 83 \%$

Availability 1997 =  $(2463-379)/2463 = 85 \%$

In figure 7.11 a perspective on the historical availability of the H- beam is presented.



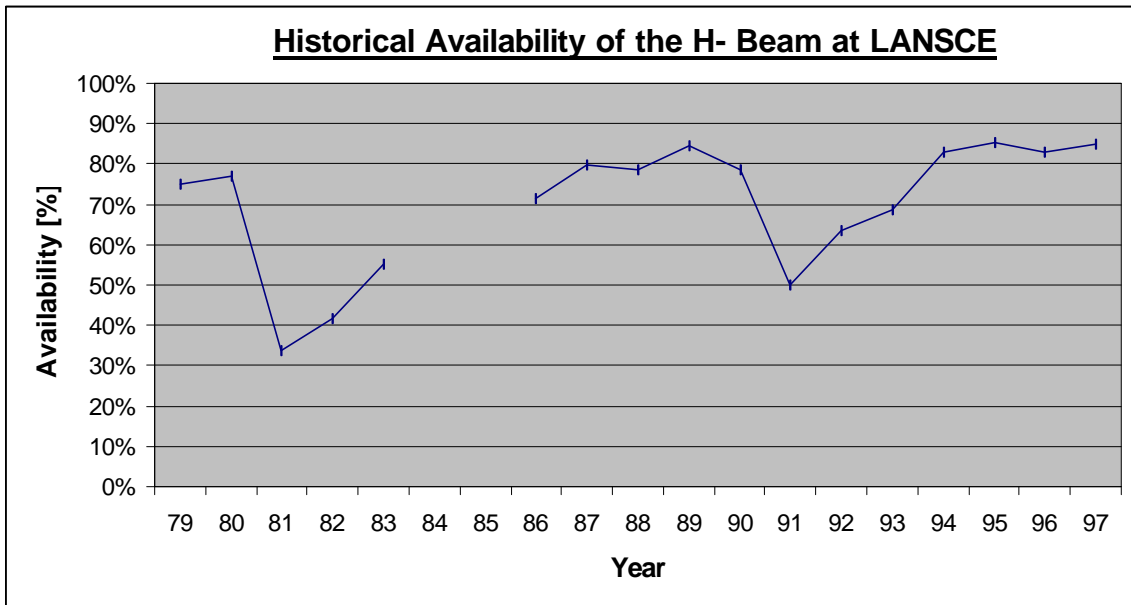


Figure 7.11 Perspective on the historical Availability of the H- Beam at LANSCE (1979-97) [17]

1984-85 the Proton Storage Ring was under construction, hence no H- beam was delivered.

Obviously the historical availability of the H- beam has changed significantly from year to year, but the last 4 years (1994-97) the availability has been in the region of 80-90 %.

### 7.3.3 Conclusions

In the overall reliability balance of the entire LANSCE accelerator, the injector is responsible for most of the trip events. For short interruptions (<1 min) the H+ injector is accountable for 90 % of all trips of the H+ beam. In other words, a more reliable injector in combination with, for example, an RFQ could substantially reduce the number of beam interruptions. For long down times (>5 min) the injector is no longer the main source of trips, but instead the RF System is the primary generator of trips. A short summary of all beam trips produced by the H+ and H- beam is presented in table 7.4.

SUMMARY OF THE LANSCE ACCELERTOR					
Beamline	Period	Cycles	Scheduled Beam Time [h]	Total number of trips	Average number of trips per hour [trips/h]
H+ Beam	1997	74-76	2870	4655	1.62
H- Beam	1996-97	71-76	5144	4020	0.78

Table 7.4 Summary of Beam Trips produced at LANSCE

One may conclude that the H+ beam experiences twice as many trips per hour than the H- beam. When operating, the H+ beam experiences almost 40 trips/day. That is mainly due to problems with the H+ injector. One should keep in mind that the injector

used at LANSCE is an electrostatic Cockcroft-Walton type injector. It is therefore justified to exclude many of its trips when using these numbers for future accelerators. Modern microwave ion sources present a significant increase in reliability. For example, the new microwave proton injector developed for the APT project proves to be very reliable. In figure results from the LEDA Injector Availability Test [9] is presented.

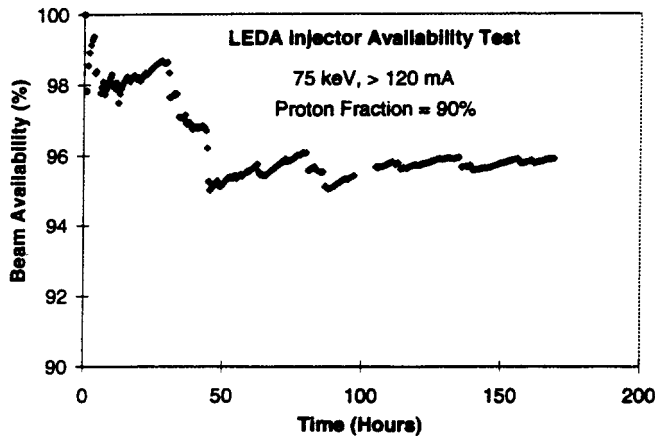


Figure 7.12 LEDA injector beam availability test

LEDA is the Low Energy Demonstration Accelerator developed to demonstrate the LEBT system for the APT accelerator [9]

Two important means when measuring reliability is the Mean Time Between Failure (MTBF) and the Mean Down Time (MDT). In Table 7.5, the Availability, MDT and MTBF for the entire accelerator are shown.

OVERALL RELIABILITY OF LANSCE				
Beamline	Classification	Availability [%]	MDT [h:mm]	MTBF [h:mm]
H+ Beam	All trips included	86 %	0:05	0:31
	Injector trips excluded	90 %	0:15	2:22
H- Beam	All trips included	84 %	0:12	1:05
	Injector trips excluded	87 %	0:14	1:35

Table 7.5 Overall Reliability of LANSCE

The overall availability of the machine is in the region of 80-90 % for both the H+ beam and the H-. This level of availability is in the same range as that observed in other accelerators. MDT for the H+ and H- are both found shorter when the injector trips are included compared to the case when the injector trips are excluded. This is obvious since the injector produces mainly short interruptions (see figure 7.2 and 7.7). MTBF for the H+ beam is significantly shorter due to the large amount of injector trips produced.

In the case where the injector trips are excluded, it is interesting to note that the MDT is almost the same for H+ and H- even though these numbers originate from two different data sets. This makes sense since both beam lines utilize, for most of their length, the same accelerating structure. Where the beam lines are separate, the components are very similar. MTBF for the H+ beam when the injector trips are excluded is longer in comparison to the MTBF for the H- beam. The reason is that the H- beam

line is more complex, since it includes the Proton Storage Ring, and hence more components are subject to failure.

**The conclusion is that upgrading the injector would result in a more stable beam with less interruptions, especially short ones. This would significantly increase the MTBF. The RF System and the Magnet Power Supplies are next in order important. Upgrading the RF System would reduce the total down time and the accelerator would gain a better availability. A shorter MDT would be also be achieved since the RF System is responsible for many long interruptions.**

## 8 Subsystem and Component Reliability

### 8.1 Introduction

In this chapter the reliability of major LANSCE accelerator systems are investigated. For this purpose, the raw data is divided into categories corresponding to individual subsystems and subsequently estimates of failure and repair rates are obtained. With the progression towards individual components, the available statistics become more and more scarce. To address this issue, the analysis combines the data from the H+ and the H- beam for six run cycles to enlarge the size of the samples.

The objective of the present data collection and analysis effort is to understand the behavior of existing operating accelerator facilities so that better, more reliable systems can be designed and built in the future. Previous work has identified the current state of the art lacking in the area of reliability database information for components typically used in rf accelerator systems, such as rf stations, rf drives, rf transport, cooling, vacuum systems, magnets, and magnet power supplies. Thus, while it is possible to use the reliability theory to model accelerator systems, the input data currently available for such analyses lacks credibility. This led to the initiation of an effort of data collection and analysis of which this study is one of the tasks. The present work examines the data set of failure events for the LANSCE accelerator facility.

### 8.2 Method

From the input data (section 8.2.1) failures associated with the following main systems were extracted and analyzed.

#### **Main Systems for which reliability analysis has been performed:**

- 1) 805 RF System
- 2) DC Magnets
- 3) Magnet Power Supplies
- 4) Pulsed Power
- 5) Water System
- 6) Vacuum System

Individual failures corresponding to these systems were thoroughly investigated with the help of logbooks, operational reports, operators, maintenance personnel and other experts in particular fields. The aim was to detect the root cause (down to component level) of each failure. Each failure was classified into subsystems (see table 8.1). Trips were then entered along with their failure causes into different databases (see table 8.2) depending on which system and subsystem the trip affected. Trips affecting the H+ and the H- beam line were merged into the same records. From the databases further reliability statistics were obtained.

#### 8.2.1 Input data

In this investigation beam trips associated with the H+ beam to Area A and the H- beam to Lujan Neutron Scattering Center are analyzed. The records obtained cover run cycles 71 through 76, over the period of 1996-97.

The first, and most time intensive task of this effort was collecting the input data. Thanks to the cooperation of the LANSCE Operations Group, a large amount of data was collected. This included the:

- 1) **Operational data records from LANSCE-6**
- 2) **Central Control Room Logbook (CCR Logbook)**
- 3) **Operations Shift Supervisor's Summary Reports (OSS Reports)**

The data includes all beam delivery trips during cycles 71-76 ordered by time of occurrence for H+ and H- beams. The Operational data records are the same records that were used for reliability calculations in Chapter 7 (Overall LANSCE Reliability). The Central Control Room logbook contains operational information such as trips, down time assignments (section 6.2), repairs and other maintenance activities in progress etc. The logbook is used to determine the underlying cause of each event down to the level of subsystem and component. At the end of each shift the shift supervisor summarizes a report. The OSS Report contains information concerning significant events during the shift. The report may include additional information that was not included in the logbook. In case the cause of the trip is uncertain, experts in particular fields are consulted to correctly classify each event

Due to the extra knowledge that was added, a few failure assignments were changed from the original assignment. Sometimes the real cause of a failure is realized several days or weeks after the failure incident. This may initially lead to an incorrect classification of the failure at the time of occurrence.

### 8.2.2 Subsystems

In order to categorize the trips, each system to be studied was broken down to subsystems. These subsystems are listed in table 8.1

*Table 8.1 Classification of Subsystems*

<b>MAIN SYSTEMS</b>	<b>SUBSYSTEMS</b>		
<b>805 RF</b>	Klystron assembly	Phase and Amplitude Control	Other
	High Voltage system	Resonance Control	Unknown
	805 Tank	Module Control	
<b>DC Magnets</b>	Magnet Hardware	Water	Vacuum
	Interlocks		
<b>Magnet Power Supplies</b>	Electronics	Transformers	Interlocks
	Capacitors	Water cooling	Unknown
<b>Pulsed Power</b>	Harmonic Buncher	Chopper	Kicker
	Deflector		
<b>Water System</b>	Water Pump	Piping	Unknown
	Other		
<b>Vacuum System</b>	Ion Pump	Piping	Unknown

A detailed description of the subsystems is outlined in section 8.4, "LANSCE Subsystems".

### 8.2.3 Database

Trips associated with the H+ and H- beam lines were merged and classified into different databases depending on what System the trip affected. Since merging of two databases "Area A" and "Lujan" occurred, trips that affected both beam lines were originally present in both databases. In other words, some trips overlapped in both databases. Therefore identical trips were recognized and only one trip was finally recorded in the merged database. Within each database trips were classified into subsystems. In table 8.2 an illustration of the final database format is presented. In this case, the 805 RF System database and trips corresponding to the Klystron Assembly are shown.

*Table 8.2 Illustration of final database*

*In this case, the database for failures in the Klystron Assembly of the 805 RF System is presented. Similar databases are compiled for each subsystem. The database contains trips that affect both the H+ and the H- beam line.*

DURATION OF BEAM INTERRUPTION			LOCATION OF FAILURE			CAUSE OF FAILURE	
Date & Time of Outage	Date & Time of restoration	Down Time [h:min]	Area	System	Subsystem	Component failure or other reason	Comment
<b>Klystron Assembly</b>							
10/29/96 22:19	10/29/96 22:37	0:18	LINAC	805	Klystron	Water flow	Sector D tripped on Module 21 Klystron water flow
11/01/96 02:09	11/01/96 02:29	0:20	LINAC	805	Klystron	Flow switch	Module 21 Klystron water not okay. Mechanically agitated flow switch and it made up.
11/23/96 09:43	11/23/96 09:56	0:13	LINAC	805	Klystron	Water flow	Sector D off. Module 21 klystron water flow trip. The klystron magnet supply valve has been opened 1/8 of a turn.
11/23/96 23:17	11/23/96 23:32	0:15	LINAC	805	Klystron	Water flow	Module 21 klystron water flow trip
03/17/97 07:25	03/17/97 07:40	0:15	LINAC	805	Klystron	Ion Pump	Module 46 (Sector H) Klystron ion pump supply failed. It was replaced.
03/26/97 07:22	03/26/97 07:33	0:11	LINAC	805	Klystron	Klystron	Sector B trip on Main Amplitude Overcurrent. RFON aborted. Locally recovered. Loud hum from klystron/switchtube
04/18/97 23:23	04/18/97 23:24	0:01	LINAC	805	Klystron	Voltage adjustment	Linac excursion. Adjustment of voltage in Klystron 1 in Sector D recovered linac.
05/24/97 07:24	05/24/97 13:14	5:50	LINAC	805	Klystron	Klystron	Module 36 Main Amplitude crowbar. Sector F tripped a second time and the fire alarm went off. Acrid smell from the capacitor room. Module 36 klystron was replaced.

The database is for practical reasons divided into three major sections: One section deals with the Duration of the Interruption. It contains the date and time of the beam outage and restoration. It also includes the Down Time of each interruption. The second section considers the Location of the Failure. The Area defines the geographical location of the failure. The System and Subsystem columns specify in what System and Subsystem the failure is located. The third section gives detailed information on the Cause of the Failure. The cause may be a component failure that needs repairment, a bad condition such as a water flow problem or a bad adjustment failure. In the comment column, extra text has been added to explain the failure.

### 8.3 Scheduled Beam Time

In the analysis scheduled beam time of the H- beam for 1996-97 and the H+ beam for 1997 is considered. This means that the total scheduled beam time embraces the scheduled H- beam time for 1996 plus the merged scheduled beam time of the H+ and H- beams for 1997. The analysis investigates accelerator operation during scheduled operation only. In Appendix 1, a detailed beam schedule of the H- and the H+ beams are available. In table 8.3 the merged beam schedule of the H+ and H- beams for 1997 is presented.

Table 8.3 Merged Beam Schedule for 1997 of the H+ and H- Beams at LANSCE

<b>LANSCE: 1997 SCHEDULED DELIVERY OF H+ AND H-</b>			
<b>Active Beam Line</b>	<b>Beam On</b>	<b>Beam Off</b>	<b>Beam Time [h:mm]</b>
<b>CYCLE 74</b>			
H- On	03/06/93 08:00	03/17/93 17:00	273:00
H+ and H- On	03/17/93 17:00	03/21/93 08:00	87:00
H+ On	03/21/93 08:00	03/22/93 17:27	33:27
Both Off	03/22/93 17:27	03/24/93 19:28	
H+ On	03/24/93 19:28	03/25/93 21:50	26:22
Both Off	03/25/93 21:50	03/27/93 08:00	
H+ and H- On	03/27/93 08:00	04/12/93 20:00	396:00
H+ On	04/12/93 20:00	04/20/93 08:00	180:00
<b>Scheduled Beam Time for Cycle 74:</b>			<b>995:49</b>
Minus 1 hour daylight savings time			-01:00
<b>Adjusted Time:</b>			<b>994:49</b>
<b>CYCLE 75</b>			
H+ and H- On	04/22/93 08:00	05/13/93 08:00	504:00
H+ On	05/13/93 08:00	05/18/93 08:00	120:00
Both Off	05/18/93 08:00	05/19/93 22:50	
H+ On	05/19/93 22:50	05/20/93 07:30	8:40
H+ and H- On	05/20/93 07:30	06/08/93 04:00	452:30
H+ On	06/08/93 04:00	06/15/93 08:00	172:00
<b>Scheduled Beam Time for Cycle 75:</b>			<b>1257:10</b>
<b>CYCLE 76</b>			
H+ and H- On	06/17/93 08:00	07/11/93 08:00	576:00
H+ On	07/11/93 08:00	07/13/93 08:00	48:00
Both Off	07/13/93 08:00	07/15/93 04:41	
H+ On	07/15/93 04:41	07/16/93 08:00	27:19
H+ and H- On	07/16/93 08:00	07/23/93 10:00	170:00
H+ On	07/23/93 10:00	07/26/93 08:00	70:00
<b>Scheduled Beam Time for Cycle 76:</b>			<b>891:19</b>
<b>Total Scheduled Beam Time for H+ and H-, 1997</b>			<b>3143:18</b>

By merging the statistics of two beams the total scheduled beam time increases and thereby more trips are included in the analysis. For 1997, the H+ beam alone, was scheduled for 2870 hours and the H- beam was scheduled for 2463 hours. The merged beam time was 3143 hours. Sometimes the H- beam is scheduled while the H+ beam is not and the other way around. For 1996, the H- beam was scheduled for 2681 hours and hence the total scheduled beam time used in the analysis is 5824 hours

## 8.4 LANSCE Subsystems

### 8.4.1 805 RF System

The rf system is the most complicated and also the most expensive system of an linear accelerator. The rf system supplies the necessary power to the accelerator and controls this power within specified limitations. There are different rf systems for the DTL and the SCL. The DTL operates at 201.25 MHz and is powered by triode power tubes. The SCL operates at 805 MHz and rf power is produced by klystrons, this system is sometimes referred to as the 805 RF System. The RF System for the envisioned ATW accelerator is more similar to the 805 RF System than the 201 RF System. Therefore, reliability analysis has been performed for the 805 RF System and not the 201 RF System. No further explanation of the 201 RF System will be made.

The 805 RF system is divided, basically, into two parts:

- 1) RF Reference System - which provides a stable phase and amplitude reference for each accelerator section.
- 2) The Klystron System - which provides rf power for the beam. This system also includes phase and amplitude control circuits.

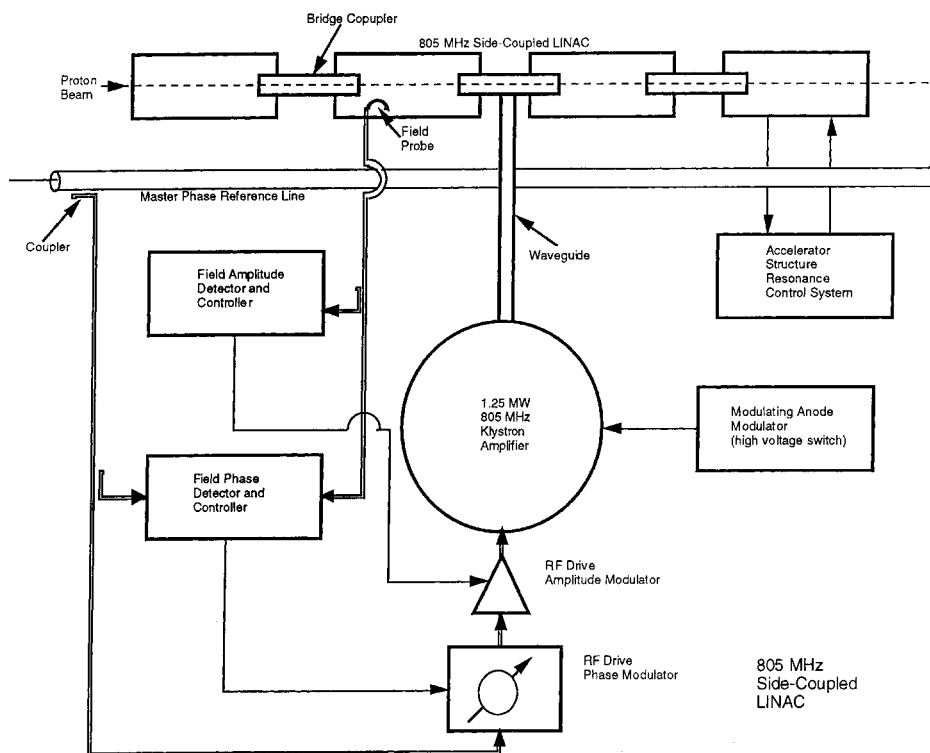


Figure 8.1 805 MHz Side Coupled Linac (805 RF System)



### 8.4.2 RF Reference System

The rf reference system provides precisely controlled power at 201.25 MHz and 805 MHz for distribution throughout the accelerator. This power is also used to drive all rf equipment other than the more power demanding modules and bunchers. It is used as a standard of comparison in all systems for phase relationships, power levels, and timing. The rf reference system consists of a low frequency oscillator, multipliers to derive the two operating frequencies, power amplifiers, distribution system, distribution system temperature control, and the source phase and amplitude control equipment.

The basic reference is a sophisticated crystal oscillator operating at the relatively low frequency of 6.289 MHz. It is followed by multipliers which derive 201.25 MHz and 805 MHz. Since the power output of the multipliers is only 1 W and because of transmission line losses, power amplifiers are required at each frequency. This power is then distributed along the accelerator and when a reference or drive power is required, roughly 6 W is coupled out of the transmission line.

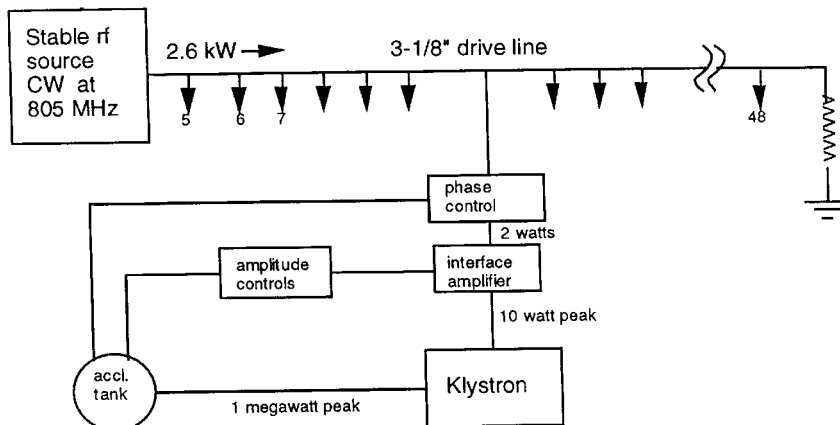


Figure 8.2 The RF reference system for the Side Coupled Linac

Since almost every operation connected with the accelerator is dependent upon the rf reference system, there are two identical units of the oscillator, multiplier and amplifier system. These are designated the A and B chains. One is in service 24 hours a day, while the other is in standby mode but pretuned and ready for service.

### 8.4.3 The Klystron System

The heart of the 805 MHz rf system is the klystron system. The klystron system provides rf power at 805 MHz to the side coupled linac. The SCL is divided into 44 modules. Each module contains its own klystron system. Modules are clustered into groups of six or seven, each group is fitted into a cluster building (sectors B to H):

*Table 8.4 Count of Klystron Systems and High Voltage System*

Sector or cluster building	Modules	No of Klystron Systems	No of High Voltage Systems
B	5-10	6	1
C	11-17	7	1
D	18-24	7	1
E	25-30	6	1
F	31-36	6	1
G	37-42	6	1
H	43-48	6	1
Total		44	7

The number of klystron systems used for the SCL is 44.

#### **8.4.3.1 The Klystron**

Two types of klystrons are used at LANSCE; the Varian (VA-862) and the Litton (L-5120), both klystrons produces 1.25 MW pulses of rf power with a time duty factor of up to 12% (duty factor during normal operation is 6%). The klystron provides a power gain of more than 100,000. An input rf drive of about 10 Watts results in an output of 1.25 MW.

The LANSCE klystron is comprised of three parts:

- 1) The electron gun, where the beam is formed and focused. The gun end is under oil in the modulator tank. In this end are the filament, cathode, beam focus electrode and the modulating tank.
- 2) The rf interaction region, where the actual amplification of the rf signals take place. The rf interaction region contains five cavities and four drift spaces.
- 3) The collector, where the electron beam is intercepted. The collector is water cooled as considerable beam power is dissipated there, especially when low levels of rf drive are used.

These components are shown in greater detail in figure 8.3.

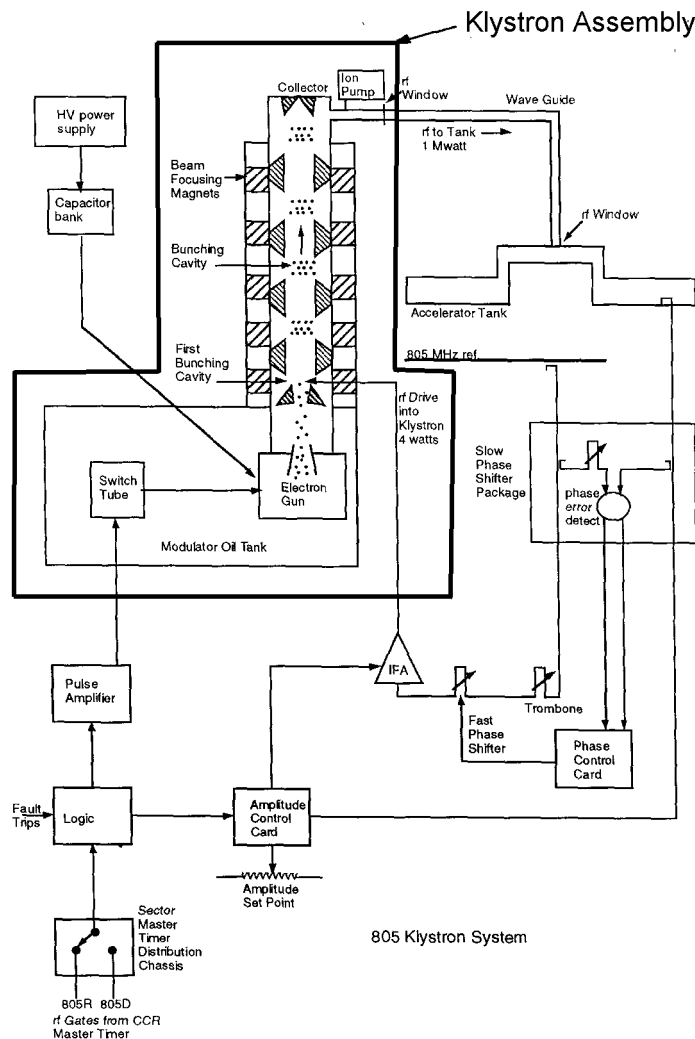


Figure 8.3 The Klystron System and the Klystron Assembly subsystem

The High Voltage System, the Phase and Amplitude Control System, and the accelerator tank are not included in the Klystron Assembly.

Some other equipment associated with the Klystron Assembly are:

- a focusing klystron magnet
- a klystron magnet power supply provides DC power for the focusing magnet
- a klystron ion pump is used to maintain the vacuum within the klystron
- an ion pump power supply provides high voltage power for the ion pump
- a klystron water system including a flow switch and a bypass flow switch

#### 8.4.3.2 The Klystron Modulator

The main purpose of the modulator is to switch the electron beam in the klystron on and off. The Pulse Amplifier turns the modulator switchtube on and off. The switchtube turns the klystron beam on and off. Another important function of the modulator is to prevent arcing and corona discharge from the cables which is connected

to the electrodes of the klystron. Thus, the large modulator tank is filled with transformer oil to provide good high voltage insulation. The oil is circulated within the modulator tank by an oil pump. The oil pump circulates oil through a heat exchanger in the modulator tank and supplies cooling oil to the high voltage switchtube and other heat sources in the tank.

### 8.4.3.3 Phase and Amplitude Control System

When the beam is turned on, energy is transferred from the cavity fields to the beam. Beam loading up to 40% is anticipated in the LANSCE accelerator. That is, up to 40% of the total rf power supplied will be transferred to the beam, with the remaining 60% lost in the cavities. Beam loading in a cavity in which the rf phase and amplitude are not controlled results in a decrease in the amplitude of the accelerating gradient and a shift in the apparent synchronous phase angle. The result is reduced acceleration and loss of particles. Since the beam is somewhat "sucking" power from the cavity fields correction signals must be applied to both amplitude and phase to keep them within tolerance at all times when there is beam in the cavities.

The phase and amplitude control systems are designed to maintain the rf field in the cavities within the specified limits of 1° in phase and 1% in amplitude during the entire rf pulse. One system controls amplitude another controls phase. A magnetic pickup loop located inside the tank is used to obtain a "sample" of the rf cavity field. The control system operates by comparing the actual tank amplitude or phase to a reference value and then applying a correction signal to the rf amplifier chain to produce the desired result.

This phase and amplitude loop is sometimes referred to as the servo loop and a fault in this chain is called a servo fault.

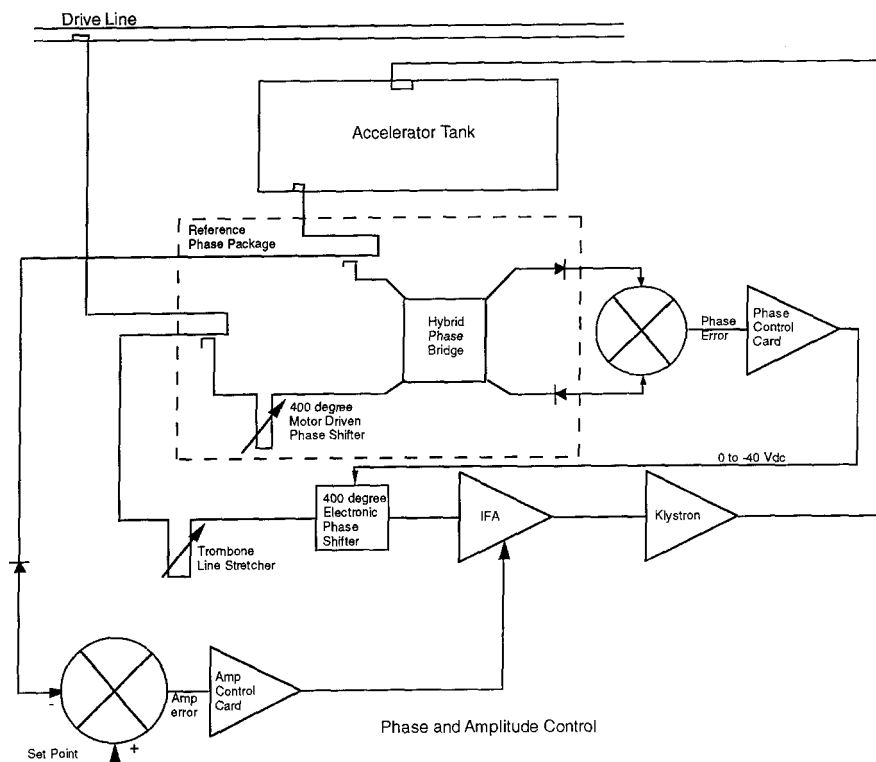


Figure 8.4 Phase and Amplitude Control System

#### 8.4.4 High Voltage System

The High Voltage (HV) system provides HV power to the 6 or 7 klystrons in each sector. The capacitor room is a large metal enclosed structure which contains the HV distribution system and the crowbar system. Each HV distribution system consists of:

- HV switch
- capacitor bank, including 50 capacitors
- 84 Amp fuse + air cooling blower
- two crowbar resistor banks
- shorting bar switch
- voltage divider
- current meter shunt
- cable fault detection system
- klystron duty factor detector

#### 8.4.5 DC Magnets

Most magnets constructed for beam transport lines are electromagnets rather than permanent magnets. Such magnets are excited by electrical current carrying coils around magnet poles. Iron magnets are the most commonly used magnets for particle beam transport systems. Quadrupole Magnets together with bending magnets are the basic building blocks for focusing devices to keep the particle beam close to the desired beam path.

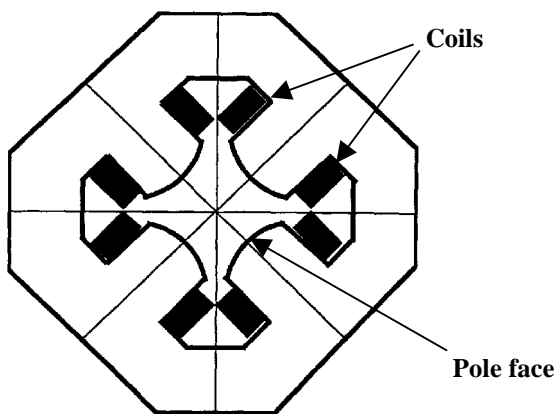


*Figure 8.5 Standard Quadrupole Magnet geometry*

*The figure shows a standard design for the quadrupole magnet geometry. The core is symmetric around the four poles, with coils mounted on the pole sides [18].*

In the LANSCE accelerator complex most magnets are supplied with DC (Direct Current) power. A table of summary of all magnets located at LANSCE is available in Appendix 2. DC magnets are used for focusing, steering, and bending actions on the beam. The most suitable device for producing a focusing effect is the quadrupole magnet. The quadrupole magnet reduces the transverse dimensions of the beam and confines it to the vicinity of the accelerator axis.

In the SCL there is a quadrupole doublet between each tank of the structure, for a total of 103 quadrupole doublets. The quadrupole magnets have a center-to-center

spacing of 20 cm. Each quadrupole doublet is protected by two interlocks, namely a thermal switch and a flow switch. The thermal switch senses that the quadrupole doublet temperature is less than 93°C (200 F), and the flow switch senses that the flow of coolant is normal. Both of these interlocks must be satisfied in order for the quadrupole doublet power supply to operate.

In the DTL, the quadrupole magnets are located inside the drift tubes. There are quadrupole magnets in every drift tube of tanks 1 and 2 and in every other drift tube of tanks 3 and 4. Totally, this system includes 132 quadrupole magnets. The quadrupole magnets of each tank are cooled by water that comes from a supply line, passes through a high pressure pump and is distributed to each magnet by a supply header. The magnet windings are cooled in parallel by water that flows from the supply header through a throttling valve. The flow is throttled so that the temperature rise in each magnet is about the same for all magnets in the tank.

#### 8.4.6 Magnet Power Supplies

In an electromagnet, the strength of the magnetic field is proportional to the current flowing in the magnet windings. Therefore, magnet power supplies are designed to deliver relatively high currents to the magnets.

The magnets used in LANSCE requires DC power for operation. In the power supplies, AC power from the building power distribution system is converted to DC power. A typical power supply generates 50 Amps of output DC current. Sometimes, for reason of economy, one power supply is providing several magnets with power. Generally, each power supply is set to deliver the maximum current required by any magnet in the group (usually the first or second magnet). The required currents for the quadrupole magnets in each group generally decrease with magnet number.

The power supplies are protected by a number of interlocks. These interlocks are power supply temperature, ground current, door interlock, transformer primary overload protection, and shunt control power.

#### 8.4.7 Pulsed Power System

The pulsed Power System includes:

*Table 8.5 The Pulsed Power System*

Count	Subsystem	Specification
1	Harmonic Buncher	The harmonic buncher is located in the Proton Storage Ring.
1	Chopper	The beam chopper is located in H- Low Energy Beam Transport.
2	Deflectors	One deflector each for the H+ and H- Low Energy Beam Transport.
3 (5)	Kickers	One Injection Kicker in Line D. Two Extraction Kickers in the Proton Storage Ring. <i>The Switchyard Kicker (includes two ferrite kicker magnets) was not in operation during 1996-97.</i>

A detailed list of components for the Pulsed Power System is available in Appendix 3 [19].

##### 8.4.7.1 Harmonic Buncher

The Harmonic Buncher is located in the Proton Storage Ring. The buncher itself is simply a resonant cavity that establishes an alternating potential across a gap in the

beam line. It is the purpose of the buncher to collect the stream of particles into clusters and time this process in a proper manner. The resonant cavity is excited with 2.8 MHz rf power.

**The Harmonic Buncher includes:**

- RF Cavity
- Low Level Electronics
- RF Preamplifier
- RF Drive Amplifier
- Output Transmission Line
- Controls/Interlocks
- Computer Interface

#### **8.4.7.2 Chopper**

The chopper is a deflecting magnetic moving the continuous beam across the opening of a slit. The chopper produces macropulses of H<sup>-</sup> ions, called bunches. These bunches are further processed by the 201 prebuncher. The Chopper system also includes a DC power supply, a slow wave structure and a distributed amplifier.

#### **8.4.7.3 Kicker Systems**

Altogether there are five kicker magnets at LANSCE, namely:

**Kicker Magnets**

- 1 Switchyard Kicker (comprised of two ferrite kicker magnets in series)
- 1 Injection Kicker
- 2 Extraction Kickers

During 1996-97 three kickers were in use, the Switchyard Kicker was not in operation.

**Injection Kicker**

The Injection Kicker is located in Line D. The Kicker injects protons into the Proton Storage Ring.

The Injection Kicker includes:

- Kicker Magnet
- Charging System
- Modulator
- Controls/Interlocks
- Computer Interface

**Extraction Kickers**

Two extraction kickers are used for single-turn fast extraction of the accumulated proton beam. The horizontally kicked beam is captured by a pair of septum magnets for transfer to the extraction line and then to the WNR target.

The Extraction Kickers include:

- 2 kicker magnets (vacuum vessels, electrodes etc.)
- Charging System
- Switching System
- Cables
- Controls/Interlocks
- Computer Interface

### 8.4.8 Summary of Subsystems

*Table 8.6 Summary of Subsystems*

System	Subsystem	Count	Definition
<b>805 RF System</b>			805 MHz Radio Frequency System (section 8.4.1): pad power supplies, capacitor rooms, amplifier systems, klystron systems, interlocks (flow, temp, etc.), resonance controllers and valves. Does not include prebunchers.
	Klystron Assembly	44	The klystron (section 8.4.3.1) and the klystron modulator (section 8.4.3.2). Klystron ion pump and magnet and their associated power supplies. Any water or vacuum failure inside the klystron system. The Phase and Amplitude, Resonance and Module Control System is NOT included in the Klystron Assembly.
	High Voltage System	7	The High Voltage System (section 8.4.4). The HV switch, capacitors, cabling, fuses etc.
	805 Tank	44	Any failure in the tank module vacuum leaks, valves etc.
	Phase and Amplitude Control	44	Phase and Amplitude Control System (section 8.4.3.3)
	Resonance Control	44	Resonance Control System
	Module Control	44	Module Control System
	Other		Extraordinary failure that is not classified into any other subsystem.
	Unknown		Unknown failure within the 805 RF System.
<b>DC Magnets</b>		800	Magnets, winding, DC cabling, flow and temperature switches, vacuum and water leaks, magnet water strainers. Does not include power supplies.
	Magnet Hardware		Any failure to the hardware (wiring, cabling)
	Water		Water cooling problems (leaks, valves, flow switches, flow problems)
	Interlocks		Magnet interlocks (flow interlocks)
	Vacuum		Vacuum leaks
<b>Magnet Power Supplies</b>		278	DC Magnet Power Supplies: electronics, trips, interlocks (flow, ripple, etc.), water leaks.
	Electronics		Power supply electronics (computer control system, SCR, regulation, filtering, shunts, overcurrent problems, magnet drifting problems)
	Capacitors		Capacitors inside the power supply (usually dry out)
	Transformers		Transformer for power supply (insulation aging)
	Water cooling		Water cooling problems within the power supply (flow switches, valves, hoses)
	Interlocks		Power supply interlocks (door interlock)
	Unknown		Unknown failure within the power supply.



<b>Pulsed Power</b>			Pulsed Power System: Kickers, Ring buncher, deflectors, inflector, choppers and their related power supplies, local controls and modulators.
	Harmonic Buncher	1	Failures connected to the buncher and power supply (water flow, arcs, crowbars, adjustments etc.)
	Deflectors	2	Failures connected to the deflectors and power supplies
	Chopper	1	Failures connected to the chopper and power supplies (water flow, adjustments, FET)
	Kickers	3	Injection kickers, extraction kickers and their associated power supplies (timing problems, Blumlein, arcs)
<b>Water System</b>			Cooling water systems: pumps, pump controls, makeup water, valves, pipes, heat exchanges. Does not include leaks and flow problems in individual cooled components such as magnets, amplifiers, cavities, etc. unless problem is caused by variations or limits in water system.
	Water pump	120	Water pumps and their associated power supplies
	Piping		Water lines, valves, hoses etc. which do not belong to any other System.
	Other		Other failures that occur in the Water System
	Unknown		Unknown failure in the Water System
<b>Vacuum System</b>			Vacuum system: Vacuum pumps, pump power supplies, roughing packages, valves, instrumentation, controls, pipes, flanges. Does not include leaks in individual components or loads such as magnets, targets, etc.
	Ion pump	250	Ion pumps and their associated power supplies.
	Piping		Vacuum lines, tanks, valves etc. which do not belong to any other System.
	Unknown		Unknown failure within the Vacuum System

### 8.5 Operational Statistics

All trips are divided into different databases depending on which system is responsible for the failure. The total number of trips corresponding to each system is presented in table 8.7.

Table 8.7 Summary of Trips produced by the Systems Analyzed

TRIPS PRODUCED BY INDIVIDUAL SYSTEMS			
Main System	No. of trips 1996	No. of trips 1997	Total
805 RF	68	162	230
Pulsed Power	127	72	199
Magnet Power Supplies	102	83	185
Vacuum System	27	47	74
Water System	30	18	48
DC Magnets	3	17	20
<b>Total</b>	<b>357</b>	<b>399</b>	<b>756</b>

The systems are presented in order of importance, starting with the system responsible for most of the trips. It must be noted that not all accelerator systems are included in the summary, only the systems which being are analyzed. The total number of trips included in this analysis (756 trips) are significantly less than the actual number of trips that occurred in the entire accelerator ( $\approx 8000$  trips). In other words, one may not

conclude that, for example, the 805 RF System is the most "troublesome" system at LANSCE. Reliability estimates of the entire accelerator and other systems are outlined in chapter 6.

In the systems analyzed, the 805 RF System is causing most of the interruptions. Next in order is the Pulsed Power System followed closely by the Magnet Power Supply system. The DC Magnets are causing the smallest number of interruptions, only 20 trips. The DC Magnets are in fact one of the most reliable systems of the entire accelerator.

During 1996, 357 trips occurred and for 1997 the number was 399. It is understandable, the accelerator was scheduled for more time in 1997 (3143 hours) than in 1996 (2681 hours).

### 8.5.1 Reliability Calculations

For all systems and subsystems identical reliability calculations have been performed. The Magnet Power Supply System is selected for the purpose of illustrating some reliability calculations. In table 8.8 the first cut of some of the calculations are presented.

*Table 8.8 Illustration of Reliability Calculations*

1	2	3	4	5	6	7	8	9	10
No	Date & Time of Outage	Date & Time of Restoration	Time Between Failures [h:min]	Cum Failure Rate [1/d]	Cum MTBF [h:min]	Down Time [h:min]	Cum Down Time [h:min]	Cum MDT [h:min]	Cumulative Availability
68	10/17/96 17:59	10/17/96 18:02	3:41	0.87	27:38	0:03	102:49	1:30	0.948139
69	10/18/96 15:51	10/18/96 15:52	21:49	0.87	27:33	0:01	102:50	1:29	0.948695
70	10/18/96 16:15	10/18/96 16:16	0:23	0.88	27:10	0:01	102:51	1:28	0.948697
71	10/18/96 20:04	10/18/96 20:05	3:48	0.89	26:50	0:01	102:52	1:26	0.948786
72	10/19/96 08:41	10/19/96 08:48	12:36	0.90	26:38	0:07	102:59	1:25	0.949051
73	10/20/96 00:53	10/20/96 00:58	16:05	0.91	26:29	0:05	103:04	1:24	0.949414

Each row represents an event or a failure that resulted in a beam interruption. In this case, event numbers 68-73 are displayed. In columns 2-3 the date and time when the beam was interrupted and restored is shown.

**Time Between Failures** - time between the end of one trip to the beginning of the next. For example, Time Between Failure = Date & Time of Outage 69 - Date & Time of Restoration 68.

**Cumulative Failure Rate** - this number reflects what the failure rate would be based on the events up to that point. In other words, if the Magnet Power Supply system only included 70 trips then the mean failure rate would be 0.88 failures per day. Cumulative Failure Rate = Event number/cumulative time between failures

**Cumulative MTBF** - Mean Time Between Failure up to that event. For example, if the Magnet Power Supply system only included 70 trips then the MTBF would be 27 hours and 10 minutes. Cumulative MTBF = Cumulative Time Between Failures/Number of failures.

**Down Time** - duration of individual trips. Down Time = Date & Time of Restoration - Date & Time of Outage.

**Cumulative Down Time** = down time 1 + down time 2 + ....

**Cumulative MDT** - Mean Down Time up to this event. For example, if the Magnet Power Supply system only included 70 trips then the MDT would be 1 hour and 28 minutes. Cumulative MDT = Cumulative Down Time/Event number.

**Cumulative Availability** = Cumulative MTBF/(Cumulative MTBF+Cumulative MDT). The probability that the magnet power supply system is functioning.

To visualize the reliability behavior of the Magnet Power Supplies the calculations have been plotted. The most important plots are presented in figures 8.6 - 8.11. All these plots apply to the Magnet Power Supply System only. Similar plots have been made for the other Systems as well.

For illustration the cumulative number of trip events as a function of time is presented for the magnet power supply system in figure 8.6.

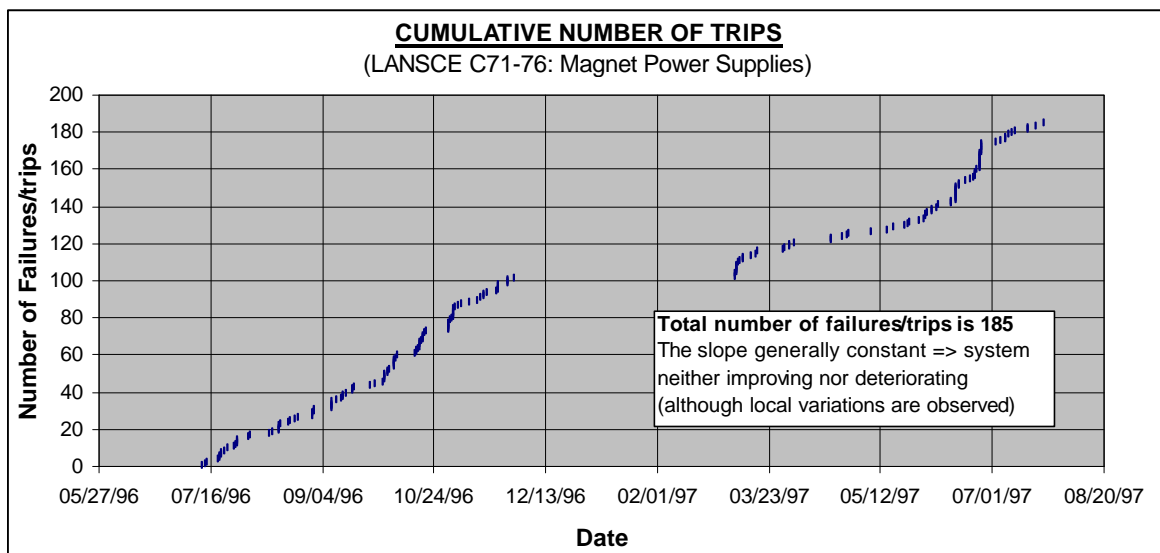


Figure 8.6 Magnet Power Supplies: Cumulative Number of Trips

This plot is remarkably straight, despite the fact that it is the sum of many different types of activities by many different people and equipment. One can see neither significant improvement nor deterioration of the system, although local variations are visible. At some instances, several trips occur in a short period of time. That is an indication of the real failure was never attended at the first time. The trip was reset but the failure was probably never investigated until numerous trips had occurred. The wide gap in the middle of the plot shows the duration of the extended maintenance period between 1996 and 1997. Some other short maintenance periods or periods when the accelerator was not scheduled are visible as well.

In figure 8.7 the cumulative down time is illustrated.

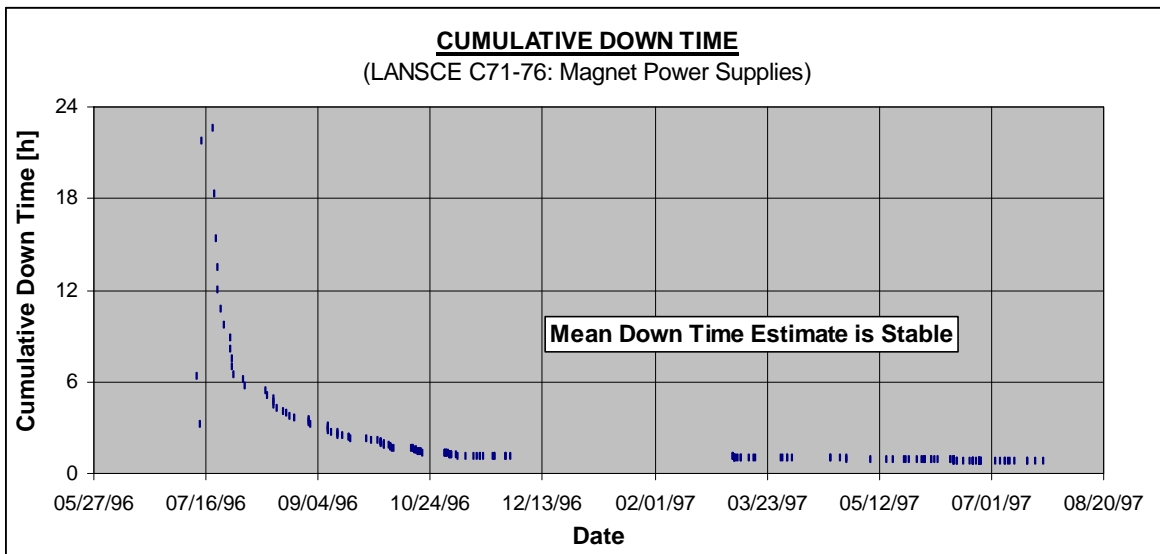


Figure 8.7 Magnet Power Supplies: Cumulative Down Time

Mean Downtime is calculated as the ratio of the cumulative downtime to the cumulative number of events as shown in figure 8.7. One indication of sufficient number of entries in the data set is the asymptotic behavior of the statistical estimators for the desired quantities, such as Cumulative Mean Down Time. The conclusion is that further data collection is not necessary, the MDT estimate appears

A histogram of magnet power supplies down times is presented in figure 8.8

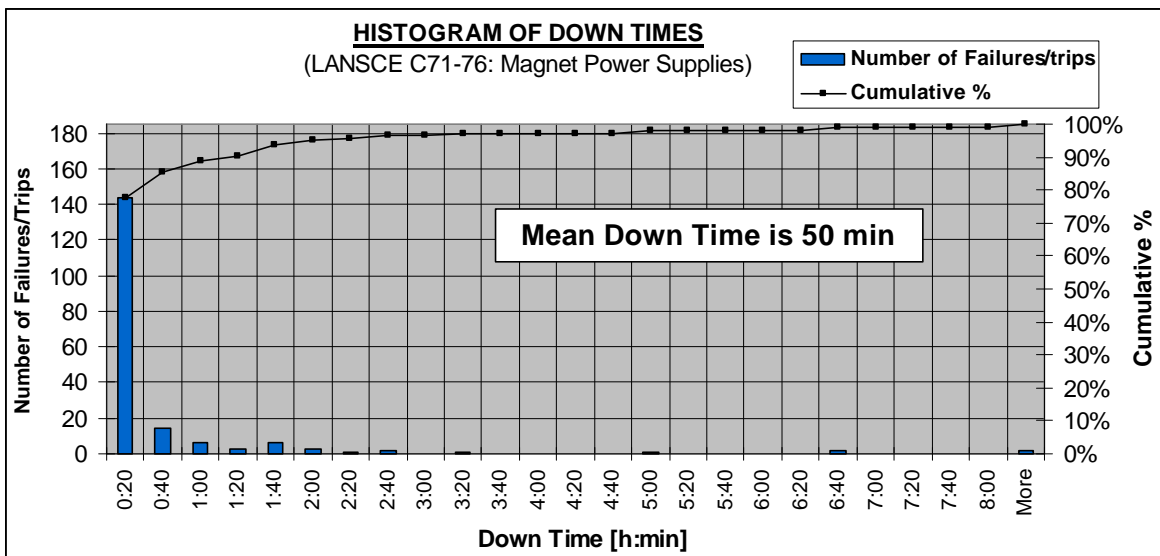


Figure 8.8 Magnet Power Supplies: Histogram of Down Times

On the x-axis different down time intervals are displayed. The y-axis displays on one side, the number of trips within each down time interval, and on the other the fraction these trips represent. The majority (80%) of the trips have down times <20 minutes. Two

trips which resulted in very long down times occurred. The Mean Down Time for the magnet power supplies is 50 min.

Cumulative Failure Rate is calculated as the ratio of the cumulative number of events to the cumulative up time. As shown in figure 8.9 the behavior is not as smooth as for the cumulative downtime but appears to converge.

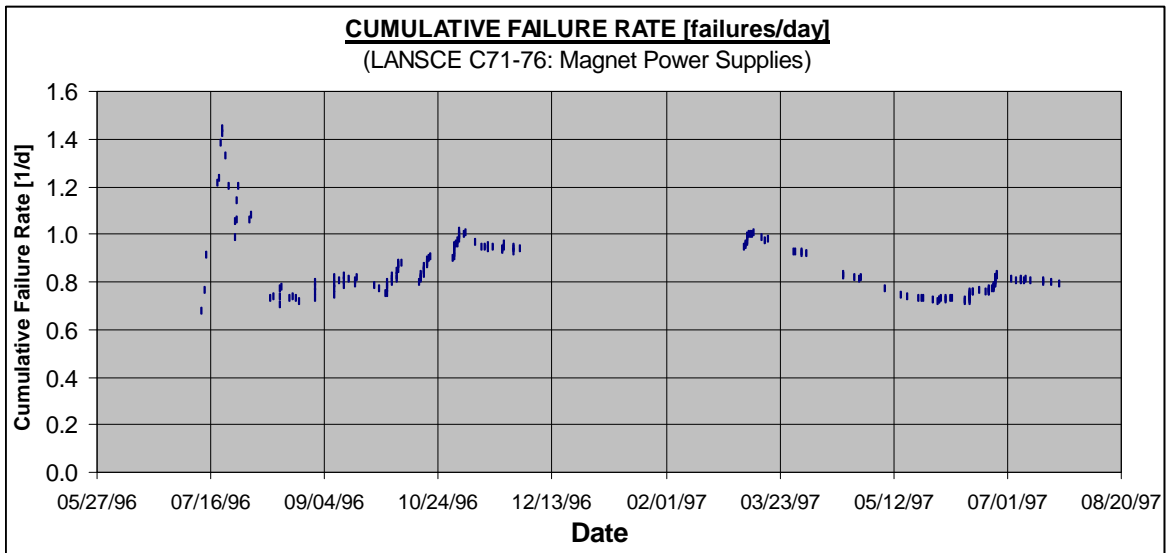


Figure 8.9 Magnet Power Supplies: Cumulative Failure Rate

Figure 8.10 shows the histogram of Times Between Failures.

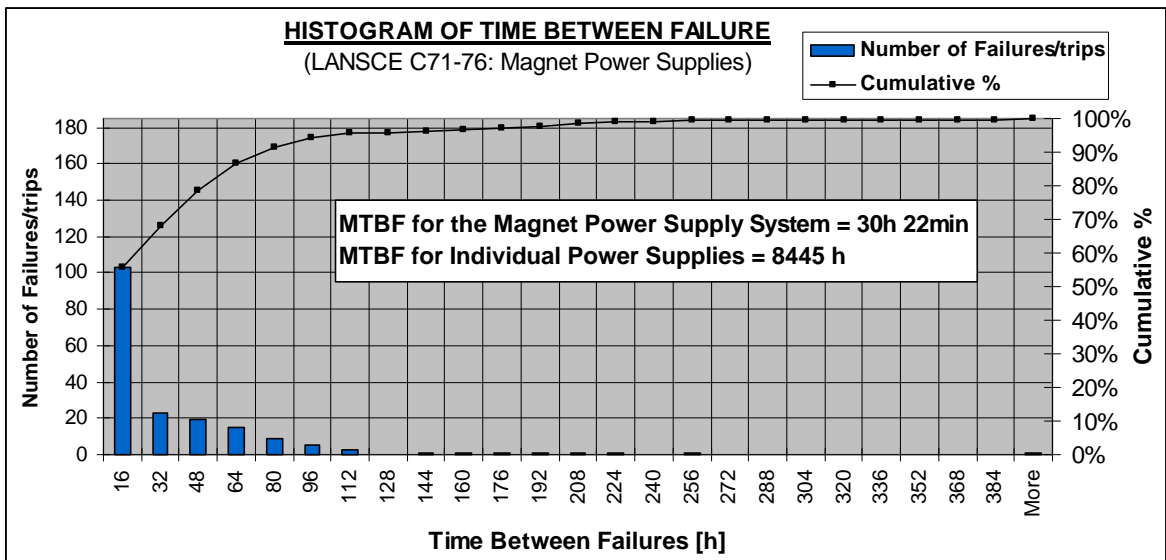


Figure 8.10 Magnet Power Supply: Histogram of Times Between Failures

The Mean Time Between Failures is 30 h 22 min. With 278 magnets power supplies total in the system, we can estimate the MTBF for an individual magnet power

supply as 8445 hours, assuming that all the supplies have the same failure rate and can be treated as a series system of independent power supplies.

### 8.5.2 Results

The results obtained via similar analyses for the other components of the LANSCE accelerator are summarized in table 8.8. Information on failure causes in the individual systems are presented in Appendix 4.

RESULTS OF RELIABILITY STUDY AT LANSCE				
Main System	Subsystem	MDT [h:mm]	MTBF for all devices [h]	MTBF for a single device [h]
<b>805 RF</b>	Klystron Assembly	0:44	262	11560
	High Voltage System	0:18	137	960
<b>DC Magnets</b>		0:53	290	232280
<b>Magnet Power Supplies</b>		0:50	30	8445
<b>Pulsed Power</b>	Harmonic Buncher	0:09	44	44
	Chopper magnet	0:08	291	291
	Deflector magnet	0:10	342	684
	Kicker magnet	1:58	185	557
<b>Water System</b>		1:20	120	
	Water pump	0:29	245	29506
<b>Vacuum System</b>		0:48	77	
	Ion pump	0:29	101	25308

Figure 8.8 Results of Reliability Investigation of Systems and Subsystems

The MTBF calculated from the raw data corresponds to the entire 805 RF system consisting of 44 klystron assemblies. An estimate of the MTBF for an individual klystron assembly was obtained by multiplying this value by 44 as 11560 hours. This value is not unreasonable when compared with the 20-50,000 hours commonly quoted for the typical klystron tube by itself. 38% of all failures in the klystron assembly are water cooling problems and 32% are amplitude crowbars (which is usually due to an old switchtube). Most of the downtime occurs when klystron replacement is necessary. During 1996-97, four klystron replacements occurred, these replacements were responsible for 54% of the downtime in the klystron system.

The High Voltage System is exposed to many short interruptions. Sometimes when a failure occurs in the High Voltage System it is not possible to point out any specific component. Usually the High Voltage system causes phase or amplitude disturbances (85% of all trips), commonly called servo faults. In this analysis, all servo-faults are classified as high voltage failures, but in some cases these failures are caused by the phase and amplitude control system. Even though many servos occur the total downtime caused by these failures is small. Sometimes the capacitors dry out and need to be replaced, this causes long downtimes. Capacitor failures are responsible for 68% of the downtime in the high voltage system.

A total of 800 dc magnets exist in the LANSCE facility. MTBF for a single magnet is 232280 hours ( $\approx 26$  years). The dc magnets at LANSCE are very reliable. This is also confirmed by maintenance personnel at LANSCE. When a magnet failure occurs it

is usually a water cooling problem inside the magnet. 50% of the magnet failures are related to the water cooling system. Water cooling failure is also responsible for 52% of the downtime. 5 failures in the magnet hardware occurred. Hardware failures accounted for 32% of the total downtime in dc magnets.

The Magnet Power Supply System includes 278 power supplies. For a single power supply the MDT is 50 minutes and the MTBF is 8445 hours ( $\approx 1$  year). A single capacitor failure inside a power supply was responsible for 80 hours, or 54% of the downtime. The most common failure cause is problems with the electronics (31% of all trips). Most of the power supplies at LANSCE are controlled by manual electronics. Modern power supplies are computer controlled and proves to be much more reliable. Many unknown trips occur in the power supplies (58%), according to expertise at LANSCE most of these trips are caused by malfunctioning electronic equipment as well.

48 trips occurred in the water system. A water system failure is usually connected to the piping subsystem (42%) or water pumps (35%). Most of the downtime is also caused by the piping (68%). Failures with hoses, valves, water lines etc are included in the piping system. MDT for a water pump is 29 minutes and MTBF is 29500 hours ( $\approx 3$  years).

In the vacuum system, 76% of the trips were caused by ion pump failures and 18% were caused by piping failures. On the other hand, piping failures were responsible for 54% of the downtime and ion pumps accounted for 45%. MDT for an ion pump is 29 minutes and MTBF is 25300 hours ( $\approx 3$  years).

## **8.6 Conclusions**

In summary, as a result of the investigation of individual systems, estimates for both MTBF and MDT were obtained for several typical accelerator components: DC magnet power supplies, DC magnets, klystron assemblies, HV power supplies, vacuum system, and water system. Both MTBF and MDT values are shorter than expected, driven by short beam trips, rather than major replacement jobs. The results will be useful in developing preliminary estimates for reliability, availability, and maintainability of high power accelerator systems planned in the future. However, before we can fully trust them, they have to be corroborated through comparison with statistics obtained from other facilities. The impact of maintenance activities outside of the scheduled production time needs to be tracked down and included in the estimates as well.

## 9 Beam Current Analysis

### 9.1 Introduction

In this chapter statistics of beam interruptions originating from current monitor data are presented. The analysis verifies the true beam performance. It does not investigate the cause of the beam failure. Mean Time Between Failure and Mean Down Time estimates of the H<sup>+</sup> beam are obtained. The analysis considers scheduled production of the H<sup>+</sup> beam for 1997 (Cycle 74-76).

### 9.2 Input data

Near the targets of Line A (H<sup>+</sup> beam) current detectors are positioned. These detectors monitor the beam continuously. Every change in beam current is registered. From the detectors the current level is read at a steady rate, about once per second. Software running on the main control computer of the LANSCE accelerator facility collects the current monitor data and automatically calculates the average current integrated over the last minute. This average value is the final input data used in the Beam Current Analysis. In figure 9.1 an illustration of this procedure is presented.

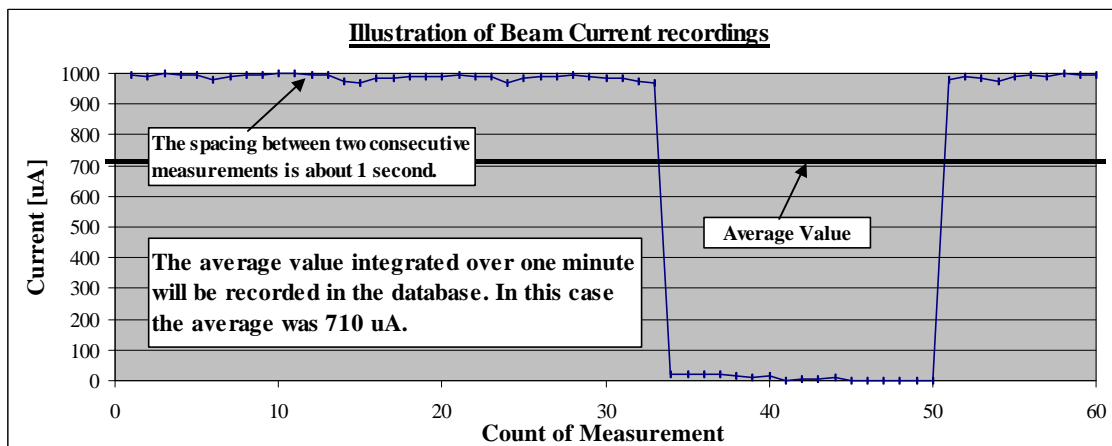


Figure 9.1 Illustration of Beam Current recordings

On average, a new current value is recorded to the database every 1.10 min. The analysis extends over the period 20<sup>th</sup> of March to 27<sup>th</sup> of July 1997 (Cycle 74-76) and the input data contains 163,000 current recordings.

### 9.3 Method

From the original database the current data is extracted and compiled into Excel spreadsheets. Due to the large amount of data the final input data is divided into several data files. In table 9.1 the final database format is illustrated. Beam recordings which occur outside scheduled production are not included in the analysis. The scheduled current is entered along with the beam current data to the final database. This is done because the beam is considered as interrupted only if the current is below a threshold current. For 1997, the threshold current was one half the scheduled current. For most of



the time the scheduled current is 1000  $\mu\text{A}$ , but sometimes other current levels are scheduled.

Table 9.1 Illustration of final database

Date	Time	Average Delivered Current	Scheduled Current	Time between measurement	Classification of event	Event Down Time	0-2 min	2-5 min	5-15 min	15-60 min	1-5 h	>5 h
		[ $\mu\text{A}$ ]	[ $\mu\text{A}$ ]	[mm:ss]	0=below threshold 1=above threshold	[h:mm:ss]	0=No 1=Yes	0=No 1=Yes	0=No 1=Yes	0=No 1=Yes	0=No 1=Yes	0=No 1=Yes
<b>Schedule On, threshold level = 0.5*Scheduled Current</b>												
97-06-11	0:00:30	996.70	1000.00	01:07	1	0:00:00	0	0	0	0	0	0
97-06-11	0:01:37	997.20	1000.00	01:07	1	0:00:00	0	0	0	0	0	0
97-06-11	0:02:43	996.90	1000.00	01:06	1	0:00:00	0	0	0	0	0	0
97-06-11	0:03:49	734.30	1000.00	01:06	1	0:00:00	0	0	0	0	0	0
97-06-11	0:04:56	387.10	1000.00	01:07	0	0:00:00	0	0	0	0	0	0
97-06-11	0:06:02	465.30	1000.00	01:06	0	0:02:13	0	1	0	0	0	0
97-06-11	0:07:09	993.30	1000.00	01:07	1	0:00:00	0	0	0	0	0	0

In the database, each current value is checked and determined whether or not the current was above or below the threshold value. Consecutive events below the threshold current are interpreted as one interruption. Interruptions are classified into down time intervals. Six down time intervals exist: 0-2, 2-5, 5-15, 15-60 minutes and 1-5 hours and >5 hours. As we shall see later, the intervals 0-2 and 2-5 minutes are combined into one interval which is denoted 0.5-5 minutes for reasons which will be explained later.

### 9.3.1 Beam Schedule

In this analysis, beam current data are only processed if they occur within scheduled production. Therefore, the beam schedule is important. The scheduled beam time used in this analysis is most similar to the beam schedule used for the H<sup>+</sup> beam in chapter 7, "Overall LANSCE Reliability" (or Appendix 1). After all, both analyses investigate the same beam during the same period of time, but small divergences exist. These are:

- Current recordings starts in the 20<sup>th</sup> of March
- Small differences in time following maintenance periods when the beam is switched on and off.

First of all, the current recordings used in the Beam Current Analysis started in the 20<sup>th</sup> of March at 07:47, where in the Overall Reliability Analysis the scheduled production started at the 18<sup>th</sup> of March at 17:00. Meaning that 38 hours of beam time is not included in the Beam Current Analysis compared to the Overall Reliability Analysis. Also, when the current data is more closely investigated it is obvious in some cases that the beam was not switched on exactly at 08:00 rather at 08:45. In order to be able to compare the two analyses this difference in time should not be considered as down time which would be the case if the schedule had started at 08:00.

In table 9.2 the final schedule used in the Beam Current Analysis is presented.

<b>H+ BEAM SCHEDULE USED FOR THE BEAM CURRENT ANALYSIS</b>		
<b>Beam On</b>	<b>Beam Off</b>	<b>Beamtime [h:mm]</b>
<b>CYCLE 74</b>		
03/20/97 07:47	03/23/97 17:27	81:40
03/25/97 19:30	03/26/97 21:49	26:19
03/28/97 09:56	04/21/97 06:09	572:13
<b>Scheduled beam time for Cycle 74:</b>		<b>680:12</b>
Minus 1 hour daylight savings time		-1:00
<b>Adjusted Time:</b>		<b>679:12</b>
<b>CYCLE 75</b>		
04/23/97 08:45	05/19/97 04:04	619:19
05/20/97 22:51	06/16/97 06:00	631:09
<b>Scheduled beam time for Cycle 75:</b>		<b>1250:28</b>
<b>CYCLE 76</b>		
06/18/97 08:00	07/14/97 08:00	624:00
07/16/97 04:42	07/27/97 08:00	267:18
<b>Scheduled beam time for Cycle 76:</b>		<b>891:18</b>
<b>Total Scheduled H+ Beam Time for 1997</b>		<b>2820:58</b>

Table 9.2 Final Beam Schedule used in the Beam Current Analysis

The total scheduled beam time is 2821 hours. Interruptions that occur during this time are included in the analysis. In the Overall Reliability Analysis the total scheduled H+ beam time for 1997 was 2870 h. In other words, the accelerator in the Beam Current Analysis is scheduled for 50 hours less beam. The difference in scheduled beam time have a very little effect on the total number of interruptions. On average

$$50 \text{ hours} / 2821 \text{ hours} = 1.8\%$$

Meaning that if the number of interruptions would be extrapolated for an extra 50 hours the Beam Current Analysis should include 1.8 % more interruptions (which is negligible).

## 9.4 Results of Beam Current Analysis

Beam current statistics originating from beam monitor data are presented. Statistics of two data runs are shown and discussed. The first computation uses a threshold factor of 0.5. The threshold factor determines at what beam current the beam should be regarded as interrupted. Threshold factor 0.5, or half the scheduled current, is the definition for an interruption used in the Overall LANSCE Reliability Analysis in Chapter 7. By comparing these two investigations a verification of the correctness and reliability of both analyses is achieved. The second computation is performed at a threshold factor of 0.8 for reasons which will be explained later.

### 9.4.1 Threshold Factor 0.5

It is interesting to compare the results of the Beam Current Analysis with the results in the Overall Reliability Analysis. In order to easily discuss and compare results from both analyses similar diagrams have been assembled. The results are presented in figures 9.2 and 9.3

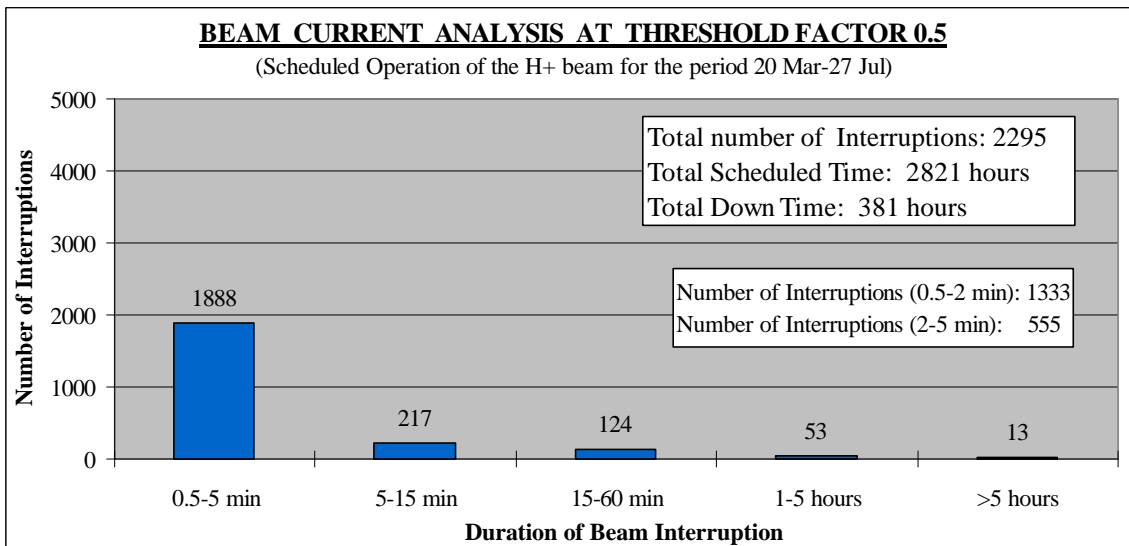


Figure 9.2 Summarize of Interruptions from the Beam Current Analysis at threshold factor 0.5

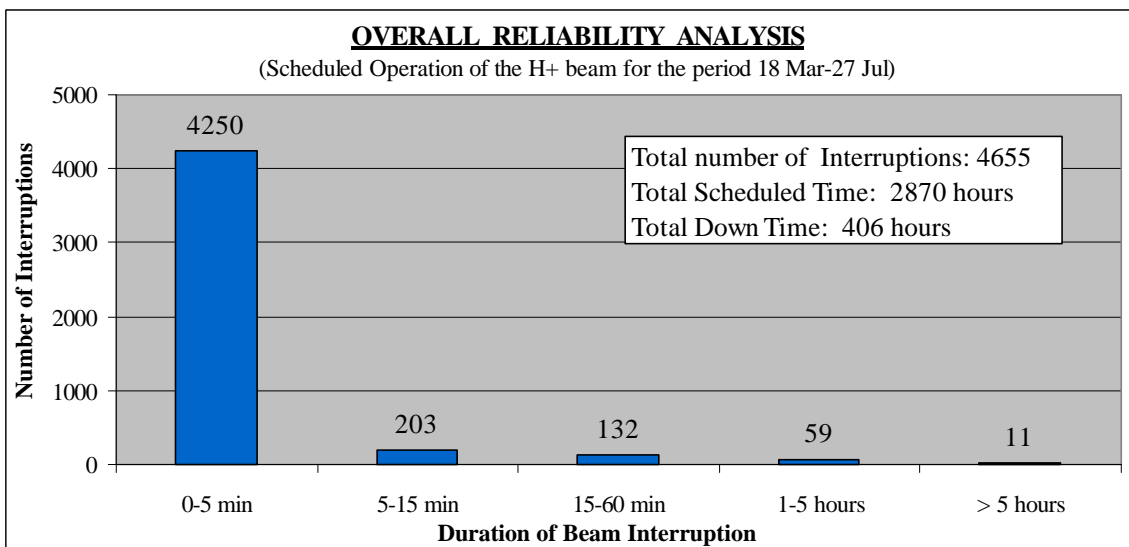


Figure 9.3 Summarize of Interruptions from the Overall Reliability Analysis

In the Beam Current Analysis, events which fall below 0.5\*Scheduled Current are interpreted as interruptions. This is the same definition for interruptions used in the Overall Reliability Analysis. Lets start by comparing the rightmost columns in both

figures. It is remarkable how well the two analyses agree even though the underlying data origins from two completely different records. The Overall Reliability Analysis is based on comments in the logbook while the Beam Current Analysis is based on current recordings from a beam monitor. In table 9.3 the number of interruptions are summarized for both analyses.

*Table 9.3 Comparison of Interruptions which occur in the Beam Current Analysis and the Overall Reliability Analysis*

Down Time Interval	NUMBER OF INTERRUPTIONS	
	Beam Current Analysis (Current Monitor data)	Overall Reliability Analysis (Logbook data)
0-5 min*	1888	4250
5-15 min	217	203
15-60 min	124	132
1-5 hours	53	59
> 5 hours	13	11
<b>Total</b>	<b>2295</b>	<b>4655</b>

*\*The interval 0.5-5 min is used for the Beam Current Analysis since interruptions shorter than 0.5 minutes are not included.*

For interruptions longer than 5 minutes both analyses agree very well. 407 interruptions with down time >5 minutes occur in the Beam Current Analysis compared to 405 interruptions in the Overall Reliability Analysis. But, in the interval 0-5 minutes significant differences occur. The reason is due to the existence of a large number of short interruptions of the H+ beam. As observed in table 7.1, 86 % of all short interruptions (0-1 min) are caused by the injector, and a typical injector failure lasts for 10-20 seconds (sparking in the high voltage column). Interruptions which last for only 20 seconds will not affect the average current sufficiently enough in order for it to fall below the threshold current. Subsequently, short interruptions will not be interpreted as a "real" interruptions in the Beam Current Analysis and therefore they will not be included in the statistics. In the Overall Analysis any interruption is included. If the beam current is below half the scheduled current an interruptions is registered no matter how short the interruption is.

During steady state operation (without any interruptions) the beam is usually delivered at the scheduled current level. Of course, this is not all true. Sometimes the operator deliberately delivers the beam with less current, for example at tuning, but this is exceptional. For most of the time the operator tries to deliver the beam at the scheduled current level. When a failure or a beam disturbance occurs it is usually the Fast Protect System or the Run Permit System which activates and shuts the beam off. The result is that the beam current drops to zero immediately. This means that during continuous operation the accelerator delivers either the scheduled current or zero current (see Appendix 5). On the other hand, the average current which is recorded in the database and used as input data may be anywhere in between, it depends on the duration of the interruption. As mentioned the input data is based on the average current during one minute (usually 70 seconds). This means that:

**At threshold factor 0.5, most Interruptions shorter than 35 seconds are not included in the Beam Current Analysis**

### 9.4.2 Threshold Factor 0.8

A similar investigation as in section 8.4.1 has been performed at a threshold factor of 0.8.

If we say that the accelerator during scheduled operation delivers either the scheduled current or zero current (during a failure) then if we raise the threshold factor from 0.5 to 0.8 we actually increase the ability to detect short interruptions. The reason is due to the nature of the input data. Each input value represents the average current delivered during 70 seconds. Since the delivered current is either full scheduled current or zero the interruption length will determine the average current. This is illustrated in figure 9.4a and 9.4b.

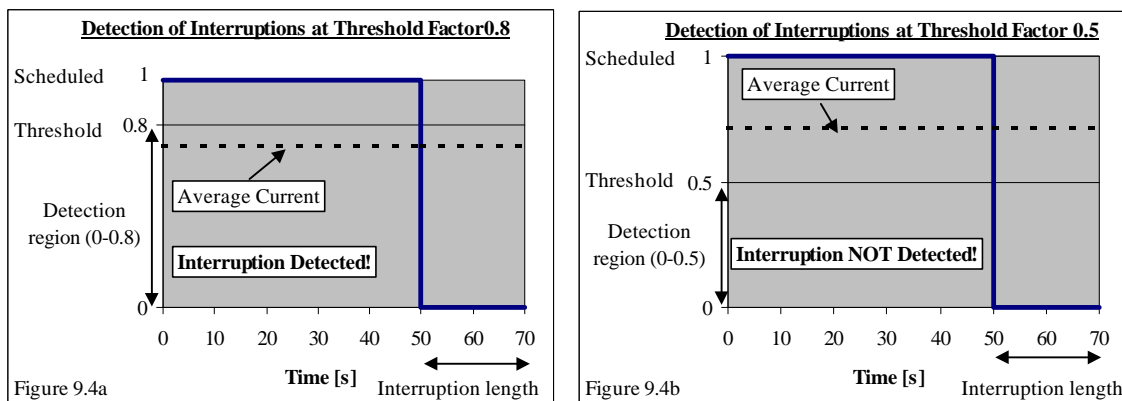


Figure 9.4a and 9.4b. Detection of Interruptions at Threshold factor 0.8 and 0.5

If the average current is below the threshold current the event will be detected and subsequently an interruption will be recorded. For example, if the threshold current is set to  $0.8 \times (\text{Scheduled Current})$  and an interruption with a duration of 20 seconds occur, the average current will be  $0.71 \times (\text{Scheduled Current})$  and the interruption will be detected (see figure 9.4a). But, if the threshold is set to  $0.5 \times (\text{Scheduled Current})$ , the average current will exceed the threshold current and the interruption will not be detected (see figure 9.4b). In summary,

- At threshold factor 0.8, interruptions > 14 seconds are detected.**
- At threshold factor 0.5, interruptions > 35 seconds are detected.**

The risk of having a too high threshold factor ( $>0.9$ ) is that you start detecting events that are actually no interruptions. For example, if the scheduled current is set to  $1000 \mu\text{A}$  but the beam is deliberately delivered at  $900 \mu\text{A}$  then the software would start to detect many false interruptions since small current fluctuations always occur.

In figure 9.5 the total number of detected interruptions at threshold factor 0.8 is presented. The analysis considers scheduled operation of the H+ beam for the period 18<sup>th</sup> of March - 27<sup>th</sup> of July, 1997.

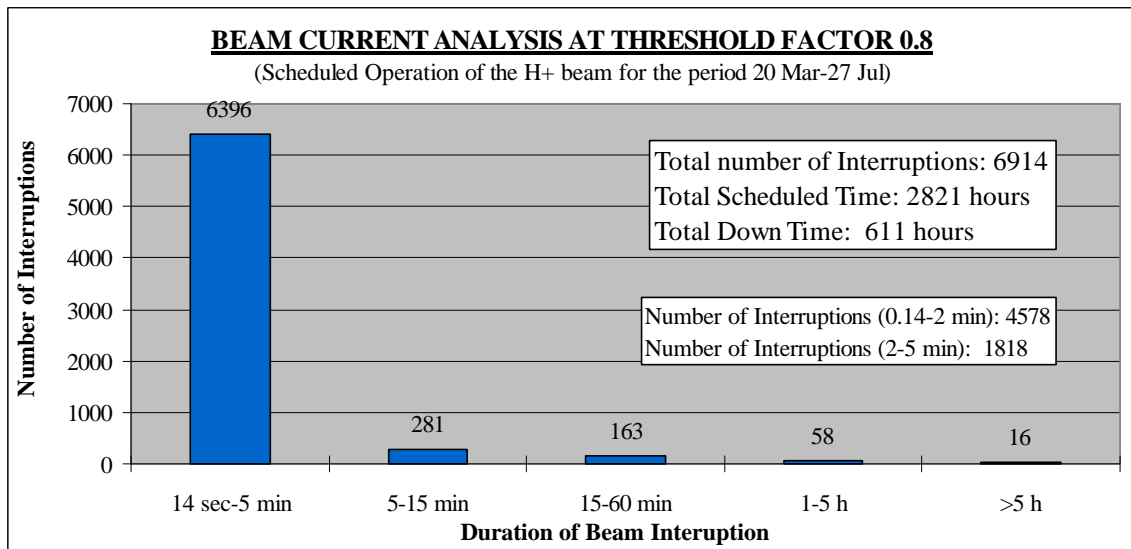


Figure 9.5 Summarize of Interruptions from the Beam Current Analysis at Threshold factor 0.8

A total of 6914 interruptions were detected. Significantly more than at threshold factor 0.5. In table 9.4 all three analyses are compared.

Table 9.4 Comparison of Interruptions which occur below threshold factor 0.5 and 0.8 and the Overall Reliability Analysis

Down Time Interval	NUMBER OF INTERRUPTIONS		
	Threshold Factor 0.8 (current monitor data)	Overall Reliability Analysis (Logbook data)	Threshold Factor 0.5 (current monitor data)
0-5 min*	6396	4250	1888
5-15 min	281	203	217
15-60 min	163	132	124
1-5 hours	53	59	53
> 5 hours	16	11	13
<b>Total</b>	<b>6914</b>	<b>4655</b>	<b>2295</b>

\*The interval 0.5-5 min is used at threshold factor 0.5 and the interval 14 sec-5 min is used at threshold 0.8

The increase in number of interruptions at threshold 0.8 is mainly due to the fact that a large number of short interruptions is detected. This is natural since the most common failure is high voltage sparking in the H+ injector column and this failure causes a down time of 10-20 seconds. At threshold factor 0.8, interruptions longer than 14 seconds are detected and hence most of the injector failures are recorded. Another important conclusion is that more interruptions are detected in the Beam Current Analysis at threshold factor 0.8 than in the Overall Reliability Analysis. This means that all short beam interruptions are not recorded in the logbook. This is also confirmed by operating personnel. For example, in periods when the injector is tripping very frequently the exact number of interruptions is not recorded, instead comments like "continuous arcing in the injector" are used.

In table 9.5 the growth of detected interruptions as a function of the threshold factor is presented.

*Table 9.5 Threshold Factor as a function of Total number of Interruptions*

Threshold Factor	Total Number of Interruptions
0.1	825
0.5	2295
0.7	4636
0.75	6558
0.8	6914
0.85	7030
0.9	6845

Obviously, the number of detected interruptions begin to grow less for threshold factors larger than 0.75, reaching a maximum around 0.85. This means that most interruptions are found at that point, and it also implies there are actually not many interruptions with down time less than 10 seconds. The reason why less interruptions are detected at threshold factor 0.9 is that individual interruptions which occur closely in time starts to "melt" together and form single interruptions with longer down time. For example, at threshold factor 0.9 22 interruptions with down time >5 hours are registered, while at threshold factor 0.8 16 interruptions are detected.

In figure 9.6 a representative plot of the average beam current is presented. A similar plot that reflects the instantaneous beam current every minute is presented in Appendix 5.

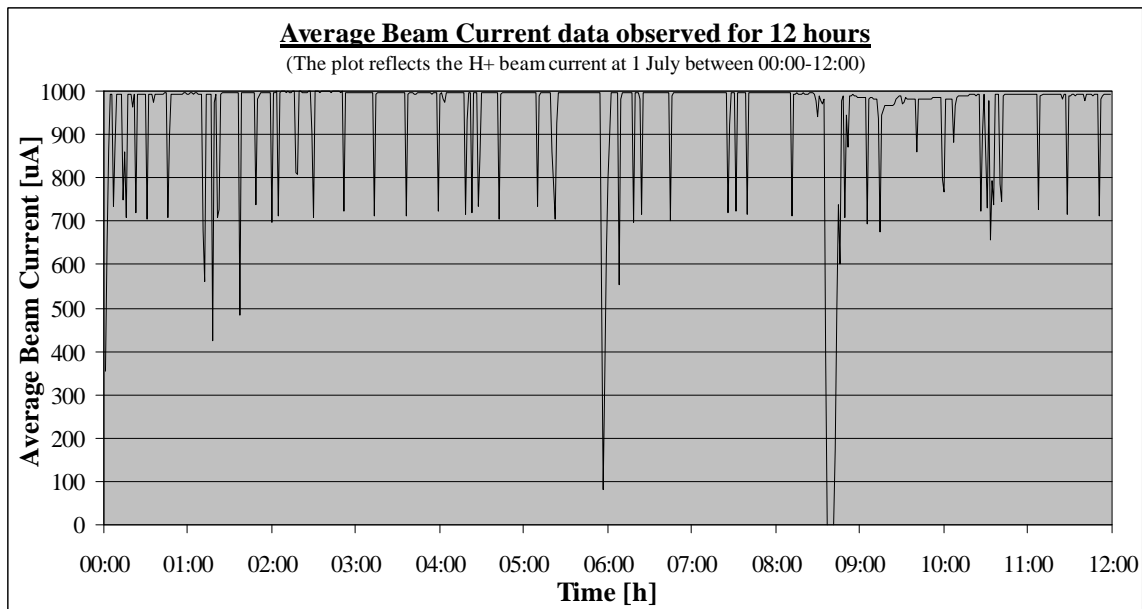


*Figure 9.6 Plot of Average Beam Current as a function of time*

The scheduled current is 1000  $\mu\text{A}$  and most of the vertical spikes reach down to the region of 700-750  $\mu\text{A}$ . This is no coincidence, the majority of the spikes represent injector failures with a duration of 15-20 seconds. As observed, very few spikes ends

above 800-900  $\mu\text{A}$ . This means that there don't occur many interruptions with down time shorter than 10 seconds. In other words, if an interruption occurs it is likely it will last for at least 10 seconds.

### 9.5 Reliability Estimates

From the beam current data estimates of the Availability, Mean Time Between Failure (MTBF) and Mean Down Time (MDT) may also be obtained. In table 9.6 these numbers are summarized for all three analyses.

*Table 9.6 Summary of the Availability, MTBF and MDT*

Analysis	Availability	MTBF [h:mm]	MDT [h:mm]
Overall Reliability Analysis (Logbook data of H+ Beam, 1997)	86 %	0:31	0:05
Threshold Factor 0.5 (Current data of H+ Beam, 1997)	86 %	1:04	0:10
Threshold Factor 0.8 (Current data of H+ Beam, 1997)	78 %	0:19	0:05

The Availability for both the Overall Reliability Analysis and the Beam Current Analysis at threshold factor 0.5 is 86 % while it is 78 % at threshold factor 0.8. Since the availability is determined by the total down time, it means a substantial amount of additional down time is included in the Beam Current Analysis at threshold factor 0.8 in comparison with the other two analyses. We know for a fact that many more interruptions are detected at threshold 0.8, but most of these interruptions are short and the contribution to the total down time should not be that much. Due to the nature of the input data any short interruption (< 70 seconds) will be assigned a down time of 70 seconds even if the interruption only lasted for 20 seconds. In other words, the calculated availability at threshold factor 0.8 does not reflect the real availability. Of course this applies at threshold factor 0.5 as well but the effect is not as pronounced. Actually, a somewhat similar problem occurs in the Overall Reliability Analysis where only discrete numbers of down time are recorded 1,2,3... minutes (every short interruption will be assigned a down time of 1 minute). The conclusion is that the overall availability of the H+ beam is most likely in the region of 85%.

MTBF in the Overall Reliability Analysis is 31 minutes which is half the value compared to the MTBF in the Beam Current Analysis at threshold 0.5. This is natural since the Overall Reliability Analysis includes twice as many interruptions. At threshold factor 0.8 even more interruptions are included and subsequently the MTBF is lower (19 minutes). The correct MTBF estimate of the H+ beam should probably be in the region of 20-25 minutes.

MDT is 5 minutes for both the Overall Reliability Analysis and the Beam Current Analysis at threshold 0.8. At threshold factor 0.5 the MDT is 10 minutes, but this number reflects more what the MDT would be if the injector interruptions were not included in the analysis. Naturally, the injector interruptions have a big influence on the MDT. Since the total down time observed at threshold factor 0.8 is too large the actual MDT is in fact shorter than 5 minutes, more likely in the region of 4 minutes.



## 9.6 Conclusions

When comparing the Overall Reliability Analysis of the LANSCE Accelerator facility with the Beam Current Analysis it is remarkable how well the results agree even though the underlying data origins from two completely different records. The Overall Reliability Analysis is based on comments in the logbook while the Beam Current Analysis is based on current recordings from a beam monitor. For down times >5 minutes a total of 407 interruptions are detected in the Beam Current Analysis compared to 405 interruptions in the Overall Reliability Analysis. That is a strong evidence for the correctness of both analyses. For down times <5 minutes, especially <1 minute, significant differences in reliability results occur. This is due to the nature of the input data in the Beam Current Analysis. When analyzing interruptions where the average delivered current should fall below half the scheduled current, interruptions with down time shorter than 35 seconds are not detected. By raising the threshold current to  $0.8 \cdot (\text{Scheduled Current})$  interruptions with down time >14 seconds are detected. At this interruption length most of the short interruptions are detected. When taking in consideration the results from all three Analyses, the conclusions are:

### **Conclusions concerning the reliability of the H<sup>+</sup> beam at LANSCE:**

- Many short interruptions with down time in the region of 10-20 seconds occur.
- The occurrence of short interruptions is larger than recorded in the logbook.
- Practically no interruptions with down time <10 seconds occur.
- The Availability is  $\approx 85\%$
- Mean Time Between Failure is about 20-25 minutes.
- Mean Down Time is about 4-5 minutes.

## 10 Acknowledgement

First of all I would like to thank Christopher Piaszczyk of Northrop Grumman Corporation for all his expert advice and help. The generous assistance of many LANSCE Operations Personnel in performing this work is greatly appreciated. Special thanks are due to Michael Oothoudt and Tim Callaway of LANSCE-6. Also, special thanks are due to Stan Cohen of LANSCE-6 for valuable help with magnet power supplies and John Lyles of LANSCE-5 for help with RF Technology.

Finally I would like to express my appreciation to Waclaw Gudowski of the Royal Institute of Technology and Francesco Venneri of the Los Alamos National Laboratory for providing the opportunity to carry out this work.

## 11 References

- [1] Francesco Venneri, "Accelerator-driven Transmutation of Waste", Technical Review MIT, 1998.
- [2] Helmut Wiedemann, "Particle Accelerator Physics", Springer-Verlag, 1993.
- [3] M. J. Smith and G. Phillips, "Power Klystrons Today", Research Studies Press LTD, 1995.
- [4] J. Le Duff, "Dynamics and Acceleration in Linear Structures", Laboratoire de l'Accélérateur Linéaire.
- [5] John W. Staples, "RFQ's- An Introduction", Lawrence Berkeley Laboratory, University of California, 1990.
- [6] Johan Carlsson, "Optimization of the neutron production in a spallation target", Royal Institute of Technology, 1996.
- [7] R.A. Jameson, "Beam Losses and Beam Halo in Accelerators for New Energy Sources", International Symposium on Heavy Ion Fusion, 1995.
- [8] George Lawrence, "Accelerator Design for ATW", Technical Review MIT, 1998.
- [9] J. Sherman, A. Arvin, L. Hansborough, D. Hodgkins, E. Meyer, J.D Schneider, H.V. Smith, Jr., M Stettler, R.R. Stevens, Jr., M. Thuot, T. Zaugg, and Robinm Ferdinand, "Status Report on a dc 130 mA, 75 keV Proton Injector", 7<sup>th</sup> International Conference of Ion Sources, 1997.
- [10] C. Rubbia, "The Accelerator Complex", IAEA Status Report on Accelerator driven systems (1997)
- [11] M. Stanley Livingstone, "A Nuclear Research Facility", LA-6878-MS, 1977.
- [12] Staffan Rosander, "Acceleratorteknik", Alfvénlaboratoriet, Royal Institute of Technology, 1997.
- [13] Oscar R. Sander, "LAMPF Transition Region", LA-9315-MS, 1982
- [14] E. A. Knapp, B. C. Knapp, and J. M. Potter, "Standing Wave High Energy Linear Accelerator Structures", Los Alamos National Laboratory, 1968
- [15] Manuel Jr. Neutron Scattering Center, Los Alamos National Laboratory, LP-95-219, 1995.
- [16] Michael Oothoudt, "Availability for cycle 75", LANSCE-6 Technical Report LANSCE-6-97-51-TR, 1997.
- [17] Olin van Dyck, "LAMPF Reliability History and Program", International Conference on Accelerator-driven Transmutation Technologies and Applications, Las Vegas, 1994
- [18] Neil Marks, "Conventional Magnets - 1", Daresbury Laboratory, Warrington, 1992.
- [19] R. Macek, "LANSCE PSR Technical Note #17", PSR-94-017, Los Alamos National Laboratory, 1994.

## Appendix 1

### A1 Beam Schedules

<b>1997 H+ BEAM SCHEDULE TO AREA A</b>		
<b>Beam On*</b>	<b>Beam Off*</b>	<b>Beamtime [h:mm]</b>
<b>CYCLE 74</b>		
03/18/97 17:00	03/23/97 17:27	120:27
03/25/97 19:28	03/26/97 21:50	26:22
03/28/97 08:00	04/21/97 08:00	576:00
<b>Scheduled beam time for Cycle 74:</b>		<b>722:49</b>
Minus 1 hour daylight savings time		-1:00
	<b>Adjusted Time:</b>	<b>721:49</b>
<b>CYCLE 75</b>		
04/23/97 08:00	05/19/97 08:00	624:00
05/20/97 22:50	06/16/97 08:00	633:10
<b>Scheduled beam time for Cycle 75:</b>		<b>1257:10</b>
<b>CYCLE 76</b>		
06/18/97 08:00	07/14/97 08:00	624:00
07/16/97 04:41	07/27/97 08:00	267:19
<b>Scheduled beam time for Cycle 76:</b>		<b>891:19</b>
<b>Total scheduled H+ beam time for 1997</b>		<b>2870:18</b>

Table A1.1 Summarize of 1997 scheduled beam time for H+ beam (Cycles 74, 75 and 76)

\*Times and dates based on Area A database.

<b>1997 H- BEAM SCHEDULE TO LUJAN</b>		
<b>Beam On*</b>	<b>Beam Off*</b>	<b>Beamtime [h:mm]</b>
<b><u>CYCLE 74</u></b>		
03/06/93 08:00	03/21/93 08:00	360:00
03/27/93 08:00	04/12/93 20:00	396:00
<b>Scheduled beam time for Cycle 74:</b>		<b>756:00</b>
Minus 1 hour daylight savings time		-1:00
<b>Adjusted Time:</b>		<b>755:00</b>
<b><u>CYCLE 75</u></b>		
04/22/93 08:00	05/13/93 08:00	504:00
05/20/93 07:30	06/08/93 04:00	452:30
<b>Scheduled beam time for Cycle 75:</b>		<b>956:30</b>
<b><u>CYCLE 76</u></b>		
06/17/93 02:00	07/11/93 08:00	582:00
07/16/93 08:00	07/23/93 10:00	170:00
<b>Scheduled beam time for Cycle 76:</b>		<b>752:00</b>
<b>Total scheduled H- beam time for 1997</b>		<b>2463:30</b>

Table A1.2 Summary of 1997 H- Beam Schedule

<b>1996 H- BEAM SCHEDULE TO LUJAN</b>		
<b>Beam On*</b>	<b>Beam Off*</b>	<b>Beamtime [h:mm]</b>
<b><u>CYCLE 71</u></b>		
07/09/92 08:00	07/15/92 08:00	144:00
07/17/92 21:30	07/27/92 08:23	226:53
07/29/92 14:00	08/23/92 08:00	594:00
<b>Scheduled beam time for Cycle 71:</b>		<b>964:53</b>
<b><u>CYCLE 72</u></b>		
08/29/92 02:10	09/02/92 08:00	101:50
09/06/92 08:00	09/20/92 08:00	336:00
09/24/92 07:00	10/20/92 07:00	624:00
<b>Scheduled beam time for Cycle 72:</b>		<b>1061:50</b>
<b><u>CYCLE 73</u></b>		
10/28/92 20:00	11/17/92 07:00	467:00
11/19/92 07:00	11/26/92 00:00	161:00
11/26/92 18:00	11/27/92 20:00	26:00
<b>Scheduled beam time for Cycle 73:</b>		<b>654:00</b>
<b>Total scheduled H- beam time for 1996</b>		<b>2680:43</b>

Table A1.3 Summary of 1996 H- Beam Schedule

**Appendix 2**  
**A2 DC Magnets and Power Supplies at LANSCE**

LOCATION	Device Area	Quadrupole Lenses QL	Quadrupole Magnets QM	Quadrupole Doublets QD	Quadrupole Triplets QT	Focusing Quadrupoles QF	Defocusing Quadrupoles QU	Bending Magnets BM	Steering Magnets SM	Vertical Magnets VM	Horizontal Magnets HM	Total Magnets	Power Supplies MP
<b>Injector Building</b>													
Transport A	TA	18						1	5			24	24
Transport B	TB	18						1	7			26	26
Transport D	TD	4						1	1			6	6
<b>Accelerator</b>													
201	M1-M4		132						10			142	16
805	M5-M48			103								103	54
<b>Transition Region</b>													
<b>Switchyard</b>													
Line A	LA		2	4				4	6			16	11
Line XD	XD		2					3				5	4
Line D (LD Kicker to RI Kicker)	LD			12	10			18		6	6	52	33
<b>Proton Storage Ring</b>													
Line D (RI Kicker to Line E)	LD			22						11	9	42	18
Ring Injection Line	RI					5	5	5		10	6	31	21
PSR	SR					10	10	10		10		40	4
Ring Extraction Line	RO					6	6	2		3	3	20	10
Bypass Beamline	BY							4		1	3	8	4
Line to Target Station 1 in Lujan	1L			6				4		3	3	13	8
Line to Target Station 2 and 4 in WNR	1R			6				2		3	3	14	11
<b>Area A</b>													
Target Station 1	1A				3				3			6	3
Target Station 2	2A				6				3			9	5
Target Station 3	3A			2					3			5	3
Mass Separator	4A			2					2			4	3
Bio-Medical Target Station	5A				3				2			5	3
<b>TOTAL</b>		<b>40</b>	<b>144</b>	<b>157</b>	<b>22</b>	<b>21</b>	<b>21</b>	<b>63</b>	<b>54</b>	<b>44</b>	<b>33</b>	<b>599</b>	<b>278</b>
Number of Dipoles								63				63	
Equivalent number of Quadrupole Magnets. (Quadrupole Doublets and Triplets have been converted into single Magnets)		40	144	314	66	21	21		54	44	33	737	
<b>TOTAL NUMBER OF DC MAGNETS</b>												<b>800</b>	

## Appendix 3

### A3 Summary of Components in the Pulsed Power System

Subsystem	Assembly	Component	
<b>Switchyard Kicker</b>	<b>Kicker Magnet</b>	Vacuum Vessel	
		Current Connections	
		Current Buses	
		Compensation Capacitor	
	<b>Charging System</b>	HVPS, EMHP	
		External Capacitor Bank	
		Charge SCR	
		Resonate Inductor	
		Do-Q SCR	
		DE-Q Shunt Resistor	
		<b>Modulator</b>	PFN Capacitors
			Output SCR
	Shunt Resistor		
	Load		
	Regulator Transistors		
	PS, Sorensen DCR40-250A		
	<b>Output Transmission Line</b>	Transmission Line	
		Cooling Blower	
		<b>Controls/Interlocks</b>	PS, PD Model 6050A
	LDK101 Run Permit Interface Panel		
	LDK102 Run Panel Permit Interface Panel		
	SCR fire Module		
	Switchyard Kicker Interlock/Control Chassi		
	Regulator Amplifier Module		
	Current Regulator Drive Module		
	Fast Protect Module		
	DAC Do-Q Module		
	Gate Generator Module		
	PS, PSR Low Voltage Group		
	<b>Computer Interface</b>		CAMAC
			<b>Injection Kicker</b>
	Current Connections		
Coils			
<b>Charging System</b>	PS, Sorensen SCR		
	Zener Diode Assembly		
	Charge Recover SCR		
	Freewheel SCR		
	Transfer Chassis		
	<b>Controls/Interlocks</b>	RIK101 Run ? Interface Channels	
NIM Crate w/6 Modules			
Short NIM Crate w/8 Modules			
<b>Computer Interface</b>		CAMAC	

<b>Harmonic Buncher</b>		
	<b>Cavity</b>	
		Ceramic Gap
		Gap Shunt Capacitors
		Ferrite
		RF Connector
		Cooling Hoses
		Bias PS, RF Choke
		Bias PS, PEI SR 1064
	<b>Low Level Electronics</b>	
		Dual TTL Fanout 63Y182451
		2.8 Mhz Harmonic Buncher
		CW Leveling Amplifier
		Hex Analog Fanout 63Y182290
		Harmonic Buncher Fast Protect
		Buncher Wide Band Amplifier
	<b>RF Preamplifier</b>	
		ENI A-300
	<b>RF Drive Amplifiers</b>	
		HVPS UVC 15 kV/3 A
		UVC Capacitor Bank
		UVC Crowbar Unit
		HVPS UVC 15 kV/6 A
		Tube 4CW25000
		Tube 8919
		Driver Filament PS Chassis
		Final Filament PS Chassis
		Final Filament Transformer
		PS, UVC 1 kV/1 A
		Pulsed Bias PS Chassis
		Screen Grid PS Chassis
		Balun Transformer
		Driver Coupling Transformer
		Final Coupling Transformer No. 1
		Final Coupling Transformer No. 2
	<b>Output Transmission Line</b>	
		Output Transmission Line
	<b>Controls/Interlocks</b>	
		UVC Monitor/Control/Interlock Chassis
		Harmonic Buncher Control/Interlock Chassis
		Buncher Cavity Bias Remote Control Chassis
		PSR Buncher Interface Chassis
		Cap Voltage Distribution/Monitor/Filter Chassis
		Master Sync System 2.8 MHz Chassis
	<b>Computer Interface</b>	
		CAMAC
<b>Extraction Kickers</b>		
	<b>Kicker Magnets</b>	
		Vacuum Vessel 71
		Vacuum Vessel 81
		Electrodes 71
		Electrodes 81
		HV Vacuum Feedthroughs
		HV Cable Connectors
	<b>Charging System</b>	
		UVC HVPS 1.6 kV/6 A
		Charge Thyatron
		Bias PS, HP 6207B
		Bias PS, Bertan Model 210-00R



		Driver, IE TD-25
		Do-Q Thyatron, HY 3002
		Do-Q Thyatron Driver
		Storage Capacitors
		Pulse Transformer
		Pulse Charging Diode Stack
		Inverse Diodes
		Ree-Htr PS
	<b>Switching System</b>	
		Switch Thyatron, CX1725
		Switch Driver
		PS, Bertan Model 210-00R
		Ree/Htr PS
		Blumlein Cables
		Heat Exchanger System
		Hydraulic Lift
	<b>Cables</b>	
		Output Cables
		Output Connectors
		Output Cables ? Modulators
		Load Cables
	<b>Loads</b>	
		Loads
	<b>Controls/Interlocks (NIM Modules)</b>	
		ESI PS-90-N
		ESI LDM-2N
		Voltage Comparator, Dual
		Fast Kicker Audio Arc Monitor
		Arc Threshold Detector
		Local/Remote Timing
		Fine Pulse Booster
		SRFK71 Fast Protect
		SRFK81 Fast Protect
		Extraction Kicker Control/Interlocks Chassis
	<b>Computer Interface</b>	
		CAMAC

*Table A3.1 List of Components for the Kickers and Buncher [19]*

## Appendix 4

### A4 Statistics of failure causes in individual Systems

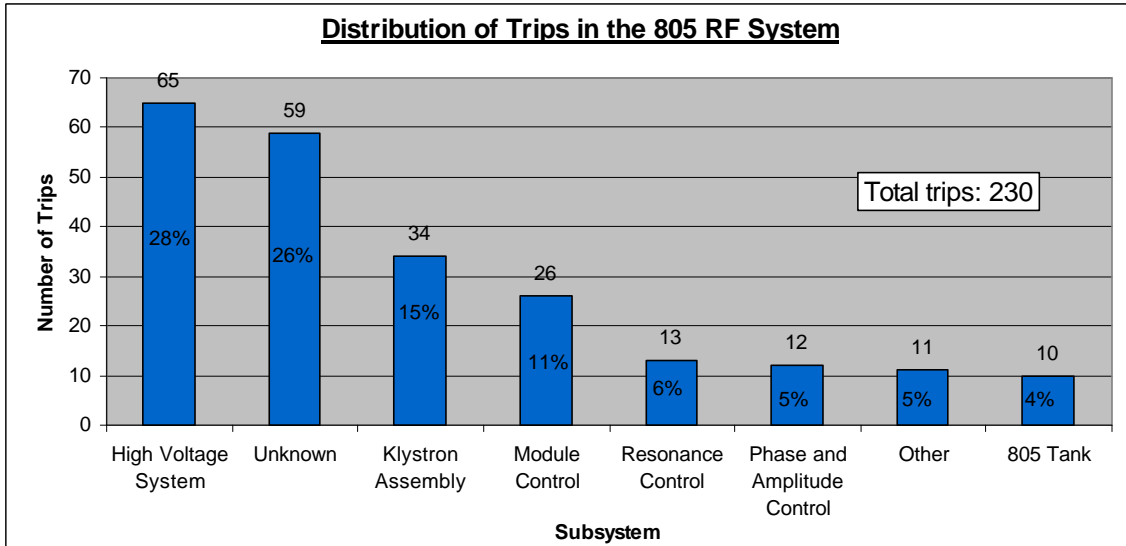


Figure A4.1 Distribution of Trips in the 805 RF System

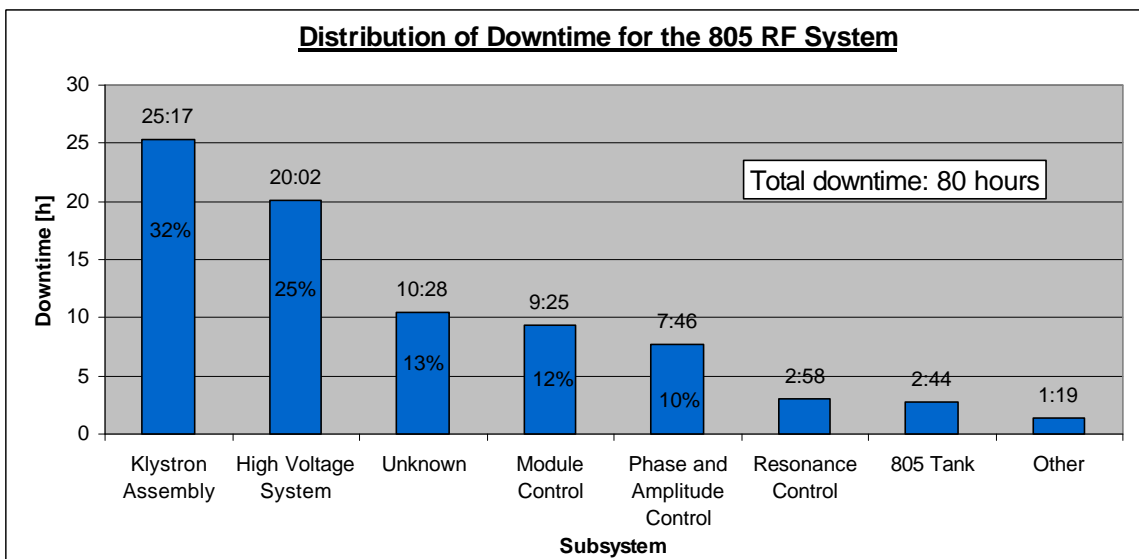


Figure A4.2 Distribution of Downtime for the 805 RF System

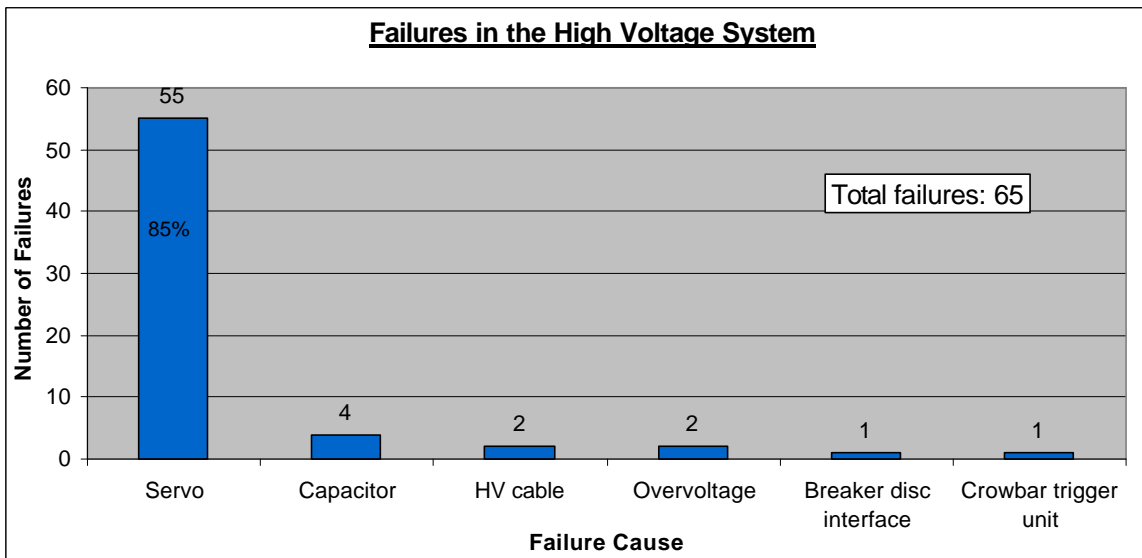


Figure A4.3 Failures in the High Voltage System

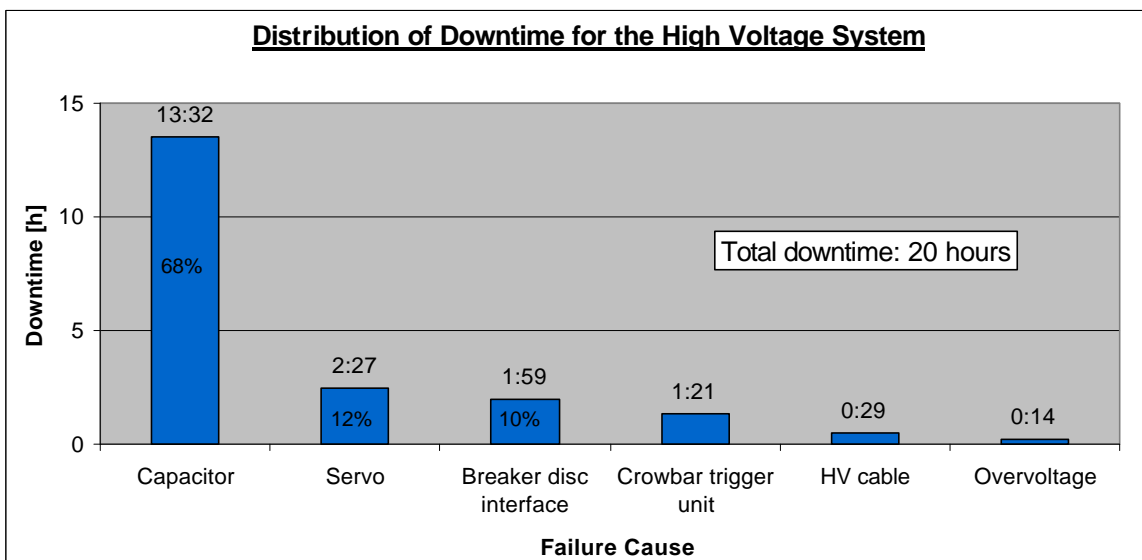


Figure A4.4 Distribution of Downtime for the High Voltage System

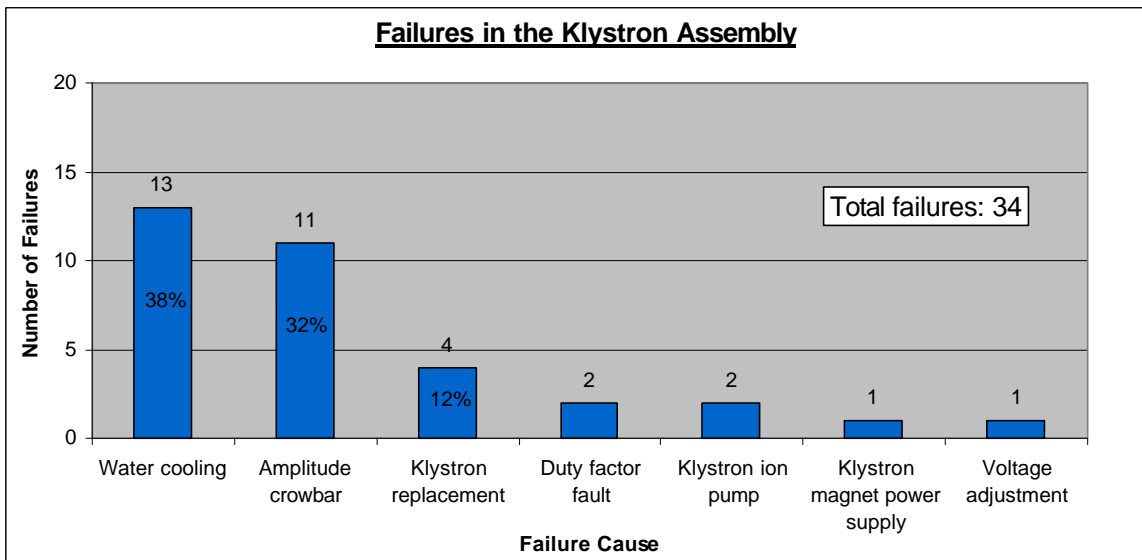


Figure A4.5 Failures in the Klystron Assembly

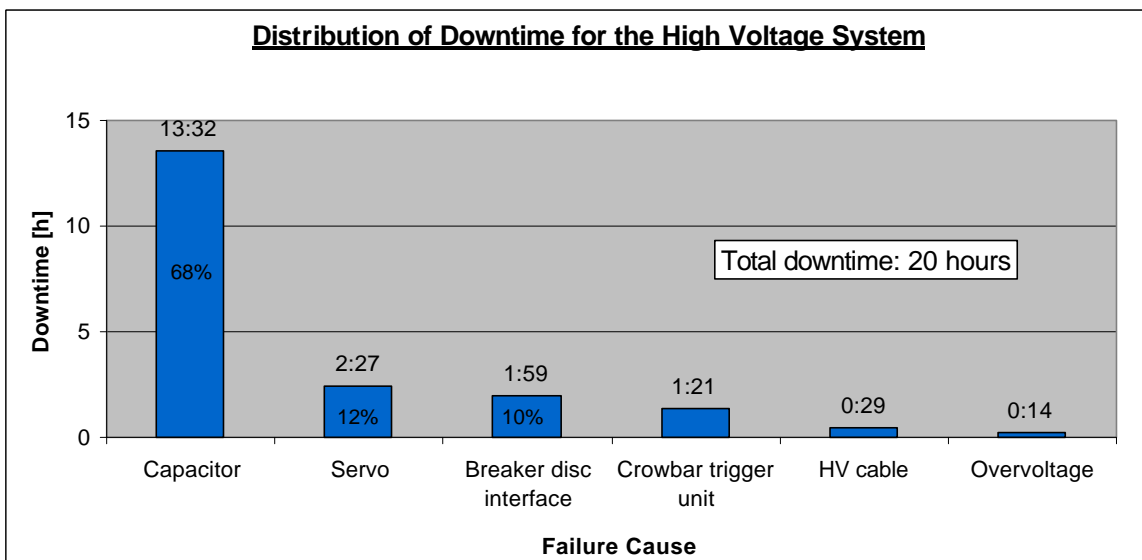


Figure A4.6 Distribution of Downtime for the Klystron Assembly

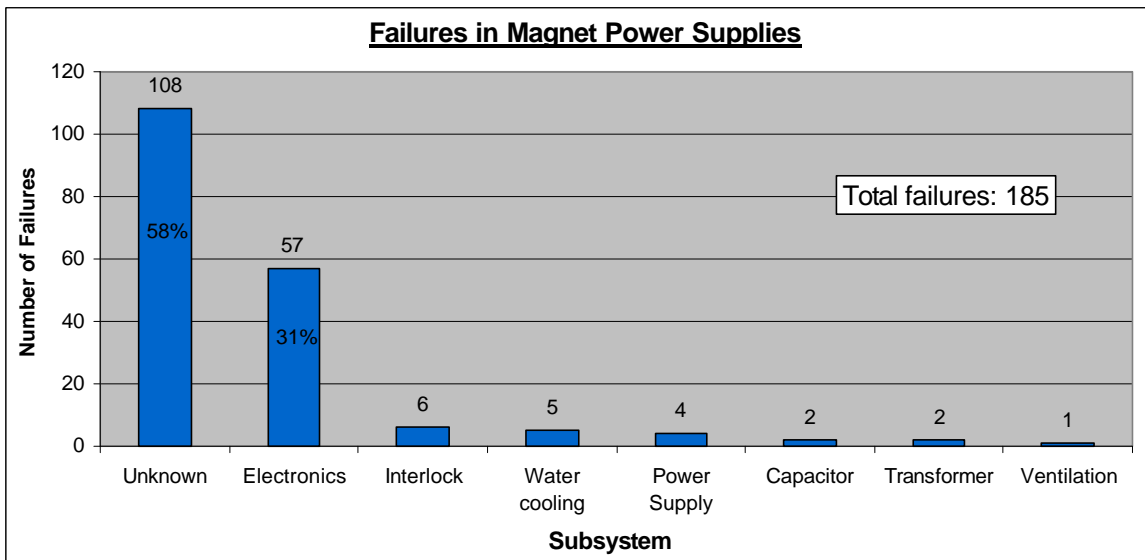


Figure A4.7 Failures in Magnet Power Supplies

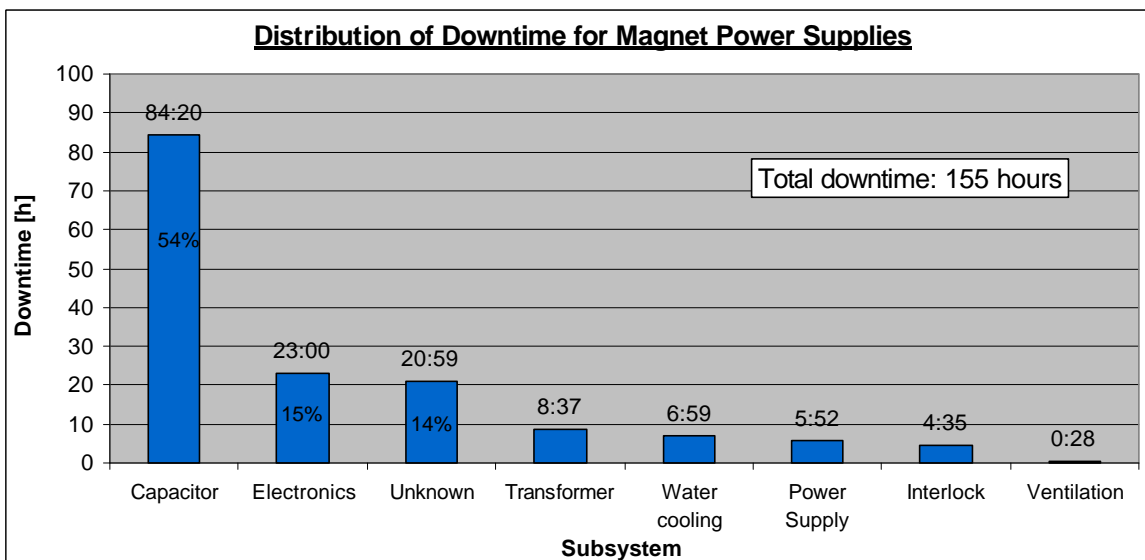


Figure A4.8 Distribution of Downtime for Magnet Power Supplies

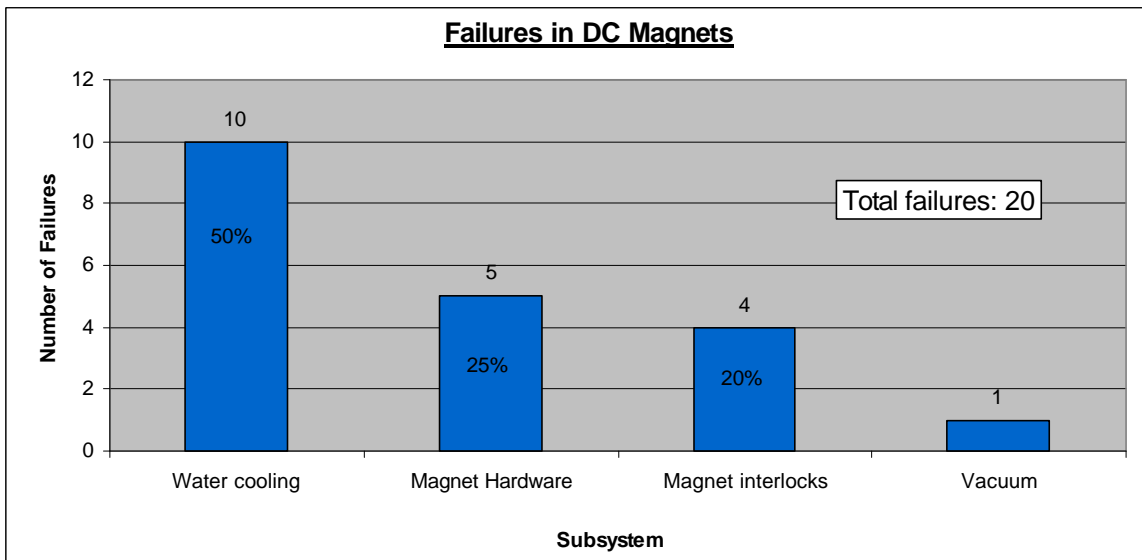


Figure A4.9 Failures in DC Magnets

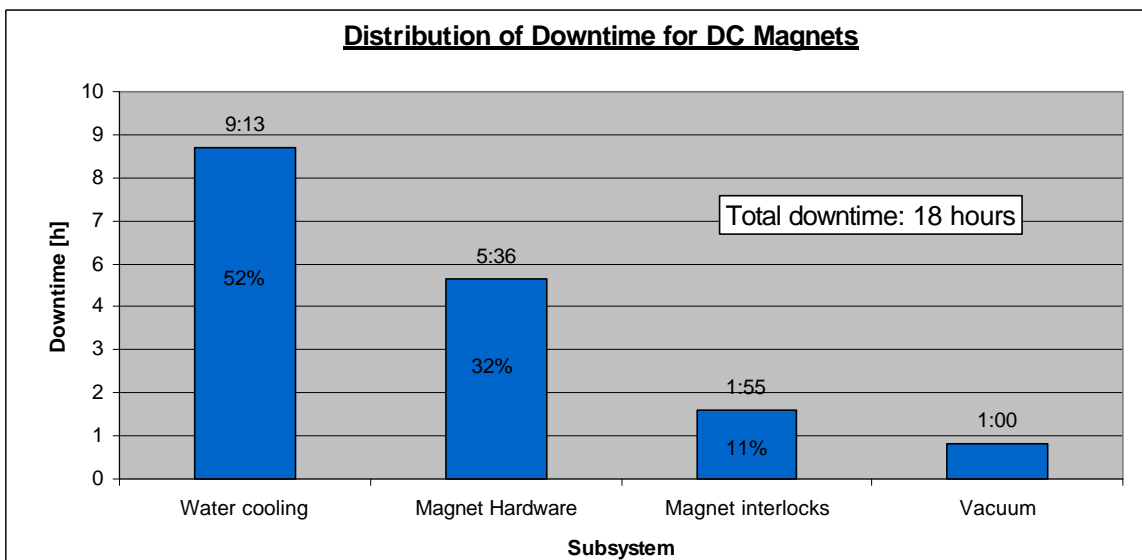


Figure A4.10 Distribution of Downtime for DC Magnets

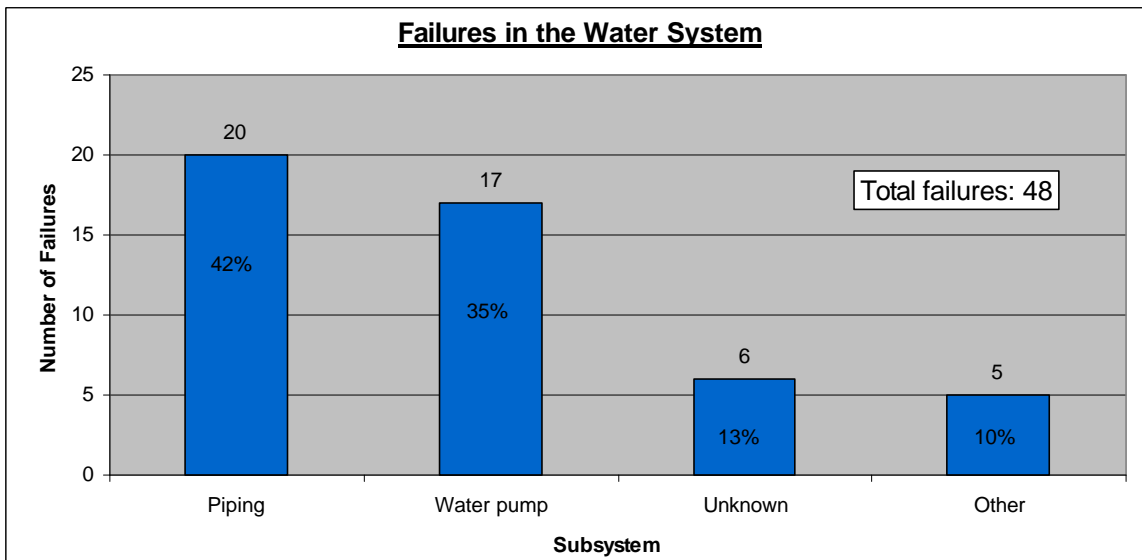


Figure A4.11 Failures in the Water System

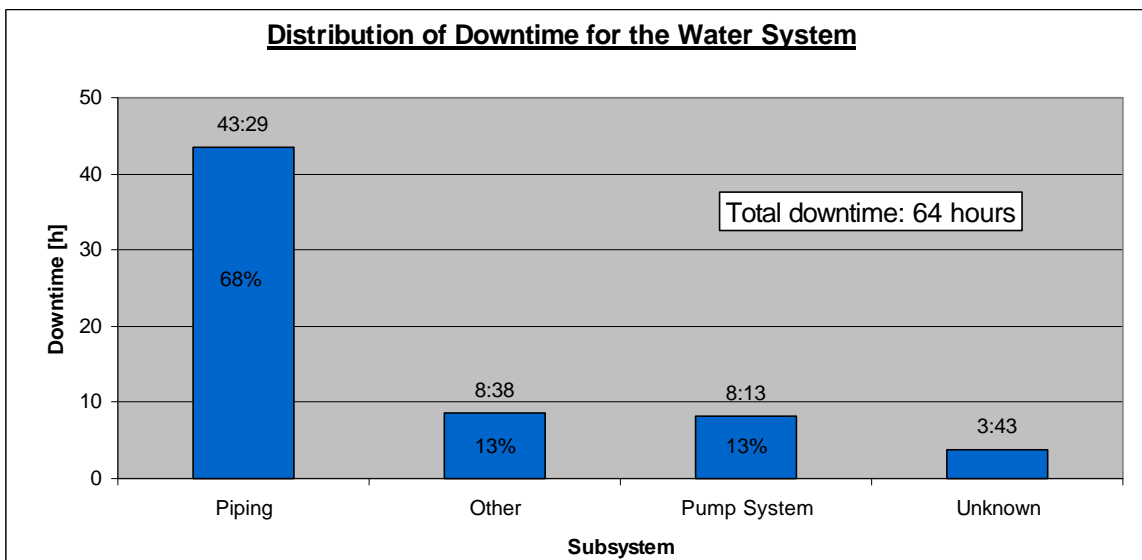


Figure A4.12 Distribution of Downtime for the Water System

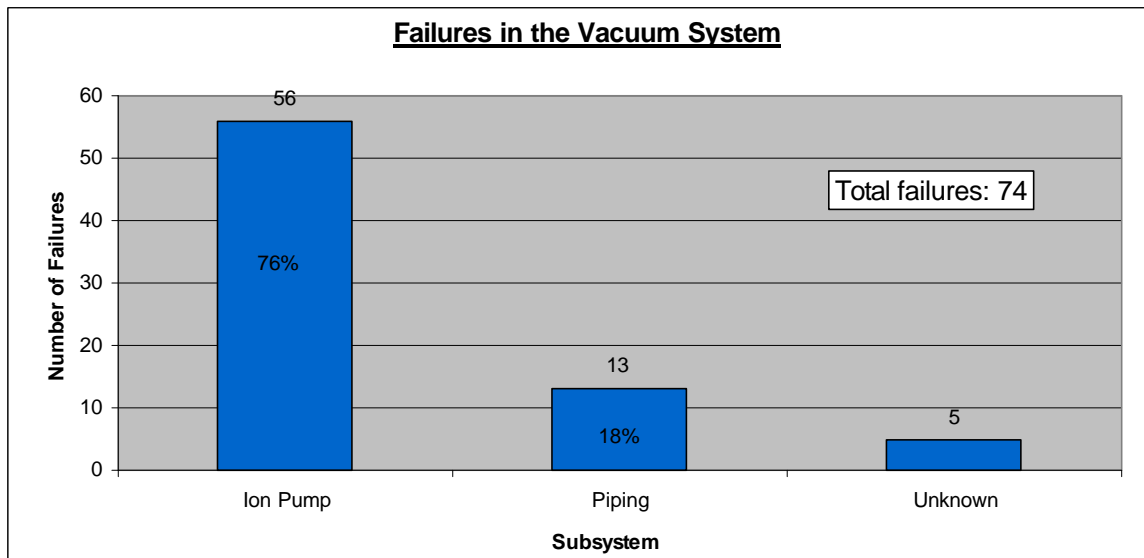


Figure A4.13 Failures in the Vacuum System

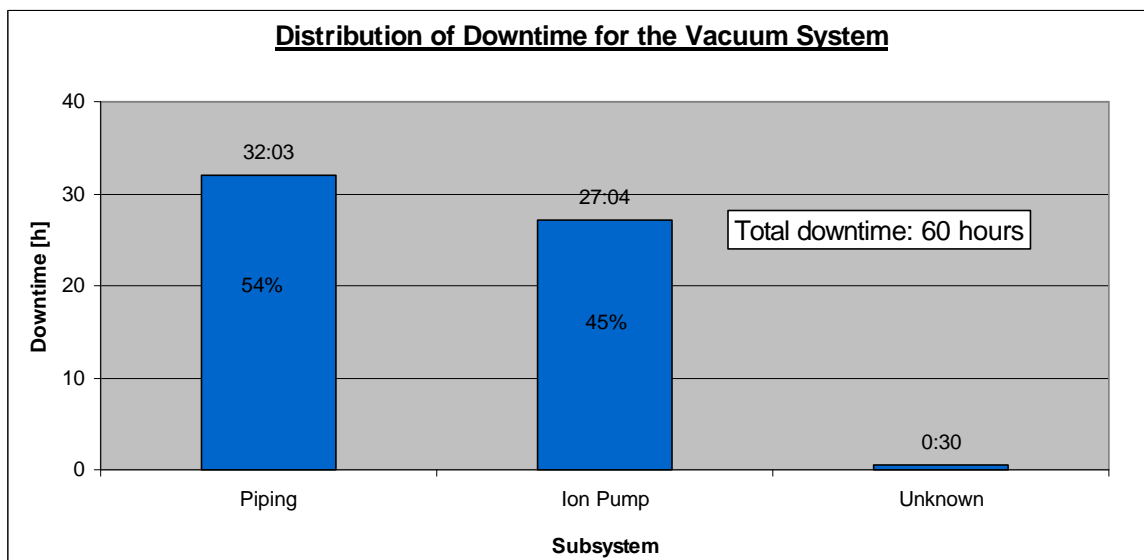
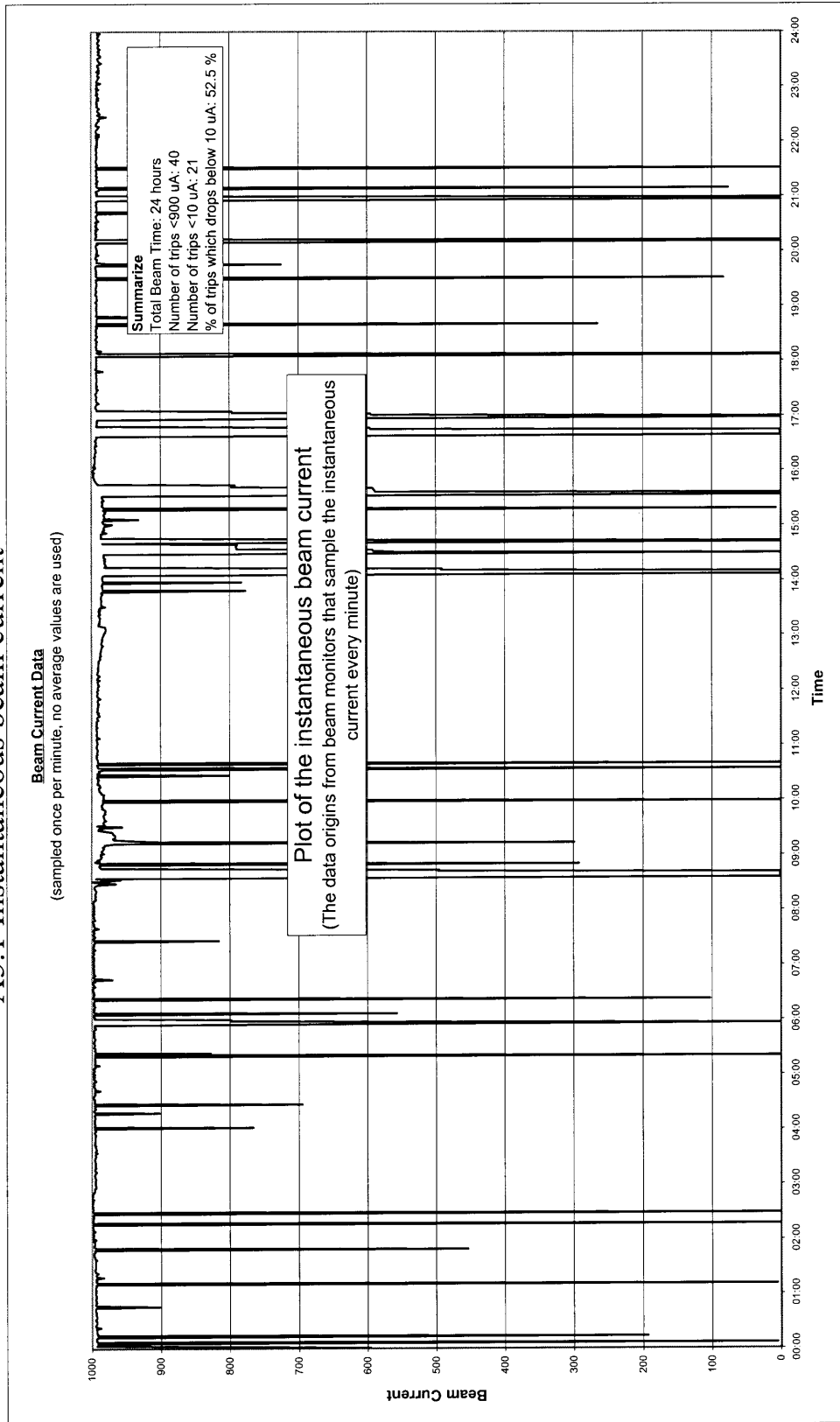


Figure A4.14 Distribution of Downtime for the Vacuum System



Appendix 5  
A5 Instantaneous Beam Current

Appendix 5  
A5.1 Instantaneous beam current



Prepared by Marcus Eriksson, RIT